National Library
of Canada

Canadian Theses Service

Ottawa, Canada
K1A 0N4

Bibliothèque nationale
du Canada

Services des thèses canadiennes

CANADIAN THESES

THÈSES CANADIENNES

NOTICE

The quality of this microfiche is heavily dependent upon the quality of the original thesis submitted for microfilming. Every effort has been made to ensure the highest quality of reproduction possible.

If pages are missing, contact the university which granted the degree.

Some pages may have indistinct print especially if the original pages were typed with a poor typewriter ribbon or if the university sent us an inferior photocopy.

Previously copyrighted materials (journal articles, published tests, etc.) are not filmed.

Reproduction in full or in part of this film is governed by the Canadian Copyright Act, R.S.C. 1970, c. C-30.

AVIS

La qualité de cette microfiche dépend grandement de la qualité de la thèse soumise au microfilmage. Nous avons tout fait pour assurer une qualité supérieure de reproduction.

S'il manque des pages, veuillez communiquer avec l'université qui a conféré le grade.

La qualité d'impression de certaines pages peut laisser à désirer, surtout si les pages originales ont été dactylographiées à l'aide d'un ruban usé ou si l'université nous a fait parvenir une photocopie de qualité inférieure.

Les documents qui font déjà l'objet d'un droit d'auteur (articles de revue, examens publiés, etc.) ne sont pas microfilmés.

La reproduction, même partielle, de ce microfilm est soumise à la Loi canadienne sur le droit d'auteur, SRC 1970, c. C-30.

THIS DISSERTATION
HAS BEEN MICROFILMED
EXACTLY AS RECEIVED

LA THÈSE A ÉTÉ
MICROFILMÉE TELLE QUE
NOUS L'AVONS REÇUE

NL-339 (r.86/06)

Canada

THE UNIVERSITY OF ALBERTA

CONTROLLING MOBILITY AHEAD OF A VISCOUS OIL BANK

by

MEHMET KADRI KALELI

A THESIS
SUBMITTED TO THE FACULTY OF GRADUATE STUDIES AND RESEARCH
IN PARTIAL FULFILMENT OF THE REQUIREMENTS FOR THE DEGREE
OF MASTER OF SCIENCE
IN
PETROLEUM ENGINEERING

DEPARTMENT OF MINING, METALLURGICAL AND PETROLEUM ENGINEERING

EDMONTON, ALBERTA
SPRING, 1987

Permission has been granted to the National Library of Canada to microfilm this thesis and to lend or sell copies of the film.

The author (copyright owner) has reserved other publication rights, and neither the thesis nor extensive extracts from it may be printed or otherwise reproduced without his/her written permission.

L'autorisation a été accordée à la Bibliothèque nationale du Canada de microfilmer cette thèse et de prêter ou de vendre des exemplaires du film.

L'auteur (titulaire du droit d'auteur) se réserve les autres droits de publication; ni la thèse ni de longs extraits de celle-ci ne doivent être imprimés ou autrement reproduits sans son autorisation écrite.

ISBN 0-315-37763-1

THE UNIVERSITY OF ALBERTA

RELEASE FORM

NAME OF AUTHOR MEHMET KADRI KALELI

TITLE OF THESIS CONTROLLING MOBILITY AHEAD OF A VISCOUS OIL BANK

DEGREE FOR WHICH THESIS WAS PRESENTED MASTER OF SCIENCE

YEAR THIS DEGREE GRANTED SPRING, 1987

Permission is hereby granted to THE UNIVERSITY OF ALBERTA LIBRARY to reproduce single copies of this thesis and to lend or sell such copies for private, scholarly or scientific research purposes only.

The author reserves other publication rights, and neither the thesis nor extensive extracts from it may be printed or otherwise reproduced without the author's written permission.

(SIGNED) ....

PERMANENT ADDRESS:

4. cadde 154/1
Bahçelievler - Ankara
TURKEY

DATED April 22, 19 87

THE UNIVERSITY OF ALBERTA

FACULTY OF GRADUATE STUDIES AND RESEARCH

The undersigned certify that they have read, and recommend to the Faculty of Graduate Studies and Research, for acceptance, a thesis entitled **CONTROLLING MOBILITY AHEAD OF A VISCOUS OIL BANK** submitted by MEHMET KADRI KALELI in partial fulfilment of the requirements for the degree of Master of Science in PETROLEUM ENGINEERING.

Supervisor

Ramon Bentsen

Date Apr 15, 87

TO MY BELOVED COUNTRY

ABSTRACT

This research presents an experimental and theoretical study of bitumen/heavy oil mobilization by solvents, gases and surfactants under cold conditions. Our experimental studies are aimed at examining several means of mobilization of highly viscous oil/bitumen employing synthetic crude, carbon dioxide and surfactant.

Athabasca oil sands and Suncor synthetic crude were used in linear and rectangular(visual) laboratory models. In the linear core runs it was observed that although a small solvent slug could move the oil locally, plugging of the formation and the cold front ahead made the displacement very inefficient. Experimental runs employing a high permeability channel were conducted in a rectangular model which allowed packing of a bottom water zone. Runs made with this model showed strong dependence on solvent slug size, thickness and permeability of the water zone. Stimulation of oil sands by the carbon dioxide and surfactant in combination with solvent did increase the incremental recovery of the bitumen and the injected solvent. Combination of gas and surfactant were not effective in the absence of a solvent. A thin bottom water zone enhanced the injectivity and interwell communication. Visual model runs were performed to obtain an idea of the flow pattern.

A simulator for solvent leaching of oils sands was extended to include a number of additional effects. Simulation runs were compared with the experimental results and good matches were obtained. It was shown that a thin bottom water zone is helpful in obtaining initial injectivity, yet not detrimental to bitumen recovery. A bitumen-to-water zone ratio of about 5 gave optimal recoveries. From the concentration profiles it was observed that the bottom water served as a transport layer for the dissolved bitumen.

An analytical method using streamlines was developed and tested to scale the linear core experimental results to confined areal pattern floods. It was found that in the first 1.5 HCPV solvent injection the bitumen recovery is controlled by the leaching process confirming the results of the numerical simulation.

ACKNOWLEDGEMENTS

I would like to thank my supervisor, Dr. S.M. Farouq Ali for his guidance, assistance and patience during the course of this study.

The assistance of Messrs. Bob Smith, Jack Gibeau and John Czuroski of the Petroleum Engineering Technical Staff is appreciated.

I would also like to thank Mr. Mustafa Oguztoreli and Dr. Ted Cyr for the beneficial discussions concerned with my research.

Last but not least, I wish to convey my gratitude to my parents for their support and patience.

Table of Contents

Chapter Page

1. INTRODUCTION AND LITERATURE REVIEW 1
  1.1 Solvent Additives 1
    1.1.1 Miscible Displacement at Unfavourable Mobility Ratios 1
    1.1.2 Solvent Stimulation 3
    1.1.3 Viscosity of Bitumen-Solvent Mixtures 5
  1.2 Effect of Gases on Oil Mobilization and Recovery 5
  1.3 Oil Expansion 8
  1.4 Viscosity Reduction 8
  1.5 Diffusion of CO_2 into Bitumen and Heavy Oil 9
  1.6 Asphaltene Precipitation 11
  1.7 Surfactants as Steamflood Additives 12
  1.8 Presence of Bottom Water 13
  1.9 Leaching Phenomena 14
2. STATEMENT OF THE PROBLEM 16
3. EXPERIMENTAL APPARATUS AND PROCEDURE 17
  3.1 Linear Sand Pack 17
    3.1.1 Packing the Core 17
  3.2 Rectangular Model 18
    3.2.1 Packing the Model 18
  3.3 Visual Model 21
  3.4 Fluid Properties 25
  3.5 Density of Sand 26
  3.6 Density of Bitumen 26
  3.7 Bitumen Content 27
  3.8 Bitumen in Place 27

3.8.1 Void Space 27

3.9 Density Measurements 28

3.10 Specific Gravity of Bitumen 29

3.11 Pore Volume and Porosity 30

3.12 Analysis of Effluent Samples 30

3.13 Volume of Carbon Dioxide 32

3.14 Fluid Injection System 34

4. DISCUSSION OF EXPERIMENTAL RESULTS 35

4.1 Results of Linear Pack Runs 35

4.2 Bottom Water Runs in the Rectangular Model 39

4.3 Effect of Hot Water on Bitumen Mobilization 41

4.4 Effect of Bottom Water Zone Thickness on Bitumen Mobilization 42

4.4.1 Solvent Stimulation 43

4.4.2 Solvent Floods 43

4.4.3 Solvent-Surfactant Flooding 47

4.5 Effect of Carbon Dioxide on Bitumen Mobilization 51

4.6 Effect of Water Zone Permeability on Bitumen Mobilization 55

4.7 Surfactant Crumble Test 60

4.8 Visual Model Experiments 64

5. NUMERICAL SIMULATION 68

5.1 Porous Region 68

5.2 Radial Dissolution 69

5.3 Convective-Diffusion with Adsorption 70

5.4 Darcy-Continuity Equation 72

5.5 Leaching 74

5.6 Simulation 76

5.7 Effect of Bottom Water on Leaching 80

6. LEACHING MODEL 93

  6.1 Analytical Formulation 93

  6.2 Experimental Runs 98

  6.3 Limitations of the Model 101

7. CONCLUSIONS 105

8. RECOMMENDATIONS 107

REFERENCES 108

APPENDIX A 112

  Derivation of Scaling Equations 113

    Streamline Model 113

    Material Balance 114

  Leaching 120

APPENDIX B 124

APPENDIX C 136

LIST OF TABLES

TABLE	DESCRIPTION	PAGE
3.1	Physical Properties of Suncor Synthetic Crude	26
4.1	Results of Experimental Runs	36-37
4.2	Effect of Bottom Water Thickness	42
4.3	Solvent Stimulation Runs	43
4.4	Solvent-Surfactant Flood Runs	48
4.5	Carbon Dioxide Stimulation Runs	52
4.6	Effect of Water Zone Permeability	57
5.1	Leaching Simulation Data	77
5.2	Effect of Bottom Water Thickness	97
6.1	β Values for Line Drive and Five Spot Patterns	97
6.2	Example Calculation for Leaching in Line Drive	101
C.1	History of Run 1	137
C.2	History of Run 2	138

C.3 History of Run 3 139

C.4 History of Run 4 140

C.5 History of Run 5 141

C.6 History of Run 6 142

C.7 History of Run 7 143

C.8 History of Run 8 144

C.9 History of Run 9 145

C.10 History of Run 10 146

C.11 History of Run 11 147

C.12 History of Run 12 148

C.13 History of Run 13 149

C.14 History of Run 14 150

C.15 History of Run 15 151

C.16 History of Run 16 152

C.17 History of Run 17 153

C.18 History of Run 18 154

C.19 History of Run 19 155

C.20 History of Run 20 157

C.21 History of Run 21 159

LIST OF FIGURES

FIGURE	DESCRIPTION	PAGE
1.1	Viscosity-temperature data for bitumen samples	6
1.2	Viscosity as a function of concentration and temperature for Athabasca bitumen-Suncor synthetic crude mixtures	7
1.3	Volumetric Solubility of CO_2 in bitumen	10
1.4	Viscosity-pressure isotherms for CO_2-saturated bitumen	10
3.1	Schematic of Rectangular Model and Fluid Injection System	20
3.2	Experimental Set up for Visual Model	23
3.3	Schematic of Visual Model	24
3.4	Absorption Spectra for Synthetic Crude-Bitumen Mixtures	31
4.1	Comparison of Runs 9 and 10	45
4.2	Comparison of Runs 9 and 11	50
4.3	Production History of Run 18	54
4.4	Comparison of Normalized Bitumen Recovery vs Solvent Used	

Breakdown 56

4.5 Production History of Run 17..58

4.6 - Comparison of Run 9 and 17 61

4.7 - Production History of Run 19 63

4.8 - Production History of Run 14 65

4.9 Residual Saturations for Run 14 67

5.1 Concentration and Recovery Profiles 79

5.2 Concentration and Recovery Profiles 81

5.3 Concentration and Recovery Profiles 82

5.4 Concentration and Recovery Profiles 83

5.5 Solvent Concentrations along the core at different times 86-87

5.6 Solvent Concentrations along the core at different times 88-89

5.7 Solvent Concentrations along the core at different times 90-91

5.8 Solvent Concentrations along the core at different times 92

6.1 Layered Presentation of Streamlines 94

6.2 Effluent Concentration History 100

6.3 Effluent Concentration History for Five-Spot Pattern 102

6.4 Effluent Concentration History for Line Drive Pattern 103

B.1 - Production History for Run 4 125

B.2 - Production History for Run 5 126

B.3 - Production History for Run 6 127

B.4 - Production History for Run 7 128

B.5 - Production History for Run 8 129

B.6 - Production History for Run 9 130

B.7 - Production History for Run 10 131

B.8 - Production History for Run 11 132

B.9 Production History for Run 15 133

B.10 Production History for Run 16 134

B.11 Production History for Run 20 135

LIST OF PHOTOGRAPHIC PLATES

PLATE..DESCRIPTION ....PAGE

Plate 1 Rectangular High Pressure Model and Fluid and Gas Injection System 19

Plate 2 Visual Model with Fluid Injection System 22

NOMENCLATURE

D_0 - liquid phase molecular diffusion coefficient

D_ℓ - apparent longitudinal diffusion coefficent

D_t - apparent transverse diffusion coefficent

D_p - grain particle diameter

D_s - solid phase molecular phase diffusion coefficient

F_r - formation resistivity factor

g - accelaration due to gravity

N_{Da} - Dimensionless Damkohler number

N_{Pe}, N_P - Dimensionless Peclet number

$\bar{p}$ - hydrodynamic pressure

q_{in} - injection rate

r_p - spherical particle radius

t_D - dimensionless time of dissolution

u - Darcy velocity

GREEK SYMBOLS

α - dispersivity

α - adsorption coefficient

ρ - density

μ - viscosity

θ - contact angle

σ - packing inhomogeneity factor

ϕ - porosity

1. INTRODUCTION AND LITERATURE REVIEW

INTRODUCTION

Conventional oil recovery methods can not be used directly in bitumen saturated oil sands because of the very low bitumen mobility. Thermal methods are often applied as a means to exploit such reservoirs, with limited success. In some instances, use of additives may help mobilizing the bitumen. Additives such as caustic, foam, polymers, surfactants, solvents, gases might increase mobility, reduce interfacial tension and residual oil. A literature survey reveals that their use is usually associated with a thermal recovery scheme. Because of the high cost of these additives and the low oil price, a careful screening of these additives is imperative to make any project economically feasible. Previous work concerning heavy oil/bitumen is relatively new and limited. Most of the work was done at the laboratory scale and has not been field-tested. The scope of this review is to look at the theoretical and laboratory studies performed on heavy oil/bitumen in general; solvents, surfactants and gases in particular.

1.1 Solvent Additives

1.1.1 Miscible Displacement at Unfavourable Mobility Ratios

When a miscible light hydrocarbon displaces an in-place viscous oil at an unfavourable mobility ratio (in the case of miscible displacement, mobility ratio is defined as the ratio of the viscosities of the displaced to the displacing phase), viscous instabilities develop. These, in turn, lead to a poor displacement efficiency. Rodriguez (1957) found that, at an unfavourable mobility ratio, viscous fingering is the controlling mechanism for the miscible recovery process. Sievert *et al.* (1957) also observed that the length of the transition zone formed depends on the mobility ratio and characteristics of the core. Blackwell *et al.*

(1959) used several methods to study the factors influencing the efficiency of miscible displacement under conditions of an adverse mobility ratio, and found that molecular diffusion is the principal mechanism causing the injected fluid to mix with the original fluids in place. They also found that in a horizontal reservoir, even if the porous medium is homogeneous, channeling and bypassing take place, and as the mobility ratio increases, the displacement efficiency and the oil recovery decrease.

Cashdollar (1959), using unconsolidated glass bead packs for his miscible displacement runs at unfavourable mobility ratio, observed that the transition zone length increased to 15% of the core length when the viscosity difference between the displaced and the displacing liquids was four-fold, for the same mobility ratio.

Alikhan and Farouq Ali (1971) studied the effects of solvent slug size, hot water, and injection rates on the recovery of heavy oil. They found that an increase in slug size, injection rate, and viscosity of the light hydrocarbon led to higher recoveries. Alikhan and Farouq Ali (1981) also did an experimental study of moderately heavy oil recovery from a porous pack by the injection of a light hydrocarbon slug, followed by a steam slug, which was in turn driven by a conventional waterflood. It was found that the light hydrocarbon slug injected prior to the steam slug in a sandpack initially containing a residual oil saturation improved the oil recovery as compared to a straight steam slug run. A large proportion of the light hydrocarbon slug was recovered by the steam instillation effects. The light hydrocarbon slug had little effect on oil recovery in the case of a high initial oil saturation. As also observed in Alikhan's previous work, recovery was found to depend on the in-place oil viscosity when employing a hot water slug. It was also found that the recovery ratio, the amount of oil recovered divided by the amount of the light hydrocarbon slug injected, was higher and the steam residual oil saturation was lower, when a steam slug was used rather than a hot water slug. In both cases, the recovery peaked after which there was no significant increase in recovery with an increase in hydrocarbon slug size.

1.1.2 Solvent Stimulation

Solvents used as diluents must be capable of dissolving bitumen and heavy oils without precipitating large quantities of asphaltenes. These solids, in sufficient quantities, can appreciably decrease the permeability of the rock. Viscosity reduction is a major mechanism for the enhancement of steam stimulation with solvents. Solvents can lower the viscosity of the unheated bitumen/heavy oil by several orders of magnitude.

Snyder (1972) investigated the recovery of bitumen by naphtha and steam injection, using Athabasca oil sands in a two-dimensional vertical model with a highly permeable channel. He concluded that solvent injection was technically feasible, recovering as much as 73.5% of the bitumen in-place, but uneconomic since the bitumen concentration in the effluent was low. Bitumen recovery was higher with lower injection rates; continuous injection led to formation plugging caused by asphaltene flocculation. Naphtha was found to be highly effective in opening a steam flow path in a homogeneous sand pack, but breakthrough occurred quickly in a sand with a high permeability channel and the naphtha was immediately vaporized and produced. He did not however investigate the naphtha injection prior to hot or cold water injection.

Alban (1975) studied the efficiency of miscible displacement for the recovery of Athabasca bitumen under conditions of gravity segregation in a two-dimensional vertical model. Synthetic crude, "Mobil Solvent" and naphtha were used to displace the bitumen. Naphtha injection gave the best recovery, more than 93% of the bitumen in-place. The process, however, was inefficient, because the richest sample recovered contained only 41% bitumen. Gravity segregation was an important factor and the effect of injection rate on recovery confirmed Snyder's finding, being higher at lower injection rates.

Note that both Snyder and Alban reported that the maximum bitumen concentrations of about 40% by volume made the continuous solvent injection process inefficient. Oguztoreli (1985), on the other hand, predicted as high as 90% bitumen concentrations in a numerical simulation study of such a process.

Redford and McKay (1980) presented results of physical model experiments. A range of hydrocarbons from ethane, propane, butane, pentane,natural gasoline, naphtha, to synthetic crude were injected with steam. Given a set of conditions of pressure and temperature, they concluded that the additives could increase recovery of bitumen. This higher recovery though was offset by increased loss of hydrocarbon additives to the formation. Redford (1982), in a similar study, extended the study of Redford and McKay to the coinjection of multi-component solvents with steam. The experiments were conducted in a two-well huff-puff model. He found an improvement in recovery for a two-component solvent injected with steam as compared to the results of individual solvents. Naphtha reduced the viscosity of the oil phase and a light solvent, carbon dioxide or ethane, provided a solution gas drive. Later, Briggs *et al.* (1982) confirmed this study and attempted to isolate the effects of each component. They found that carbon dioxide improved recovery by providing energy on the pressure depletion portion of a cyclic process.

Raplee *et al.* (1984) screened a wide range of solvents used in conjunction with steam with Alberta, Utah, California and Saskatchewan heavy oil/ bitumen resources. Comparative viscosity and solubility tests were performed. Although a majority of solvents were technically acceptable, they recommended light naphtha for Saskatchewan and California heavy oil resources based upon linear core runs.

Shu and Hartman (1985) investigated the effects of solvent on steam recovery of heavy oil using a compositional thermal simulator. They found that the placement of the solvent in the reservoir is crucial to the process performance by determining the location of the transition zone. For a particular case, the viscosity of oil was 4860 mPa.s at reservoir conditions (38°C) and there was a thin bottom water zone (13% of total thickness). Steam and solvents were injected near the bottom zone and produced near the top of the formation. They found that the coinjection of solvents with steam at up to 10% of the steam volume could increase the recovery. Medium molecular weight solvents improved recovery the most while the heavy solvents decreased recovery. Solvent recoveries were low with each type of solvent.

Schmidt *et al.* (1985) studied the dispersion of a solvent slug in bitumen injected into a communication path. They developed a one-dimensional analytical solution for breakthrough time and outlet concentration of solvent.

1.1.3 Viscosity of Bitumen-Solvent Mixtures

Extremely high viscosities at reservoir conditions are typical of bitumen deposits in Alberta or elsewhere. The Athabasca bitumen has a viscosity of 5,000,000 mPa.s at reservoir conditions. Peace River and Marguerite Lake deposits, on the other hand, have viscosities of several hundred thousand mPa.s. In other parts of the world, such as in Venezuela, the higher reservoir temperatures (67°C versus 5° in Athabasca) result in relatively low viscosities.

The viscosities of Athabasca bitumen at different temperatures are given ~~in~~ Figure 1.1. At 40°C, for example, the viscosity is 20,000 mPa.s. Bitumen-synthetic crude mixtures show large reductions in viscosities. Viscosities of bitumen at different solvent concentrations and temperatures are shown in Figure 1.2. Greater viscosity reduction occurs at lower concentrations. For example, at 49°C (120°F), the viscosity reduction is five-fold at 10% solvent volume whereas, from 40 to 50%, it is only three-fold.

1.2 Effect of Gases on Oil Mobilization and Recovery

Use of gases to increase the recovery of oil has been extensively studied and there have been numerous field applications with varying success. For the case of heavy oil/bitumen, various immiscible displacements and well stimulation schemes have been proposed since the 1950's. Regardless of how gases are utilized in any given scheme, reduction of oil viscosity, crude oil expansion, increasing injectivity, and solution gas drive may contribute to mobilization and recovery. Among gases, carbon dioxide seems to have the most extensive data and considerable promise as it will be apparent in the following sections.

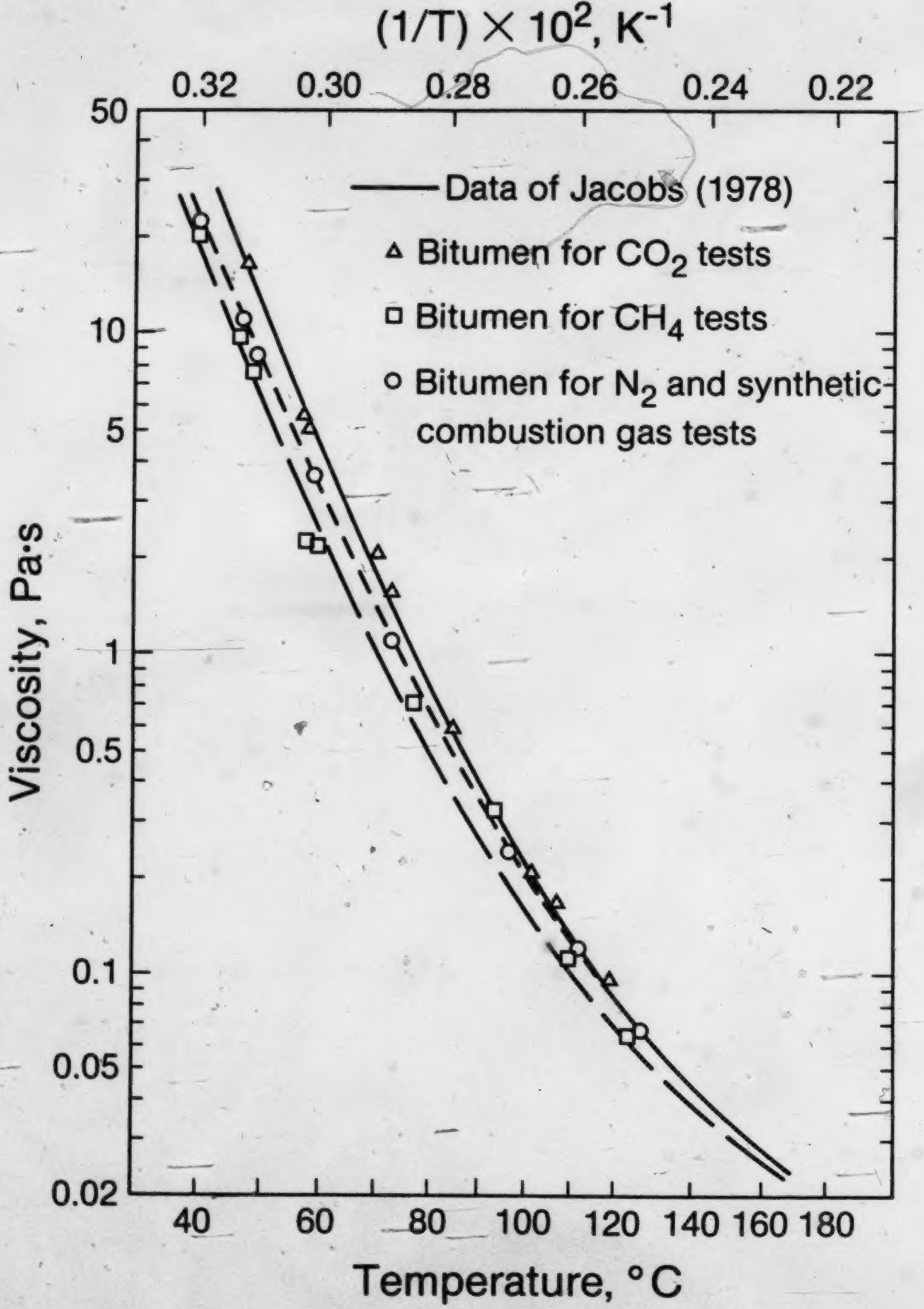

FIGURE 1.1 Viscosity-temperature data for bitumen samples (taken from Svrcek and Mehrotra (1982))

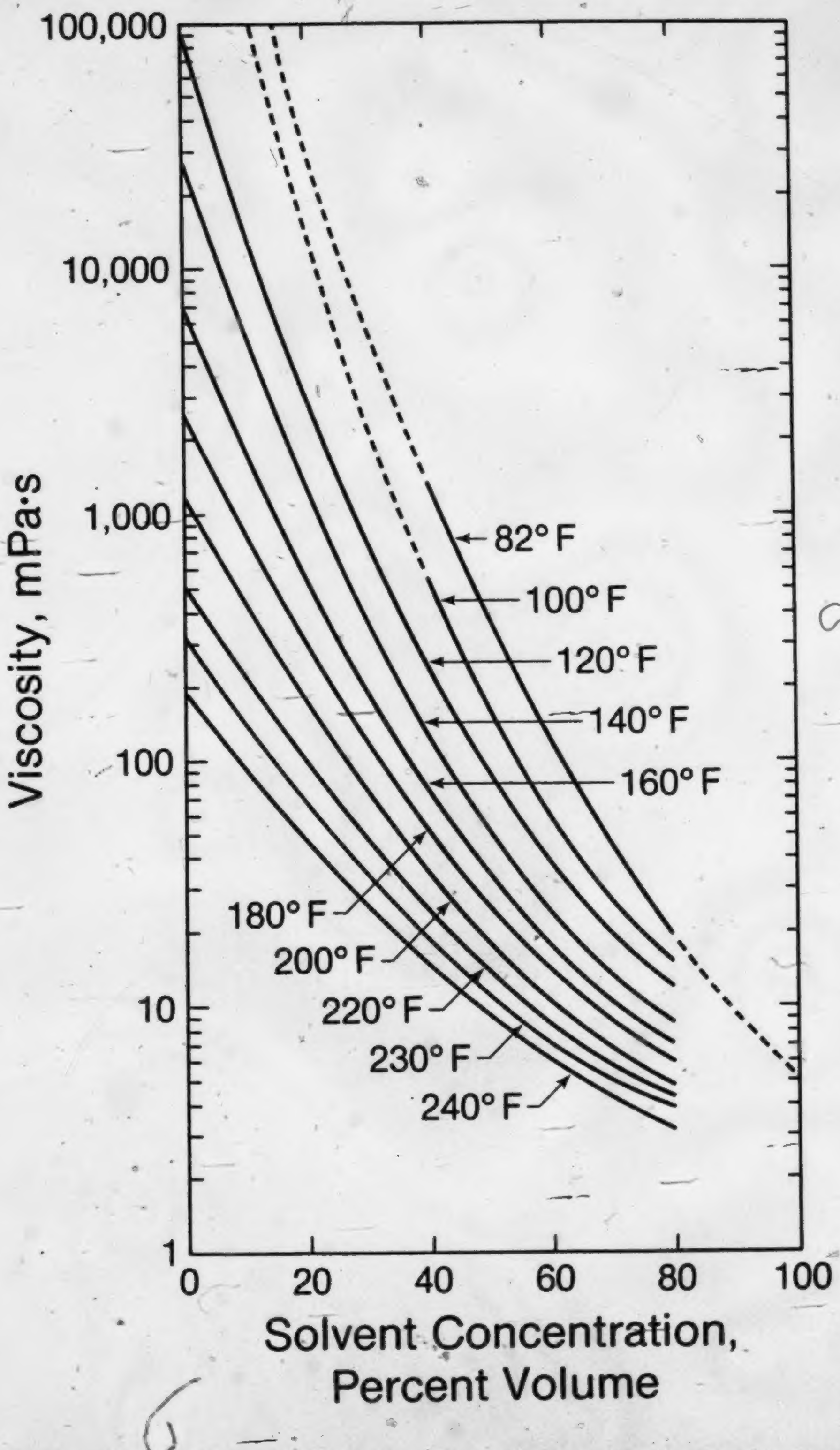

FIGURE 1.2 Viscosity as a function of concentration and temperature for Athabasca bitumen - Suncor synthetic crude mixtures (taken from Farouq Ali and Abad (1976))

1.3 Oil Expansion

Solubility of gases in bitumen and heavy oil was found to be dependent on pressure, temperature and crude composition. Mehrotra and Svrcek (1982, 1984, 1985) measured the effects of gases on density and viscosity of Peace River, Athabasca, and Marguerite Lake bitumen. In their findings, solubilities of gases, measured at several temperatures and pressures, increased in the following order: $N_2 < CO < CH_4 < CO_2 < C_2H_6$. Similarly the effects of dissolved gas on the live bitumen viscosity[1] also followed the above order. The volumetric solubility of CO_2 increased almost linearly up to a pressure of 6 MPa. Beyond this pressure, the rate of increase was smaller. Solubility of carbon dioxide in Athabasca bitumen as a function of pressure is shown in Figure 1.3. For carbon dioxide-saturated bitumen, the solubility increased with pressure and decreased with temperature. The density of saturated bitumen decreased with increasing temperature but pressure had no effect on the density. Miller and Jones (1984) studied the solubility of CO_2 and the swelling of heavy oils (15-17° API) experimentally. The PVT curves showed a sharp break at approximately the condensation pressure of carbon dioxide when it went from the gas to the liquid phase. Very little CO_2 went into solution after carbon dioxide was in the liquid phase.

Note that Svrcek and Mehrotra did not observe the sharp break that Miller and Jones reported, possibly because they worked at relatively low pressures.

1.4 Viscosity Reduction

A large viscosity reduction occurs in bitumen and heavy oils when they are saturated with certain gases at increasing pressure. The viscosities of dead and live Athabasca bitumen in contact with CO_2, CH_4 and N_2 were published by Jacobs *et al.*(1980).

The viscosity, density and gas solubility data for Athabasca bitumen saturated with CO_2, CH_4, and N_2 were published by Svrcek and Mehrotra (1982). Their experiments were carried out over a temperature range of 25-100°C and up to a pressure of 10 MPa. Figure 1.4

---

[1] bitumen saturated with gas

shows the viscosities of the CO_2-saturated bitumen at different pressures. At a similar pressure and temperature, saturation with CO_2 yielded a maximum reduction in bitumen viscosity. Again, Mehrotra and Svrcek (1982) reported the viscosity of Peace River bitumen saturated with different gases. The solubility of dissolved gases increased in the following order: $N_2 < CO < CH_4 < CO_2 < C_2H_6$. For all five gases, an increase in temperature and pressure resulted in a reduction in the live bitumen viscosity.

Raplee *et al.* (1984) screened a number of gases (H_2, N_2, CO_2, CO, CH_4, C_2H_6, C_3H_8, Freon 22) for the *in situ* steam processes for Alberta, Utah bitumen and Saskatchewan, and California heavy oils. Their oil reaction tests revealed no significant reactions between gas and resource oils. Based on solubilities, they chose CO_2 and C_3H_8 for the Alberta resources but did not obtain any additional recovery in the experiments limited to a one-dimensional physical model. Briggs *et al.* (1978) measured the viscosities of Cold Lake bitumen and Aberfeldy oil at subsaturation concentrations. Viscosity decreased linearly with concentration at a given temperature and pressure.

1.5 Diffusion of CO_2 into Bitumen and Heavy Oil

Carbon dioxide mixes with heavy oils by diffusion as well as by solution. If oil and CO_2 are in contact with an initially sharp interface, they will diffuse into each other. The sharp interface will become a diffuse mixed zone with time. This tendency for mass transfer to take place in such a way as to cause the concentrations to become uniform, in the absence of any convection within the system, is defined as molecular diffusion. Diffusion helps carbon dioxide to penetrate into heavy oil and may reduce viscous fingering. A need arises for accurate knowledge of the diffusion coefficient to determine the amount of oil contacted by gas; it enables the optimum soaking time to be determined.

Information available on the molecular diffusion coefficient of carbon dioxide into bitumen and oils is restricted to experiments performed at atmospheric pressure. For dense gases and liquids, molecular theory has not advanced enough to allow diffusion coefficients to

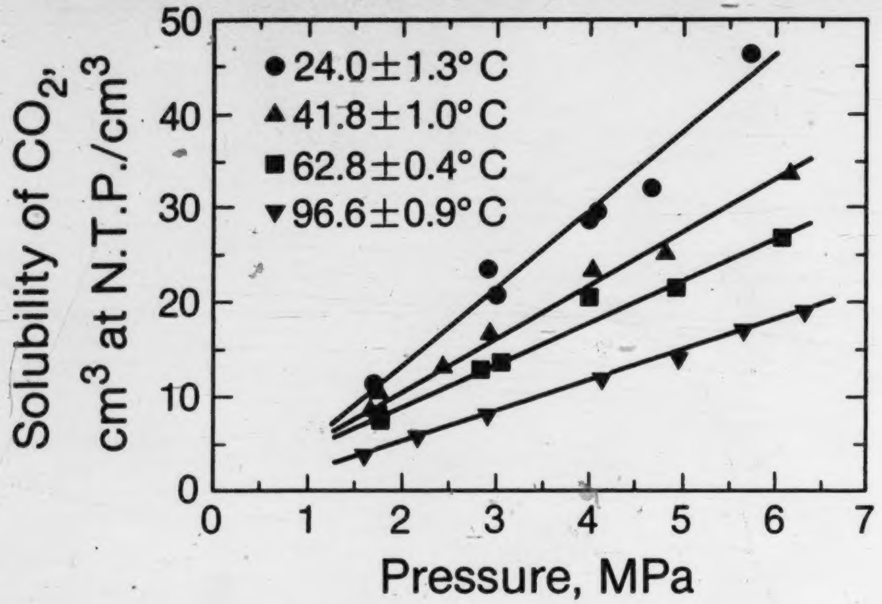

FIGURE 1.3 Volumetric solubility of CO_2 in bitumen (taken from Svrcek and Mehrotra (1982)).

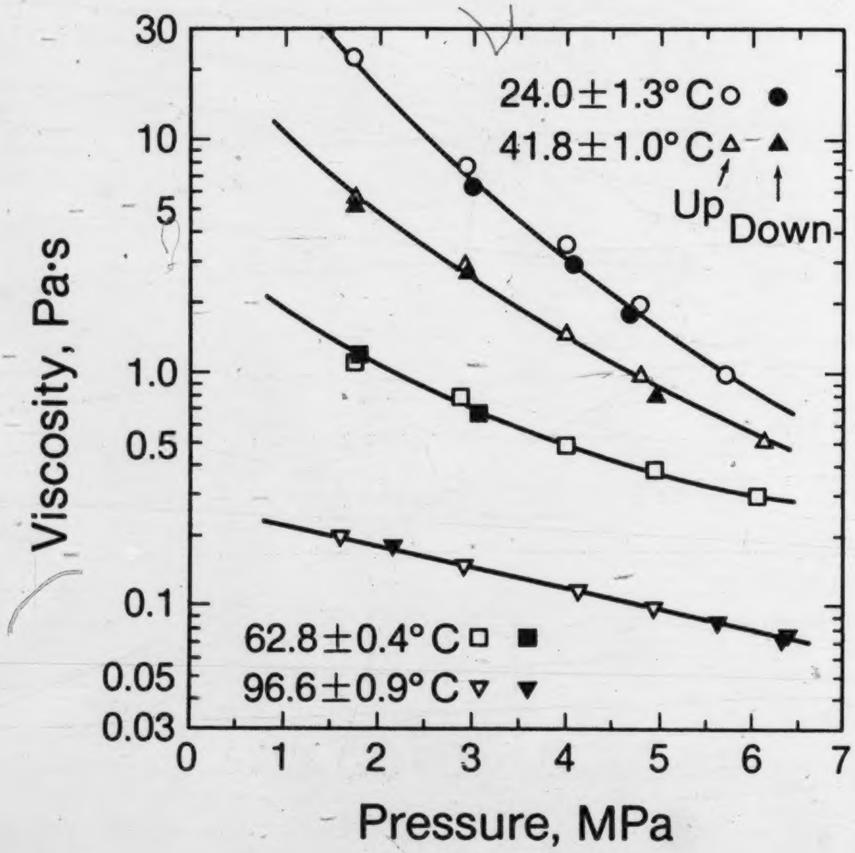

FIGURE 1.4 Viscosity-pressure isotherms for CO_2-saturated bitumen. (taken from Svreck and Mehrotra (1982)).

be calculated. Davies *et al.* (1967) reported the diffusion coefficients of carbon dioxide for a number of organic liquids and hydrocarbon mixtures. For a gas oil of 26.5 mPa.s viscosity, the diffusivity was 0.728 x 10^{-5} cm^2/s at 25° C and at atmospheric pressure. They suggested that the diffusion coefficient was a function of $\frac{1}{\sqrt{\mu_o}}$.

McManamey and Woollen (1973) proposed an equation in which the the diffusion coefficient was a function of $\mu^{-0.47}$. Schmidt *et al.* (1982) concluded that carbon dioxide diffusivity into bitumen is of the order of that observed in most liquid systems. They also indicated that the diffusivity was concentration dependent, increasing with higher concentration. More recently, Denoyelle and Bardon (1984) found that the diffusion coefficient of CO_2 increases with pressure. At 15 MPag, diffusion coefficients increased five-fold over those reported in the literature at atmospheric pressure. For example, they reported a diffusion coefficient of 4.6 x 10^{-5} cm^2/s at 15 MPag and 80° C for a 570 mPa.s viscosity oil.

It is interesting to note that both researchers, in spite of extreme viscosities, reported high values of diffusion coefficients. It should be pointed out, however, that the high values reported could have been affected by convection streams induced by density changes and pressure gradients at the beginning of the experiments, and by swelling or expansion of the oil by solution of CO_2 (Rojas, 1985).

1.6 Asphaltene Precipitation

One of the problems encountered in the bitumen recovery is the asphaltene precipitation which may cause plugging. Asphaltene precipitation causes reduction of flow, which gives rise to problems in wellbore equipment, flow lines and possibly reduces formation permeability.

Asphaltenes are polynucleic aromatic sheets containing about 15-25 rings, with various aliphatic and alieyetic residues on their perimeters. Asphaltene precipitation occurs when asphalt-based crude oils lose their ability to disperse colloidially the suspended solid particles.

Solvents and gases are known to cause precipitation under certain conditions; thus this phenomenon should be considered in a possible application of solvents.

Mitchell and Speight (1973) investigated precipitation of asphaltenes from Athabasca bitumen at room temperature by a number of solvents. Aromatics and cycloparaffins by precipitating little were found to be good solvents. Paraffins, especially low molecular weight ones, were found to precipitate asphaltenes up to 17 weight percent of the original bitumen. Later, Raplee *et al.* (1984) tested precipitation at elevated temperatures. It was indicated that asphaltene precipitation decreased with increasing temperature. For the Athabasca, Utah bitumen and California heavy oil, Suncor naphtha did not leave any precipitation at all. Graue and Zana (1981) studied the phase behaviour of CO_2/light oil systems. They observed a dark solid precipitate at carbon dioxide concentrations of 44% mol or higher. The solid precipitate was estimated to be 2-5 volume% of the original reservoir oil. Diaz (1978) observed that Suncor synthetic crude effectively reduced crude oil viscosity, and did not cause any asphaltene precipitation.

1.7 Surfactants as Steamflood Additives

Currie *et al.* (1980) evaluated the relative effectiveness of a number of surfactants crumble test for promoting the breakup of the oil sand matrix. The crumble test, expressed in terms of the cohesive strength of compressed oil sand pellets, was shown to be sensitive to surfactant type and concentration, pH, ionic strength, presence of counterions, temperature and oil sand composition. Heterogeneity of the sand pellets affected the results, depending on the source. Handy *et al.*(1980,1982) evaluated the thermal stabilities of several surfactants at elevated temperatures. The results they obtained were inconclusive. Isaacs, McCarthy and Smolek (1982) examined the use of surfactants as additives to steam-based processes. The authors reported that displacement experiments showed a substantial increase in bitumen recovery efficiency in the presence of surfactants for both hot water and steam injection.

Raplee *et al.* (1984, 1983) investigated the type of surfactants which could be used as steam additives in bitumen/ heavy oil recovery They performed a series of thermal stability, crumble and adsorption tests on various surfactants. Their criterion was based on the capability of the surfactant withstanding elevated temperatures in the presence of steam, its effectiveness in the mobilization of oil or bitumen from the oil sand matrix with the crumble test, and adsorption of surfactants by sands and clays. As a result of these experiments, the most effective surfactants were the alkyl aryl and alpha olefin sulfonates. Later hot water runs instead of steam in one-dimensional cores showed the greatest improvement in recovery with the high molecular weight anionic and alkyl benzene sulfonate surfactants.

Although it is agreed that the surfactants enhance the recovery when used as additives, a precise understanding of the enhancement mechanism is not established. In heavy oil/ oil sands, viscous forces are much more important than capillary forces. When the viscosity of oil is reduced by steam injection, the capillary forces play an increasingly important role. The surfactants, by reducing the interfacial tension, can increase the displacement efficiency.

1.8 Presence of Bottom Water

In many heavy oil/ oil sand formations a water sand occurs below the oil sand in communication with it. The water zone may be a transition zone, part of an aquifer, or a zone of high water saturation. The thickness and permeability of the water layer may vary considerably.

Several laboratory studies have been reported. Pursley (1974) used a scaled model to simulate a 0.5 ha pattern with 43 m sand, 15% of the thickness being water zone, and 100 Pa.s oil. Recovery was 36% with one pore volume of steam injection. Steam was found to override the oil and the water zone enhanced the injectivity. Ehrlich (1977), and Huygen and Lowry (1979) investigated the recovery of Wabasca bitumen in a laboratory scale model with bottom water present. The heated bitumen was found to be swept into the water zone by the condensate.

Use of low pressure scaled models for bottom water steamfloods has been reported by Stegemeier *et al.* (1980) and Prats (1977)). Prats reported results for Peace River conditions (200 Pa.s oil) with oil-to water zone thickness ratios of 2.0, 4, and 10. The operational strategy consisted of injecting steam into the water zone, pressurizing, and then blowing down to raise the temperature of the overlying oil zone. In each case of bottom water, a different operating scheme was found to be optimal.

Stegemeier *et al.* (1980) used low pressure vacuum models to simulate the Mt. Poso field, which has a water drive, and developed a successful operating strategy.

Islam and Farouq Ali (1985) investigated the effects of bottom water in laboratory models. For light and medium viscosity oils, the water zone was found to be detrimental to most recovery processes.

1.9 Leaching Phenomena

There have been a number of studies concerning leaching in porous media in recent years. Although the minerals sought are other than oil and gas, the underlying reservoir dynamics are similar. The term leaching, also called solution mining, refers to the leaching of minerals in situ by circulation of the solvent over and through the ore body (Treyball (1980)). Similarly the solvent dissolves the interstitial bitumen in an oil sand matrix.

Bommer and Schechter (1979) made use of the streamline method for computer simulation. Later, Schechter and Bommer (1982) studied the optimization of uranium leach mining . They found that the reaction rates of the competing minerals should be taken into account. The reaction rates are controlled by the Damkohler number and there is a minimum distance between injection and production wells to utilize oxidant most advantageously.

Hekim and Fogler (1980) studied the different rates of dissolution for minerals in porous media. They developed a mathematical model describing the movement of multiple reaction zones and the depletion of the reactive fluid in porous cores. Wang *et al.* (1981) and

Kabir *et al.* (1982) presented various aspects of in situ uranium leaching using the streamline models.

Oguztoreli (1984) treated solvent leaching of the oil sands by developing a two dimensional mathematical model using finite difference techniques. He used three dimensionless groups controlling the leaching. The dissolution of bitumen is governed by the Damkohler number and solvent capacity numbers.

Kabir *et al.* (1985) presented a new scaling method for modeling in situ leaching of uranium. They simplified a 2-D problem to a bundle of 1-D problems. When dispersion is neglected, the bundle of 1-D problems is further reduced to a single 1-D problem. The 1-D calculation accommodates chemical-rock interactions and the streamline model accounts for areal sweep. The agreement between the results of the scaling model and the numerical model was excellent.

2. STATEMENT OF THE PROBLEM

Current enhanced recovery techniques for bitumen and heavy oil are impeded by virtually immobile oil in the reservoir and lack of interwell communication. Recovery from oil sands is also limited by the low injectivity associated with the displacement of highly viscous bitumen. This research, in general, is aimed at improving fluid mobility ahead of a cold oil front by various experimental methods. The objectives are to investigate the following:

1. The effectiveness of solvents in mobilizing bitumen and heavy oil in a linear laboratory model.

2. The recovery efficiency of oil by solvent and surfactant additives, for
    i) continuous injection of solvent at constant rate.
    ii) injection of slugs followed by surfactant solution at a constant rate.

3. The use of subcritical carbon dioxide to increase mobility ahead of a heavy oil bank.

4. The utilization of the bottom water layer for transporting the displaced fluids and increasing injectivity in a rectangular model.

5. The comparison of numerical simulation results with experimental results.

6. The prediction of the effluent concentrations at the production end using the leaching theory.

3. EXPERIMENTAL APPARATUS AND PROCEDURE

The three physical models used in this work are described in this chapter along with the respective packing procedures. Fluid properties, injection system and data analysis are also discussed under the appropriate headings.

3.1 Linear Sand Pack

The basic structural element of the model is a 122 cm long and 6.25 cm in diameter cylindrical core. The maximum working pressure is 10.3 MPa. In addition to the core, the apparatus consists of

1. A Milroyal pump to inject water and solvent at constant rates
2. Two back pressure regulators
3. Single stage separation system
4. A heater for hot water injection
5. Carbon dioxide supply.

The separator is used to separate gas production from fluid recovery. The heater is used when hot water is required during the runs as well as mobilizing the heavy oil in saturating the core.

3.1.1 Packing the Core

The linear cylindrical cores were packed with the oil sand by crushing fresh sand with an air gun. Each time about 200 grams of sand were taken out of the closed container, weighed, and placed in the core. Then an air gun with a steel rod was used to crush the sand manually. Although packing the core was time consuming, it assured that the packing was tight and the density of the oil sand was close to the field values. After packing, the core was tightly closed and connected to a vacuum pump. It was then saturated by imbibition of distilled water.

3.2 Rectangular Model

The model is made up of a tubular aluminum block, which is capable of withstanding pressures up to 4200 kPa. The inside dimensions of the core are 60.5 cm length, 6.25 cm depth, and 3.75 cm width. The depth was chosen to be deep enough so that two different layers could be packed. A picture of the model is shown in Plate 1.

The model has one inlet and one outlet at the middle of the inlet/outlet faces. These are used to pack glass beads and measure the absolute permeability. The injection and production wells are located at 1.5 cm from each end of the core. The wells are 0.635 cm in diameter and are perforated and fitted with porous metal caps at the ends. The porous caps are fitted in the wells in order to prevent any flow of glass beads and sand particles. There are also four more wells located along the core for effluent sampling during the runs. A schematic of the apparatus is given in Figure 3.1

In order to pack the oil sand and include a bottom water layer, the core had a lid along the bottom side. For packing purposes, the core was rotated along the ends to pack the oil sand first and the bottom water glass beads later.

3.2.1 Packing the Model

Before the model was packed, the oil sand was prepared in an attempt to obtain uniform compaction. In order to do so, the sand was sorted to remove any foreign material and finely divided and mashed. After this lengthy process, the sand was spread inside the model in small amounts and was tightly packed after each addition so as to obtain a homogeneous pack. This packing of the model was done manually, taking about six hours. The whole process was repeated for each run.

The glass beads (80-120 mesh) as received from the supplier were used for the heavy oil runs. The wet packing technique was used to obtain packs with consistent properties. The core holder was suspended in a vertical position and filled with distilled water up to a few cm in height. The glass beads were dropped into the core holder thorough the open end while a

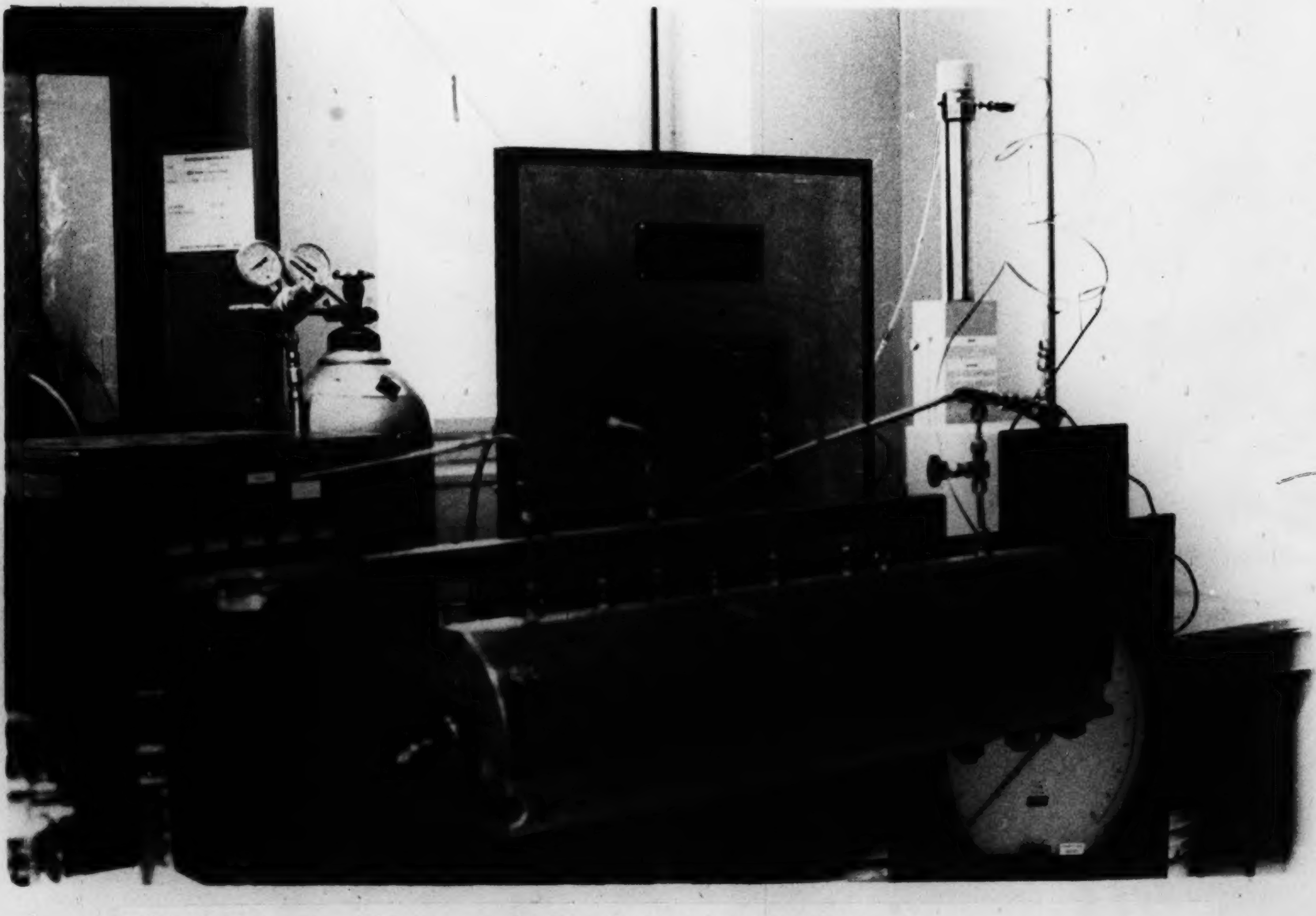

Plate 1 Rectangular High Pressure Model and Fluid and Gas Injection System

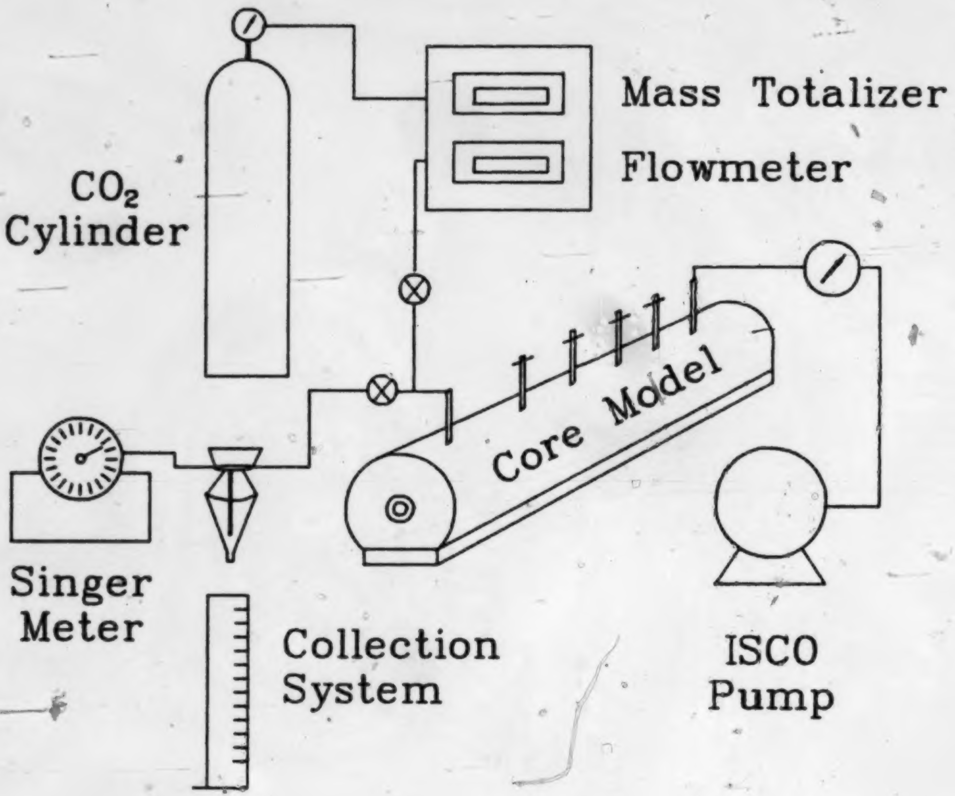
Mass Totalizer
Flowmeter
CO_2 Cylinder
Core Model
Singer Meter
Collection System
ISCO Pump

Figure 3.1 Rectangular Model and Fluid Injection System

constant water head was maintained on top of the beads. Following packing, the model was saturated by imbibition of distilled water into the sand which had been under vacuum. To saturate the core, it was connected to a beaker containing a known volume of distilled water greater than the previously estimated pore volume of the pack. After the glass beads in the core had imbibed distilled water, the inlet was connected to the ISCO pump and water was pumped through the core at a flow rate of about 150 ml/h. When the flow stabilized, the pressure drop along the length of the core was recorded for that particular flow rate in order to calculate the absolute permeability of the core. Since the oil was very viscous, the pumps were not able to inject into the core efficiently. A steel cylinder of four liters was filled to three quarters capacity with heavy oil. Nitrogen gas from a high pressure cylinder was employed to push the oil from the top of the cylinder. The oil under high pressure was then able to move from the bottom of the cylinder to the core. Heating straps were wrapped around the cylinder to warm the oil. It took a full day to saturate the core with oil to the irreducible water saturation (WOR of 100).

3.3 Visual Model

A picture and schematic of the system is shown in Plate 2 and Figure 3.2. The model consists of a 33 cm x 33 cm x 2.5 cm thick Plexiglass sheet, upon which was glued another sheet of the same size, with a 30.5 cm x 30.5 cm x 2.5 cm square cut out inside it. Figure 3.3 illustrates a schematic of the model. This space was packed with the Athabasca oil sand, finely divided, leveled and covered with a 0.16 cm thick rubber sheet which served as the pressurizing diaphragm. This was covered with another 33 cm x 33 cm x 2.5 cm Plexiglass sheet with a 0.32 cm fitting. The complete model was held tightly together by a number of bolts which were placed 2.5 cm apart each. The bottom Plexiglass sheet hole was connected to an air cylinder in order to pressurize the rubber diaphragm and thus insure that the oil sand was tightly packed against the top Plexiglass sheet to avoid any channeling. The top plate was provided with a port at each corner to serve as wells. In a typical run, one pair of diagonally

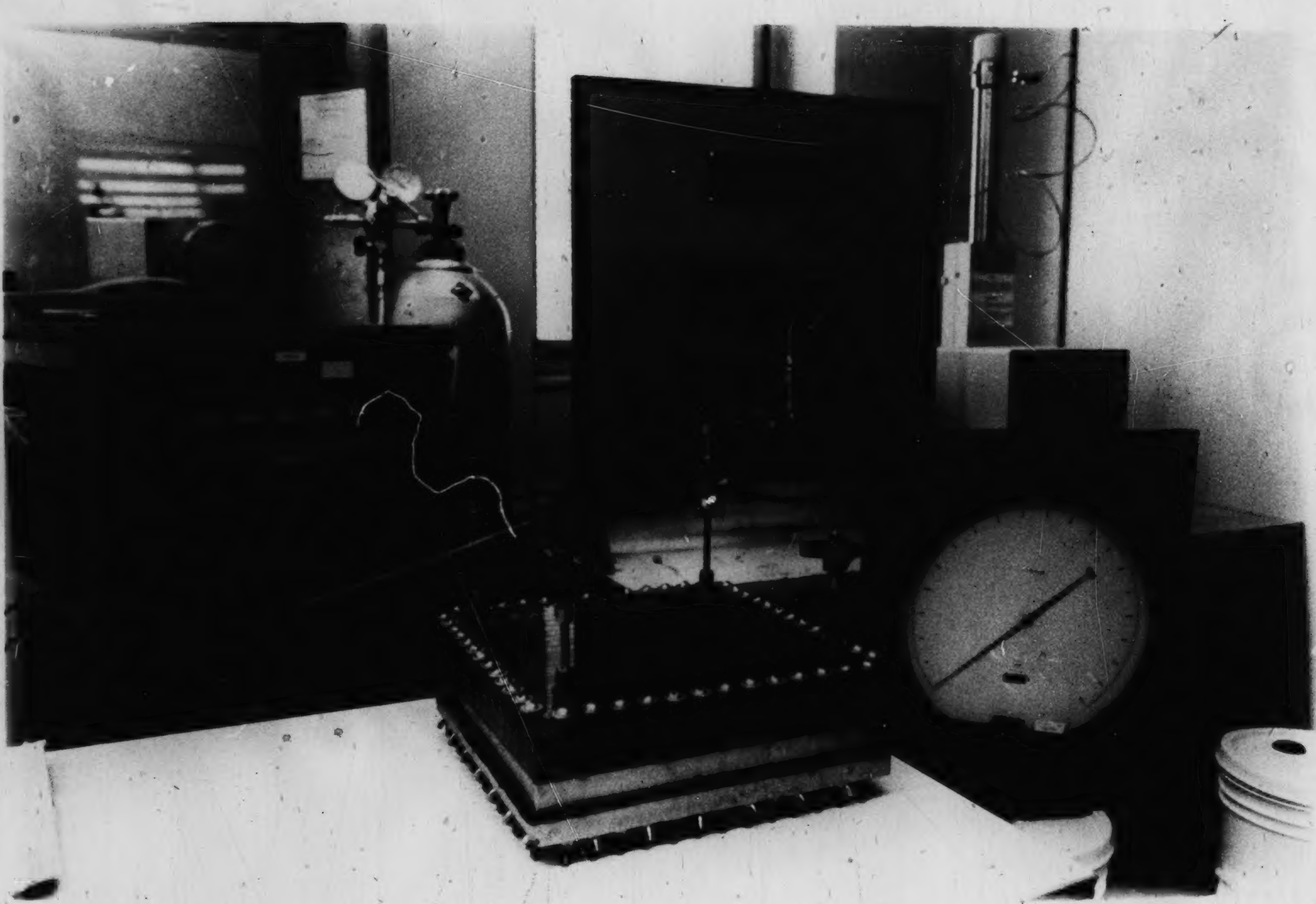

Plate 2 Visual Model and Fluid Injection System

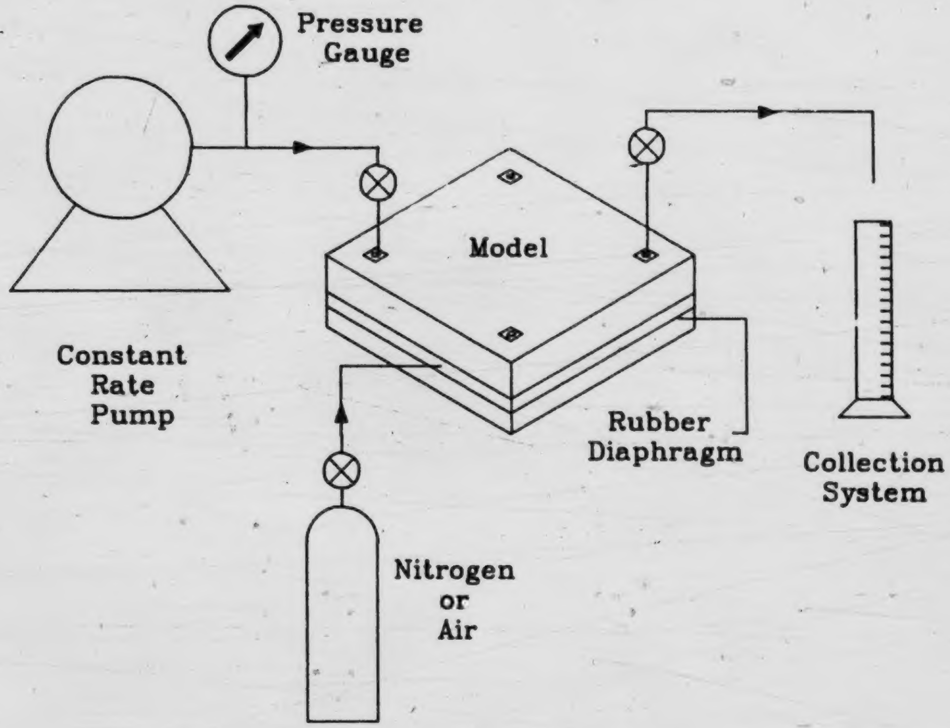
Pressure
Gauge
Constant
Rate
Pump
Model
Rubber
Diaphragm
Collection
System
Nitrogen
or
Air

Figure 3.2 EXPERIMENTAL SET UP FOR VISUAL MODEL

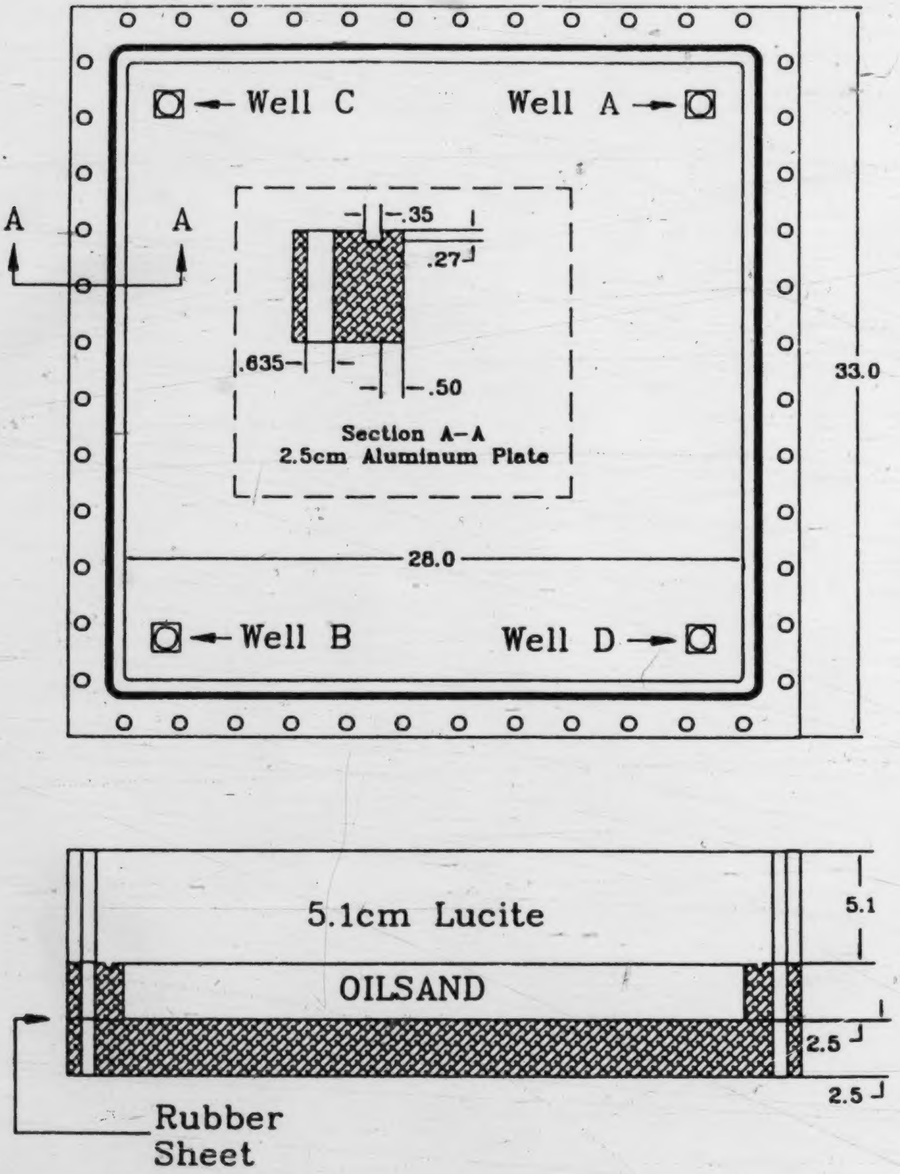
Well C
Well A
Well B
Well D
A
A
.35
.27
.635
.50
Section A-A
2.5cm Aluminum Plate
28.0
33.0
5.1cm Lucite
OILSAND
5.1
2.5
2.5
Rubber Sheet

Figure 3.3 SCHEMATIC OF VISUAL MODEL

opposed holes were closed while the other two were kept open to represent the injection and production wells, in 1/4 of a five-spot pattern.

A constant rate pump was used to inject the fluids at any desired constant rate. The injection pressure was measured by means of a pressure gauge connected between the pump and the model. The wells were perforated with small holes at the ends to assure sand-free bitumen production. It should be pointed out that the smaller holes used in the early runs caused high injection pressures. The holes used later were 0.10 cm in diameter.

The production well in the model was connected to a 0.32 cm well tubing. A sample collector and a timer were used for collecting the effluent produced in each run.

3.4 Fluid Properties

The oil sands were obtained from the Suncor corporation's open mining site at Fort McMurray. High grade oil sand, as obtained in a container, was kept closed and frozen until it was used. Each time it was packed, the bitumen and water content were determined by solvent extraction. The bitumen content varied between 14.2% and 17.5% while the water content varied between 1% and 2%

The surfactant used was an alkyl benzene sulfonate. The surfactant, under the trade name of Stepanflo 80, was obtained from the Stepan Chemical Corporation. It had active components of 56.3% and was used as received.

The Suncor synthetic crude used as solvent obtained from the same company as it is a product of bitumen. The properties of the solvent are given in Table 3.1.

Table 3.1. Physical Properties of Suncor Synthetic Crude

Density g/ml	Specific Gravity	Colour	Viscosity mPa.s	Solubility in bitumen
0.827	0.829	Dark Yellow	4.56	All Proportions

3.5 Density of Sand

A random sample of oil sand was placed in a graduated cylinder. It was then extracted with a solvent until it was clean and there was no trace of bitumen in the sample. The clean sand was dried in an oven or left outside for a long time, and weighed by using an electronic balance. Next, a specific volume of solvent was added to the sand contained in the graduated cylinder and the total volume was recorded. Knowing the total volume and the volume of the solvent, the sand volume was calculated.

The density of the oil sand was then calculated by dividing the weight of the sand by its volume. A value of 2.65 g/ml was determined and used in this work.

3.6 Density of Bitumen

As above, a known volume of toluene was added to a sample of tar sand of known weight. By subtracting the solvent volume from the total volume, the oil sand volume was determined. Following extraction by toluene, the dried sand sample was weighed. Then, the bitumen weight was calculated. Obtaining the sand volume as above, the bitumen volume was the difference of the oil sand volume and the sand volume. By dividing the weight by volume, the density of bitumen was calculated. A value of 1.037 g/ml was found and used in this experimental work.

3.7 Bitumen Content

The bitumen content of oil sand changes somewhat with time due to exposure to air. Therefore, it was decided to determine the bitumen content of oil sand for each run individually.

A sample of oil sand was placed in a container and weighed. By subtracting the weight of the container from the weight of the sample and container, the weight of oil sand was determined.

Extracting and drying the sample, the weight of the oil sand was calculated by subtracting the weight of the clean sand from the weight of the original sand.

The bitumen content was then calculated by dividing the weight of bitumen by the original oil sample weight. The values of bitumen content by weight ranged from 14.2 to 17.5% by weight.

3.8 Bitumen in Place

The bitumen in place for each run was determined by multiplying the bitumen content (by weight) by the weight of the oil sand packed into the model. In order to obtain the volume of bitumen in place, the weight of bitumen was divided by the density of the bitumen previously calculated.

3.8.1 Void Space

The void space in the pack was determined by subtracting the volume of pure sand and the volume of bitumen in place from the inside volume of the model.

3.9 Density Measurements

The density measurements were needed for the fluids and the effluent samples taken throughout the experiments. When a surfactant was present in a bitumen-solvent mixture, the absorbance readings from the spectrophotometer were not able to give any useful readings. Thus the effluent concentrations were determined from the effluent density measurements. A high precision density meter, DMA 60 by PAAR, was used in the measurements. A brief explanation of the procedure used is given in the following paragraph.

After a sufficient time for temperature equilibration, the period T is read for the sample tube filled with air. Then, about 1 ml of distilled water is introduced by means of a syringe into the lower entrance port of the sample tube. It is ensured that the introduction of water or any other liquid takes place slowly enough to enable the liquid to properly wet the walls of the sample tube. The period, T, is again read from the digital screen after the desired temperature reading is obtained. At the end of each measurement procedure the water or effluent is drawn back into the syringe and the sample cell is briefly flushed with acetone or a similar solvent. The sample cell is dried with the air hose from the built-in air pump. Next the period, T, of the sample is recorded by repeating the above procedure. With three T values the density of the sample can be obtained as follows

$$e_s = e_1 + ((T_s^2 - T_1^2) \, . \, K)$$

where

$$K = \frac{e_1 - e_2}{T^2_1 - T^2_2}$$

e = density in g/ml

where subscripts 1 and 2 are assigned for water and air, respectively. Density of the air, e_1, is obtained from the following formula

$$e_{air} = \frac{0.001293}{1 + 0.00367\,t} \cdot \frac{H}{76}$$

where t = temp in °C

H = pressure in cm Hg

the density of water at different temperatures is obtained from the tables provided with the instrument.

3.10 Specific Gravity of Bitumen

The specific gravity of bitumen was determined at room temperature following the procedure outlined in the "Standard Methods for testing Petroleum and its products." ASTM Designation 59/49.

The specific gravity of the bitumen is given by the formula:

$$SG = \frac{W_{ps} - W_{p})}{(W_{w} - W_{psw} + W_{ps})}$$

where

W_p = weight of pyconometer

W_{ps} = weight of pyconometer and bitumen

W_p = water equivalent

W_{psw} = weight of pycnometer, bitumen, and water.

W_w = weight of water

The value obtained was 1.034 which agrees with values reported in previous studies.

3.11 Pore Volume and Porosity

The weight of the sand packed in the model was calculated by subtracting the weight of the model from the model plus packed sand. The weight of the bitumen was then calculated by multiplying the weight of the sand with the saturation (wt%) of the oil in the sample and the volume of bitumen was obtained by dividing the weight of bitumen by its density.

The weight of the pure sand was obtained by subtracting the weight of the bitumen from the weight of the packed sand; and the volume was equal to the weight of pure sand divided by its density.

The pore volume was calculated then as the sum of the volume of the bitumen in place and the void space in the pack. The porosity was obtained by dividing the pore volume by the inside volume of the model.

3.12 Analysis of Effluent Samples

The analysis of the effluent samples was done by means of a Perkins-Elmer infrared spectrophotometer. First a calibration graph was prepared. The Suncor synthetic crude and Fort McMurray bitumen were mixed in different volumetric proportions. To ensure thorough mixing, samples were stirred for about thirty minutes. The mixtures were analyzed over the wavelength range of 2.5 microns to 16.6 microns. A wavelength with a distinct peak was chosen. It was observed to be 6.21 microns.

The absorbances of the samples for different bitumen proportions are shown in Figure 3.4. The absorbances of the mixtures were scanned at the range of the peak and the absorbance values at 1607 cm^{-1} were read from the spectrophotometer. As seen in Figure 3.4, the pure bitumen has the highest absorbance while the pure solvent has the lowest absorbance.

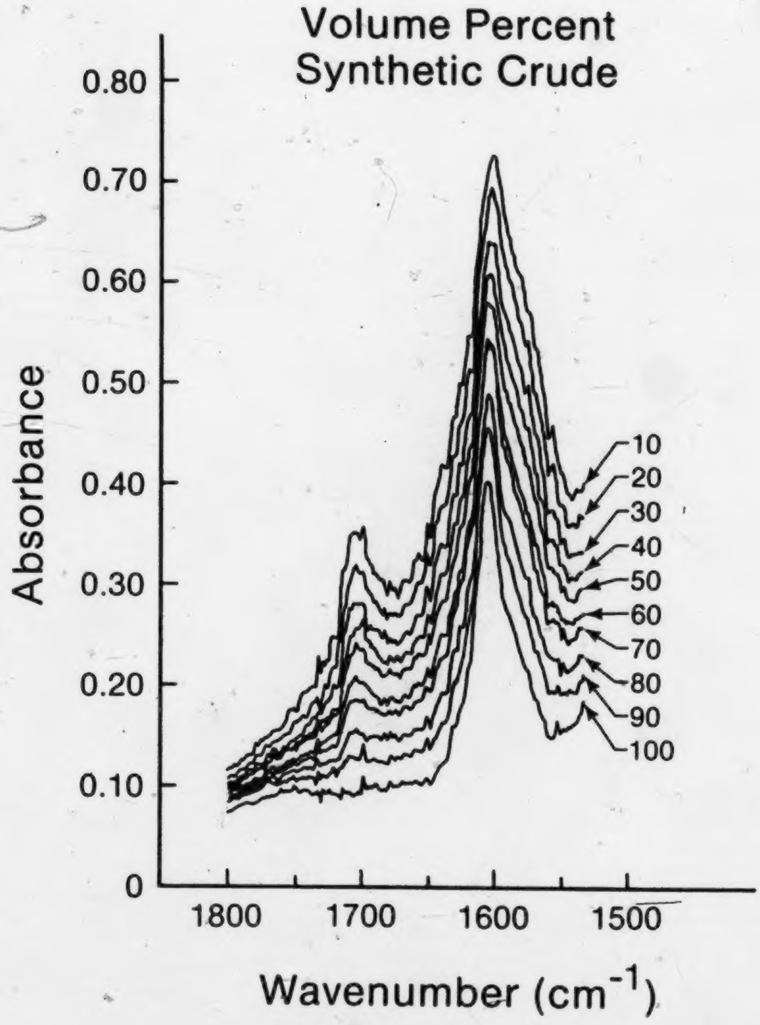

Figure 3.4 Absorption Spectra for Synthetic Crude-Bitumen Mixtures.

In order to analyze the produced effluent, a small sample was introduced into a special cell by means of a plastic syringe. The sample was then scanned in the 1900 to 1500 cm^{-1} range and the absorbance value at the peak was recorded. This value was then converted into volumetric and weight concentrations using the calibration curve in Figure 3.4

In carbon dioxide displacement runs, the effluent from the model was separated in a glass separator operating at atmospheric pressure. The top of the separator was connected to a dry test meter(DTM) to measure the amount of gas produced. Liquids from the separator were collected in graduated cylinders.

3.13 Volume of Carbon Dioxide

The amount of CO_2 injected was measured by means of a mass flow meter and a totalizer. A Matheson model 8250 mass flowmeter for CO_2 gas was used in conjunction with a Matheson Model 8122B totalizer. With this combination the totalizer was able to record the quantity of gas that had flowed over a period of time. The flowmeter has a full scale flow rate of 3.5 standard liters per minute. It can be set to any fraction of the full scale. The totalizer is also programmed for a desired count rate through the switch at the back of the device.

In order to calculate the volume of the carbon dioxide at the system pressure and core temperature, the Starling (1973) equation of state for CO_2 was used to calculate the moles of

CO_2 injected and produced. This equation of state has the following general form.

$$P = \rho RT + \left(B_0RT - A_0 - \frac{C_0}{T^2} + \frac{D_0}{T^3} - \frac{E_0}{T^4} \right) \rho^2$$

$$+ \left(b\rho R - a - \frac{d}{T} \right)\rho^3 + \alpha \left(a + \frac{d}{T}\right) \rho^6$$

$$+ \frac{c\rho^3}{T^2} (1 + \gamma\rho^2) \exp(\gamma\rho^2)$$

A set of constants in SI units were used in the equation. For P in MPa, T in °K and ρ in kg-mol/m^3 the following constants apply:

$B_0 = 0.024588$ $A_0 = 0.176976$ $C_0 = 2.45187E04$

$D_0 = 188.3481E04$ $E_0 = 2.61156E04$ $b = 0.003781$

$a = 0.009434$ $d = 0.055761$ $\alpha = 0.961229E-04$

$c = 1419.7888$ $\gamma = 0.006421$ $R = 0.008314$

A trial and error procedure with an accelaration approach was used in a program to determine the molar density of CO_2 using the above equation. This equation predicts experimental density data with an average uncertainty of 1.0% by Starling's own assessment.

3.14 Fluid Injection System

A constant rate Milroyal pump was used for the first three runs. The Isco LC-5000 pump was then used for the remainder of the runs. It is a syringe pump with a 500 ml capacity, flow rate range of 0.1 ml/h to 400 ml/h, and 25.5 MPa rating. The pump operates in a constant flow mode and has a digital display of pressure in psi or MPa. The syringe barrel and piston are made of 304 stainless steel. It is designed for applications requiring precise, pulse free delivery of liquids. It has a flow rate accuracy of 1% of range. The pump has a maximum refill rate of 100 ml/min. Since it had to be refilled at least once for every run, each run had interruptions of 5 to 10 minutes. The pump barrel was connected to the injection well through flexible steel tubing. At the entrance of the core, a Heise pressure gauge was connected for pressure measurements.

Commercial grade carbon dioxide (99.5% purity) from a high pressure cylinder was used in the experiments. The volume of the gas out of the cylinder was measured, as explained in the previous section.

4. DISCUSSION OF EXPERIMENTAL RESULTS

The contents of this chapter are the results and discussion of the experimental runs performed in the physical models. A total of 22 experimental runs were performed in the three models. A summary table of these runs is given in Table 4.1. Appendix B gives the respective figures of Runs 4 through 22. Finally, the history of the runs are tabulated in Appendix C. For two of the runs, heavy oil was used to saturate the core packs and for the remaining runs oil sand was used to pack the cores. The problems addressed are however common in both cases.

Three linear core experiments, which were qualitative and exploratory in nature, led to the design of later experiments in the rectangular cross-section core. The runs in the rectangular model are discussed according to distinctive aspects of each and they are not necessarily in chronological order. Finally, two visual model experiments are presented when discussing the flow patterns.

4.1 Results of Linear Pack Runs

Runs 1, 2 and 3 were conducted in the linear cores packed with heavy oil/bitumen. A combination of carbon dioxide, synthetic crude and hot water were employed in an attempt to mobilize the oil under cold or low heat conditions. These runs essentially consisted of injecting a slug of solvent followed by water with slight variations.

Run 1: Carbon Dioxide & Solvent Stimulation

This run was performed to mobilize the bitumen with small slugs of carbon dioxide and synthetic crude. A slug of gas and 36% HCPV solvent injection was followed by hot water injection.

A core 122 cm in length and 6.25 cm ID was packed with the Athabasca oil sand. The oil sand density in the pack was 1.81 g/ml, close to that found in the field, and the bitumen content was 15.7 percent by weight. By carbon dioxide injection, it was intended to decrease

TABLE 4.1 Results of Experimental Runs

Run No.	Core Type	Run Type	h_b/h_w	PV (ml)	Porosity (%)	Permeability (darcies)	S_o	Solvent Slug (% HCPV)	Surfactant (%)	CO_2 (% HCPV)	Recovery (%IBIP)
1.*	Linear	Bitumen	--	1224.6	33.9	1.1	81.6	36.	-	Yes	10.
2.*	Linear	Bitumen	--	1130.5	31.3	1.0	92.1	10.	-	-	Nil
3.*	Linear	Heavy Oil	--	1372.6	38.0	22.8	90.9	46.	-	-	[illegible]
4.[1]	Rect.	Bitumen	1.5	319.6	34.5	2.6	87.7	20.	-	-	2.1
5.	Rect.	Bitumen	5.25	459.7	38.9	1.8	87.1	20.	-	-	2.0
6.[2]	Rect.	Bitumen	--	569.8	40.5	1.1	76.7	10.	-	-	1.8
7.[3]	Rect.	Bitumen	5.25	463.7	39.2	1.9	89.6	20.	5.0	-	14.8
8.[4]	Rect.	Bitumen	5.25	426.7	36.1	1.9	89.9	20.	1.	-	7.6
9.	Rect.	Bitumen	5.25	428.0	36.2	2.4	86.9	361.	-	-	80.0
10.	Rect.	Bitumen	5.25	423.4	35.8	2.5	92.7	376.	-	-	82.0
11.	Rect.	Bitumen	5.25	440.7	37.3	2.4	87.1	104.	1.0	-	68.2
12.	Rect.	Bitumen	6.0	460.3	38.1	2.6	83.0	--	1.0	5.0	Nil
13.	Rect.	Bitumen	7.0	410.2	38.2	1.6	82.1	35.0	--	-	Nil
14.	Visual	Bitumen	--	870.6	41.1	2.7	80.1	20.	--	-	4.1

CONTINUED

15.	Visual	Bitumen	--	841.6	42.9	2.8	78.4	55.	--	--	23.8
16.	Rect.	Bitumen	5.25	422.6	35.8	1.9	91.0	217.	--	--	23.8
17.	Rect.	Bitumen	5.25	429.7	36.4	58.4	89.1	317.	--	50.0	25.1
18.	Rect.	Bitumen	5.25	396.0	33.6	1.9	87.9	100.	--	45.0	51.
19.	Rect.	Bitumen	--	510.0	34.3	0.45	90.1	197.	1.0	40.	56.8
20.	Rect.	Bitumen	5.25	495.0	35.5	1.09	83.5	18.		--	Nil
21.	Rect.	Bitumen	--.	501.9	35.7	0.56	90.2	331.	--	--	41.8
22.	Rect.	Heavy Oil	5.25	436	36.1	16.1	88.7	--	1.0	32.0	Nil

* Only in these runs the solvent + water were injected with the Milroyal pump. In the rest, the fluids were injected with the constant flow rate pump.

[1] Solvent + water injection

[2] Water + solvent slug + water Injection

[3] Surfactant + solvent + surfactant injection

[4] Solvent + surfactant injection

the viscosity of the bitumen. Carbon dioxide was injected into the core until the pressure reached 3.5 MPa. At this stage, the amount of gas injected could not be measured without proper instruments. Next, synthetic crude was injected into the core until it broke through at the outlet. Hot water injection at 60° C followed the synthetic crude. It had to be stopped when the injection pressure exceeded 10 MPa, which was the maximum pumping pressure. At 60% HCPV injected, the recovery was 10% of the bitumen in place. The injection rate was was set to 95 ml/h; however, it was observed to decrease under high pressure. The copper lid, which was used as a production well, was observed to contain clay particles. These fine particles might have blocked the pore space causing injectivity problems.

Run 2: Solvent Stimulation

This run was conducted to overcome the low injectivity encountered in Run 1 by not employing carbon dioxide and using a smaller slug of solvent preceding hot water injection. The carbon dioxide injection along with solvent was believed to cause the swelling of the bitumen and thus the blocking of the flow channels.

A solvent slug of 10% HCPV was chosen for injection prior to hot water. As in the previous run, hot water injection resulted in a rapid increase of the injection pressure to 10 MPa, when it had to be curtailed. After about two hours, injection was resumed, but the high pressure again led to the stopping of injection. No fluid was produced in both attempts. Temperature of the water arriving at the injection port was 80° C but the effect of hot water was only felt around the injection well. While a considerable heat loss occurred near the inlet, it could be concluded that the water was not able to move much further than the inlet. The analysis of the sand pack after the run showed that the solvent and water injected concentrated around the injection well. In this run, the oil sand density of 1.95 g/ml in the core was higher than that of the previous run; tighter packing may have been the cause of the plugging.

Run 3: Solvent Stimulation in Heavy Oil

This run involved injection of solvent and then hot water injection in a heavy oil packed core. It was undertaken to see if there was any mobility improvement with the use of less viscous oil pack.

A heavy oil with a viscosity of approximately 50,000 mPa.s was wet packed with glass beads of 80-120 mesh in a 122 cm long core. Since the oil was too viscous to inject with a pump, it was heated in a closed cylinder and driven by nitrogen gas in order to saturate the core. Solvent, synthetic crude, was first injected, until the solvent-oil ratio became about 5. Then, hot water at 50° C was injected, until the WOR became 20. The injection rate was set to 100 ml/h but the observed rate varied with increasing pressure. The oil recovery was 17% of initial oil in-place.

The three runs above show that it is difficult to mobilize the bitumen or heavy oil with a limited amount of solvent and transport it in the absence of a suitable path. Oil mobilized by solvent could not move through the cold zone, even at the maximum pumping pressure.

4.2 Bottom Water Runs in the Rectangular Model

Solvents, viz. synthetic crude, naphtha or a gas, carbon dioxide, can mobilize the heavy oil by way of viscosity reduction, solution and diffusion. When a solvent contacts bitumen of several million mPa.s viscosity, which is virtually immobile, a miscible displacement does not take place immediately. The oil sand matrix absorbs the solvent to a certain critical concentration and the bitumen swells to a degree. Once the critical concentration is reached, the bitumen is dissolved. The solvent-bitumen mixture can then be displaced by a solvent or another displacing agent. Since this process involves the solution of one of the constituents of a solid mixture, it may be treated as a leaching problem.

In Runs 1 through 3, it seemed that the solvent dissolved the bitumen locally around the injection point but the bitumen-solvent mixture was not able to move through the solid zone ahead under the applied pressure gradients.

Many heavy oil formations in Alberta and Saskatchewan are characterized by a water saturated sand located directly below the oil zone, and it usually has communication with it. The water zone may be merely a high saturation zone, or a transition zone. In the context of this research, "bottom water" refers to a zone of silica sand or glass beads having a water saturation of 100%.

In any oil recovery process, the presence of bottom water is likely to have an inhibiting effect on oil recovery. The injected fluid will tend to channel into the low resistance water sand. The magnitude of such channeling will depend on the oil viscosity, relative water zone thickness, injection rate, oil saturation in the water zone, if any, and vertical permeability. Although a bottom water zone is undesirable, it may serve the purpose of providing initial injectivity in very viscous oil formations.

Kasraie and Farouq Ali (1984) reviewed the field case histories of thermal recovery methods in the presence of bottom water. The authors concluded that a water leg thicker than about one-fifth the oil zone thickness could make the cyclic steam stimulation uneconomical. One commercially successful field project they cited is Murphy's Lindbergh cyclic steam stimulation project. The oil viscosity is 50,000 mPa.s. As many as eight cycles have been conducted, with oil-steam ratios averaging 0.25, close to the predicted value of 0.3. The predictions took into account steam in the bottom water. The formation thickness is 15-20 m, with varying amounts of bottom water, on the order of 3 m.

Ehrlich (1977) investigated the recovery of a 5 kPa.s bitumen, with bottom water present. It was found that the heated bitumen was swept into the water zone by the condensate. He notes, once the water zone is preheated, it cannot be plugged off, and must be saturated with oil by gravity flow before steam will advance into the oil zone and the resulting oil-steam ratio is low.

Considering the results of the aforementioned runs and the leaching process, it was decided to design the experiments in a rectangular core (details of the model are given in the previous chapter). The model was made to allow packing of a bottom water zone underlying the oil zone. The highly permeable water zone of variable thickness was intended to serve as a transporting medium for bitumen. In the following sections, the runs conducted in the rectangular cross section model will be discussed with or without a bottom water present.

4.3 Effect of Hot Water on Bitumen Mobilization

Hot water was used in Run 4 to observe if low level heat would mobilize the bitumen effectively. Heating pads were wrapped around the steel tubing along the section from the pump to the injection well. A thermocouple placed at the injection point was used to record the injection temperature. There were also three other thermocouples placed at equal distances inside the core and at the production well. The temperatures were recorded every two minutes during the run. It was observed that during the earlier phase of the run, the heating effect of hot water was not felt even in the middle of the core. Heating pads were then wrapped around the core near the injection point in the later stages of the run, thus heating the model throughout. The reason for heating the model was that the temperatures near the production well did not change by hot water injection.

As it is shown by the history of the run (Appendix C), bitumen mobilization was of small extent and the recovery was about 2% of the bitumen in-place. Although this run had a thick water zone, it could nevertheless be said that low level heat is not sufficient to mobilize the bitumen, or is not enough in a marginal reservoir of this type. Because of the difficulties in temperature control and the negligible effect of low level heat, the runs following Run 4 did not involve any heat and were performed at room temperature (24° C).

4.4 Effect of Bottom Water Zone Thickness on Bitumen Mobilization

Runs 4, 5, and 13 were conducted to observe the effects of the relative thickness of bottom water zone on bitumen recovery. Table 4.2 compares the three runs. Although hot water and more solvent were injected in Run 4, recoveries were about the same as for Run 5. Run 13, on the other hand, had a thinner water zone (bitumen-to-water zone ratio of 7). After about 20% HCPV of synthetic crude injection, the injection pressure reached the maximum pumping pressure of 4.2 MPa. Switching to water did not decrease the injection pressure, and the run had to be halted. Hence it may be seen, given the limitations of the laboratory experiments, that an oil-to-water zone ratio of 5.25 seems to be the best among the three. As a result, the following bottom water runs were done with a ratio of about 5. In the next chapter, results of the simulation study involving relative thickness effects will be discussed.

The bottom water zones in these runs had about the same permeabilities. It was reasonable to compare only the relative thicknesses. However, it is more appropriate that capacity ratios be considered when comparing the bottom layers. The capacity is the product of permeability and thickness. Since the same type of bottom layer was used in most of the runs, only the relative thicknesses were considered. On the other hand, Run 17 had a different bottom layer. The capacity ratios will be compared in discussion of this run.

Table 4.2. Effect of Bottom Water Zone Thickness

Run No.	Solvent Slug (%HCPV)	$\frac{h_b}{h_w}$	Bitumen Recovery (%IBIP)
4.	20%	1.5	2.03
5.	10%	5.25	2.0
13.	20%	7.	Halted due to high inj. pressure

4.4.1 Solvent Stimulation

Runs 6, 7 and 8 were conducted with small slugs of solvent to observe the bitumen mobilization with and without bottom water. Run 6 had no bottom water zone while Runs 7 and 8 had. Although the runs are not strictly comparable, Table 4.3 gives the slug sizes and recovery figures for these runs.

Run 6 was a waterflood with a solvent slug injected in the middle. The rectangular cross-section model was packed with oil sand with no bottom-water zone present. The run was started with 1 HCPV of water injection to see if there was bitumen produced at all. No bitumen was observed and a solvent slug of 10% was injected, followed by water again. At the end of 3 HCPV of injection, the bitumen recovery was only 1.8% of the bitumen in-place. The mixture of bitumen and solvent was in small droplets. Runs 7 and 8 had recoveries of 14.8% and 7.6% but also involved surfactant in addition to solvent. They will be discussed in the Solvent-Surfactant Flooding chapter.

Table 4.3. Solvent Stimulation Runs

Run No.	$\frac{h_b}{h_w}$	Solvent Slug (% HCPV)	Surfactant (%)	Bitumen Recovery (%IBIP)
6.	No Bottom Water	10%	-	1.8
7.	5.25	20%	5.	7.6
8.	5.25	20%	1.	14.8

4.4.2 Solvent Floods

Solvent stimulation runs, as mentioned above, had very limited recovery of oil; thus, it was difficult to compare one run with another. Solvent flood runs, in contrast, involve continuous injection of solvent and result in higher recoveries. For more meaningful comparisons and to determine the limiting cases, solvent flooding runs 9 and 10 were carried out.

Runs 9 and 10 had nearly identical packings and fluid properties. Oil sand to bitumen zone thickness ratio was 5.25 in both runs. Distilled water was displaced through the rectangular model until it broke through at the producing well only in Run 9.

Comparison of these two runs is given in Figure 4.1. Solvent breakthrough in Run 9 is earlier but the effluent bitumen concentration does not peak as high as that for Run 10. One explanation could be that the water injection in Run 9 had opened up more flow channels prior to solvent injection. Thus the solvent in Run 9 followed the flow channels of water and broke through earlier than in Run 9. In Run 10, the dissolution process has more time to dissolve the bitumen, hence the dissolution process is more competitive with convective transport than Run 9 (lower peak) in the earlier stage of the run. The differences in the concentrations decrease with more solvent injection and the final recoveries turn out to be closer for each run. After the bitumen concentrations peak in each curve, there is a drastic decrease in bitumen concentration, indicating dissolution of bitumen. Since much of the solvent is absorbed by the bitumen until about 0.8 HCPV of injection, the solvent concentration is low in the effluent during that time. Rapid dissolution begins when the bitumen no longer absorbs solvent and dissolves into the liquid phase.

Bitumen concentration declines rapidly after the initial flow channels are created (at around 1.5 HCPV injection). During the decline period, the bitumen concentration in the effluent fluctuates, as seen in Figure 4.1. One possible explanation could simply be due to sampling. The pump used in these runs had a capacity of 500 ml. In each run it had to be refilled at least twice, thus causing the experiment to be stopped for five minutes. In the first refill of the pump, which coincided with the rapid decline period of the concentration, no fluctuation in the effluent concentrations were observed. When the decline became gradual, the peaks occurred just after the run was stopped and restarted. The number of the peaks in

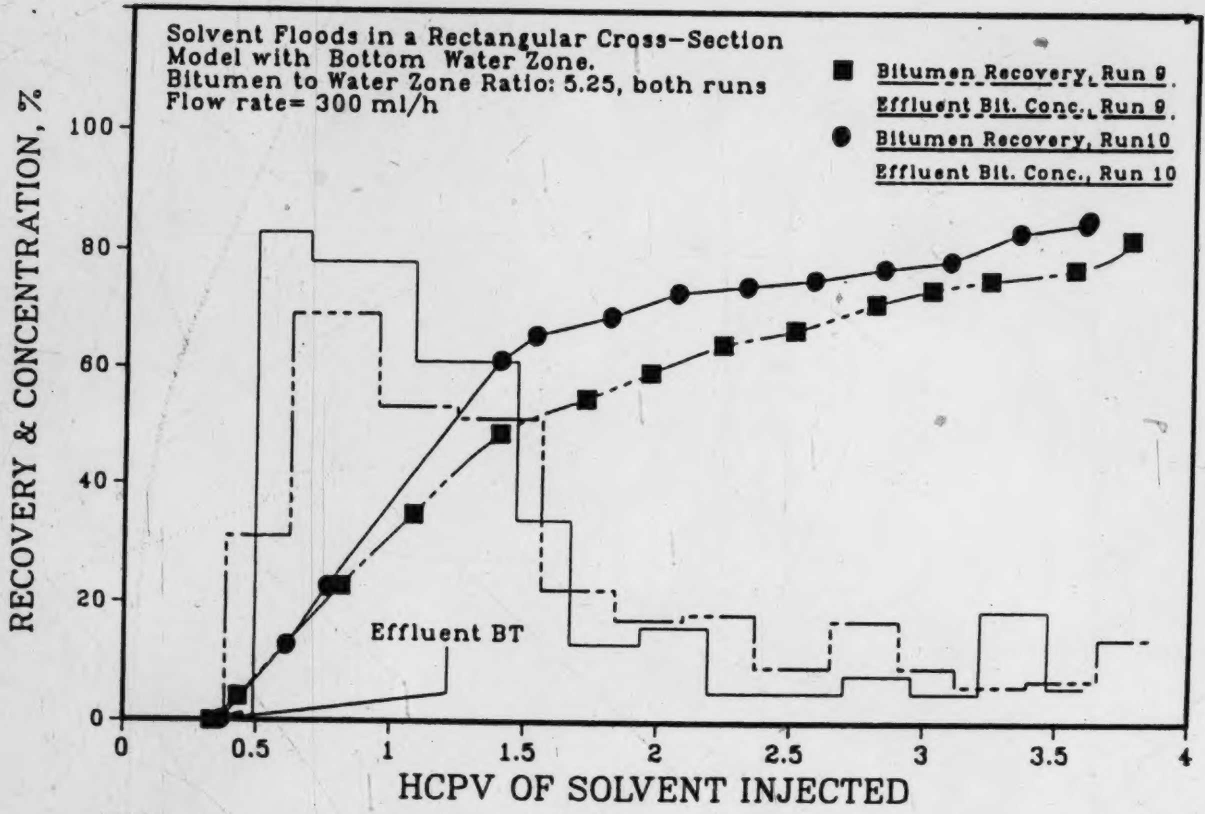

Figure 4.1 Comparison of Runs 9 and 10

the gradual decline period equals the number of refills. Such intervals might have increased the solvent diffusion into the bitumen in the absence of flow; therefore, the fluctuations were possibly a result of these interruptions. The final bitumen recoveries are 82.3% and 85.3% for Runs 9 and 10 respectively (Appendix C). The solvent recovery figures are also close to each other.

The visual post-run inspection of the core showed that the region close to the injection well was almost free of bitumen. This was indicated by the light colour of the solvent in both the water and the bitumen zones. The originally tight oil sand matrix also became soft and loose. It was also noticed that the top of the oil sand matrix retained some of the dark colour. Along the core from the injection to the production end, the bitumen content of the matrix was seen to increase; the injection end being swept the most by the solvent. The entire water zone was coloured in the same way as the oil zone although the latter was relatively darker. This observation supports the idea that the bitumen apparently flowed through the water zone. The softer sand matrix also indicates changes in porosity and thus permeability. The concentration profiles during the run will be discussed in detail in the numerical simulation chapter.

In the previous continuous solvent injection schemes reported in the literature review, the bitumen concentrations in the effluent were lower than the ones obtained in Runs 9 and 10. Farouq Ali and Snyder (1973), and and Abad (1976) reported that, in their two-dimensional vertical tar sand pack runs, the highest bitumen concentrations were around 40% by volume, making the processes inefficient. They also mentioned the predominance of the "wall effect" from a number of visual studies in vertical glass tubes packed with Athabasca oil sand. In a comparison of the packings it was also found that the packing density was higher in Runs 9 and 10. The differences in the bitumen concentrations could then be due to packing. The residual bitumen saturations near the injection port showed relatively unswept regions in Snyder's experiments.

4.4.3 Solvent-Surfactant Flooding

Surfactants have been used to alter the surface tension or wettability of oil/water/sand interfaces. Their use as waterflood additives and foams with steam drives has been established in field applications. In the case of heavy oil/bitumen, the selection of surfactants for possible use with steam on oil sand formations was studied by various researchers. Ziegler and Handy (1979) and Handy *et al.* (1982) examined the thermal stability and adsorption of surfactants. Isaacs *et al.* (1982) conducted laboratory scale experiments to examine the use of surfactants as additives to steam-based processes. Hot water and steam injection with surfactants showed substantial increase in bitumen recovery from oil sands. Raplee *et al.* (1985), in their evaluation of various additives, found that the surfactants showed greatest improvement in oil recovery. Among surfactants, alkyl benzene sulfonate, under the trade name, Stepanflo 40, demonstrated a significant improvement of recovery in Alberta oil sands.

Although it is agreed that surfactants as additives promote additional recovery in heavy oil/bitumen, a precise understanding of the enhancement mechanism is not established. Viscous forces play a far more important role than capillary forces in heavy oil/oil sand formations. When the viscosity of oil is reduced by steam, the capillary forces begin to play an important role. The increased recoveries in the presence of surfactants are therefore related to the decrease in the interfacial tension.

Runs 7, 8 and 11 were conducted to study the effect of surfactant when the viscosity of the bitumen in the formation was reduced by a previously injected solvent slug. These runs all involved injection of a solvent slug with surfactant solution at various stages. In Run 7, solvent was injected in the middle of the run whereas it preceded the surfactant injection in Runs 8 and 11. An alkyl benzene sulfonate, Stepanflo 80, was used in the experiments. It is a more effective version of Stepanflo 40 (cited above) as suggested by the vendors. A summary of these runs is given in Table 4.4.

Table 4.4. Solvent-Surfactant Flood Runs

Run no.	Solvent Slug (%HCPV)	Surfactant (%)	Bitumen Recovery (%IBIP)
7.	20	5.	14.7
8.	20	1.	7.6
11.	104	1.	68.2

In Run 7, a surfactant solution of 5% vol was injected for 2 HCPV. It was intended that such a high concentration of surfactant would mobilize some of the bitumen. Bitumen recovered in this stage was not produced continuously but rather in the form of small blobs in the effluent. Bitumen was believed to be a discontinuous phase within the porous medium. The produced fluid was mostly water and the bitumen recovery at this point was only 3.6% HCPV. Surfactant retention, as observed from the colour of the solution produced and its analysis, was estimated to be small.

Because of the low bitumen recovery in the first stage of the run, it was decided to stimulate the oil sand pack with a 20% HCPV solvent slug at the injection end. Surfactant solution injection was resumed at a rate of 300 ml/h. The total recoveries at the end of 3.4 HCPV of total injection were 14.7% of the initial bitumen in place and 54.4% of the solvent injected. In the analysis of the effluent and the remaining oil sand in the pack, the surfactant was found to be present in each phase. Although the relative amounts of surfactant in the fluids and in the formation could not be determined accurately, it is believed that only a small amount of retention by the pack occurs prior to the initiation of bitumen production, and gradually increases as more bitumen is displaced. Most of the bitumen was recovered in the second phase only after a 20% solvent slug. The additional bitumen recovery of 11.1% was more than what was recovered without surfactant with the same slug of solvent.

Run 8 was performed in a similar fashion. A solvent slug of 10% was injected first, followed by 1% surfactant solution. About 3% of bitumen in-place was recovered at 2.5

HCPV injection when another solvent slug of 10% was injected. An additional recovery of 3.7% bitumen was recovered at the end of run. Although the same amount of the slug was injected, bitumen recovery was almost twice as much as in Run 7 than in Run 8. This could be either due to the surfactant solution or the solvent injection strategy. In both runs injection of solvent was necessary to initiate the bitumen production.

Run 11 was conducted as a combination solvent-surfactant flood. About 1 HCPV of solvent and 1% surfactant solution was injected, respectively. In order for a direct comparison of solvent flood versus a solvent-surfactant flood, Run 11 was packed very similarly to Run 9. Synthetic crude was injected for 1.04 HCPV, by which time the bitumen and solvent recoveries were 34.7 and 35.8% respectively. Concentration and recovery figures for the solvent injection part were similar to those of Run 9, where the bitumen-to-water zone ratio was also 5.25. A comparison of Runs 9 and 11 is given in Figure 4.2 The second phase of the run was started with 1% surfactant solution. Surfactant solution did not break through until after 0.25 HCPV of injection. Until breakthrough, the effluent consisted of bitumen and solvent only. After breakthrough, the fluids consisted of a bitumen-solvent-surfactant mixture and surfactant solution. The bitumen concentrations in the mixture were determined by using a density meter. The spectrophotometer readings were unreliable because of the presence of the surfactant in the effluent. After breakthrough, the water-to-bitumen ratio, WOR, steadily increased. The bitumen concentration in the first effluent sample was 61% by volume as measured by the densimeter. It increased while the volume of effluent in the produced fluids decreased with more surfactant injection. In the analysis of the recoveries, 51% HCPV of solvent injected was left in place against 68% HCPV of bitumen recovery. If only bitumen recovered versus solvent lost is compared, a net 17% HCPV of bitumen is recovered. If the same comparison is used for Run 9, it is seen that Run 9 had a 82% bitumen recovery but 120% HCPV solvent was left in place. A percentage of over 100 was due to some solvent left in the water zone. Therefore, the combination of solvent and surfactant seems to

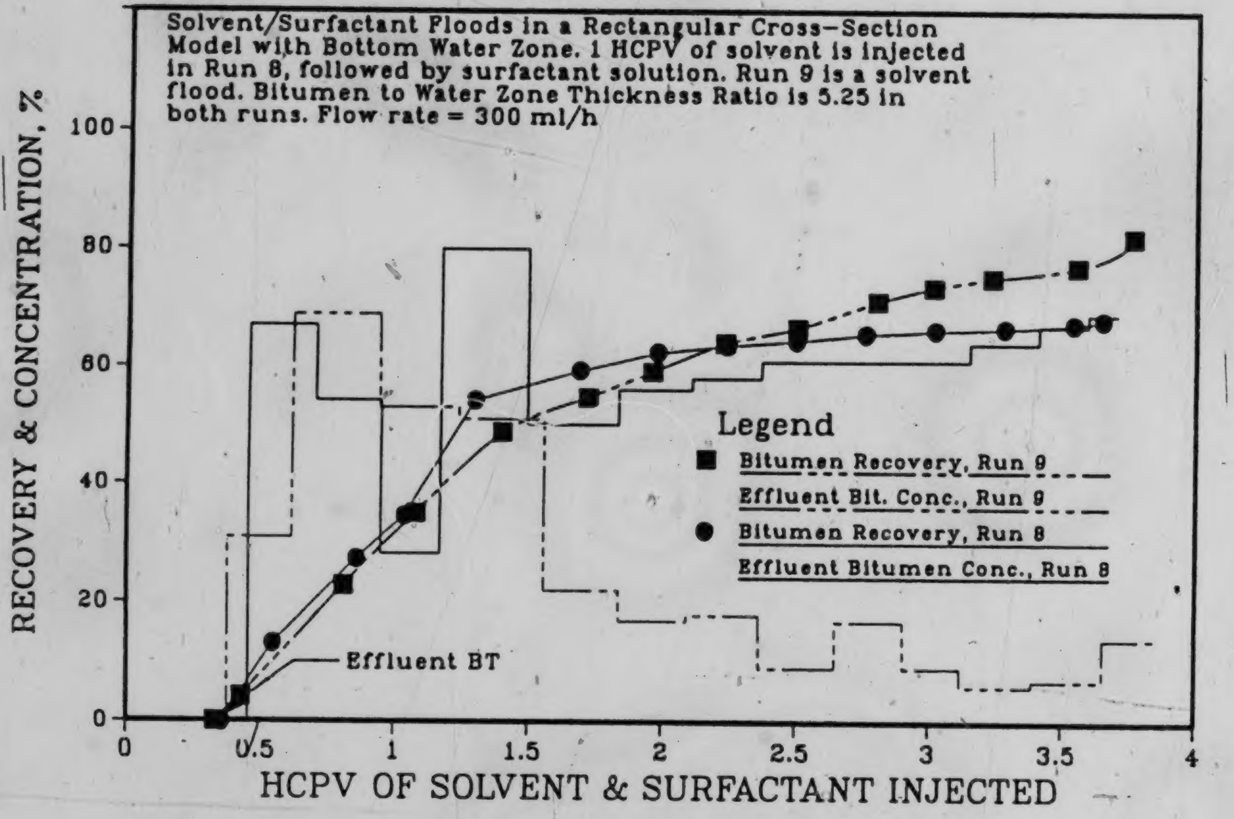

Figure 4.2 Comparison of Runs 9 and 11

be superior to solvent leaching or surfactant flooding alone. Note that the bitumen concentrations in Run 11 are measured from the bitumen-solvent-surfactant mixture. The oil cut in the produced fluid otherwise is lower because of the large water cut produced.

4.5 Effect of Carbon Dioxide on Bitumen Mobilization

As mentioned in the literature review, gases can reduce the viscosity of heavy oil and bitumen due to solution. Of gases, carbon dioxide seems to have more extensive data and promise as an enhanced heavy oil recovery agent. Carbon dioxide is viewed as a viable alternative to thermal recovery where the formation conditions do not warrant heat injection. Carbon dioxide can be injected into a reservoir in the liquid or the gas phase. Rojas (1985) cited findings that in the case of heavy oils it is better to inject the carbon dioxide in the gas phase rather than in the liquid phase. Carbon dioxide either has been used in a non-thermal recovery scheme or as an additive in steamfloods. Redford (1981) and Briggs *et al.* (1981) studied a combination of additives, in which carbon dioxide and naphtha were both used as additives with steam in laboratory core experiments. They reported higher recovery of bitumen with both of the additives over each additive alone.

In this work carbon dioxide was injected in slugs to assist the displacing agent which followed the gas. Carbon dioxide was injected prior to displacement by solvent or water. There was no production while the gas was injected. Carbon dioxide was injected at the production well.

A preliminary run, in which the core packed with oil sand and a bottom water zone was pressurized by water injection, was carried out to check the system. Carbon dioxide was injected at about 4 MPa to check for possible leaks. Upon inspection, the core was corroded due to the formation of H_2CO_3. This was especially apparent in the bottom water zone. It was for this reason that the gas was initially injected into the system at low pressures in the following runs.

Runs 12, 17, 18, and 22 involved carbon dioxide injection. The gas was injected into the core starting at atmospheric pressure in the beginning or in the middle of the run. The volume of gas injected was calculated from the final pressure and flowmeter reading using Starling's equation. A summary of these runs is given in Table 4.5.

Table 4.5. Carbon Dioxide Stimulation Runs

Run No.	$\frac{h_b}{h_w}$	Slug Size (%HCPV)	Surfactant (%)	CO_2 (% HCPV)	Bitumen Recovery (%IBIP)
12.	6.	0.	1.	5.	Nil
17.	5.25	317.	-	50.	25.1
18.	5.25	1.0.	-	45.	51.1
22.*	5.25	0.0	1.	32.	Nil

* Heavy oil run

In Run 12, the rectangular cross-section core was packed with oil sand and a water zone. The bitumen-to-water zone thickness ratio was 6.0. A slug of 5% HCPV carbon dioxide (at 3.8 MPa & 25° C) was injected. Following the gas, the 1% surfactant solution injection was started. No bitumen was produced until after 2.6 HCPV of injection, at which time the run was terminated. Upon inspection of the core, the bottom water zone was observed to be free of bitumen. It was concluded from this run that the gas and surfactant failed to mobilize and transport the bitumen.

In Run 17, carbon dioxide injection followed 2 HCPV of solvent injection in an oil sand pack with a different bottom water layer. It was observed that gas injection increased the effluent bitumen concentration. Because of the different bottom layer, this run will be discussed in the next section.

Run 18 was designed to observe the combined mobilization effect of solvent and carbon dioxide. The run involved injection of 1 HCPV of solvent followed by carbon dioxide and water injection. The core was packed with oil sand and a bottom water zone. The bitumen-to-water zone thickness ratio was 5.25.

The run was started with injection of synthetic crude. At the end of 1 HCPV solvent injection, bitumen recovery of 24.8% was obtained (See Appendix C). Following the solvent, carbon dioxide was injected until the pressure reached 1 MPa. Subsequently water displaced the mobilized bitumen resulting in a recovery of 51.1% (Figure 4.3). The sharp drop in bitumen concentration which occurred in the solvent floods was not observed in the effluent taken after the gas injection. Instead there was an increase in the effluent bitumen concentration. While some of this increase could be explained by the interval during which gas injection took place (as discussed in the solvent flood section), a high bitumen content in the effluent was maintained until the end of the run. Bitumen concentration was measured by the content in the bitumen-solvent mixture of produced fluids. Although this concentration increased, the water-to-effluent ratio became larger as more water was injected (See Figure 4.3).

The total bitumen and solvent recoveries are 50.1 and 51.4% respectively. The bitumen in place was replaced by 48.6% HCPV solvent. Thus if the solvent injected versus bitumen produced is compared, a volumetric incremental recovery of 1.5% HCPV is obtained. If the solvent injection had continued instead of gas, bitumen and solvent recoveries would have been 82.3 and 68.5% respectively (from Run 9). In Run 9, while more than 68% of solvent was recovered, a substantial amount of it was left in place (1.18 HCPV). In contrast, there was 49% HCPV of solvent left in the core in Run 18 as the bitumen recovery was 32.2% less.

To make a better comparison, a "recovery ratio" is defined as the bitumen produced over solvent left in the pack. Accordingly, the higher the ratio, the more efficient is the scheme. This ratio would be 1.02 for Run 18 versus 0.70 for Run 9. If the cost of the gas and water injection were not taken into account, or assumed less than that of solvent injection, a combined solvent and carbon dioxide injection scheme seems to be more efficient compared to

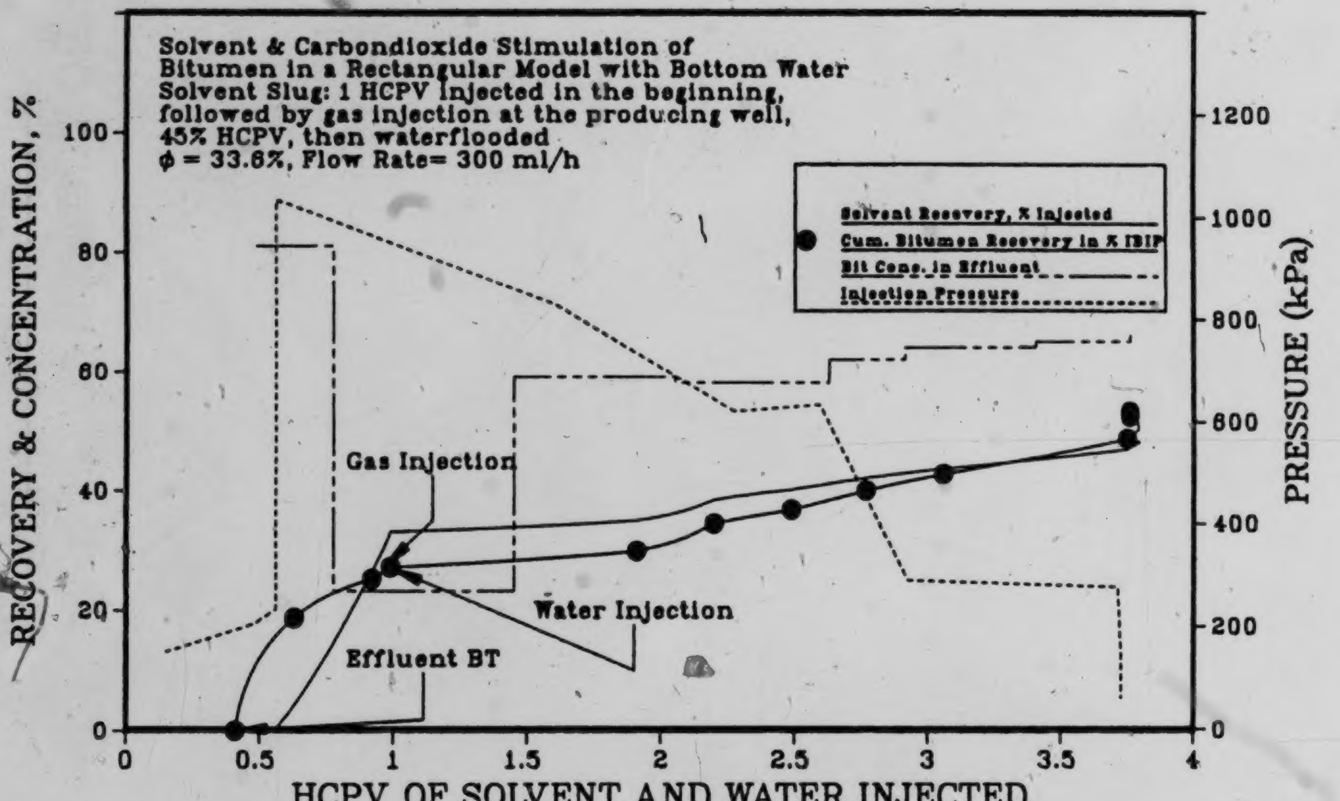

Figure 4.3 Production History of Run 18

a continuous solvent one. Yet Run 11, which involves solvent and surfactant injection is superior to both Run 9 and 18. A comparison of these runs is depicted in Figure 4.4. The figure shows the bitumen recovered against the solvent left in the pack in a normalized form for each run.

In the above runs in this section, the gas was effective when used with solvent. The oil sand pack was used in these runs. Run 22; however, was performed to study the effect of carbon dioxide and surfactant in a less viscous heavy oil pack. A 5% carbon dioxide slug was followed by 1% surfactant injection. The rectangular cross-section core was packed with heavy oil of 15605 mPa.s. The oil-to-water zone thickness ratio was 5.25. This run was performed in the same fashion as Run 12 to see if there was an improvement in mobilization when using less viscous oil. As in Run 12, no oil was ever produced after gas and surfactant stimulation. The run was terminated when a large amount of sand production occurred.

4.6 Effect of Water Zone Permeability on Bitumen Mobilization

In most of the runs the bottom water zone consisted of glass beads of 140-230 mesh. In order to see the effect of the water zone permeability, glass beads of mesh 20-30 were used as the bottom water zone in Run 17. This run consisted of continuous injection of solvent and a carbon dioxide slug of 50%.

The bitumen-to-water zone ratio in this run was chosen to be 5.25 in order to have a direct comparison with the other solvent flood runs. The permeability of the water zone was calculated to be about 360 darcies by the Kozeny equation. Table 4.6 gives the comparative recovery and capacity ratio for Runs 9 and 17. Although the thickness ratios are the same, the capacity ratios are greatly different. The capacity ratio for this run is a better indicator of the bitumen recovery.

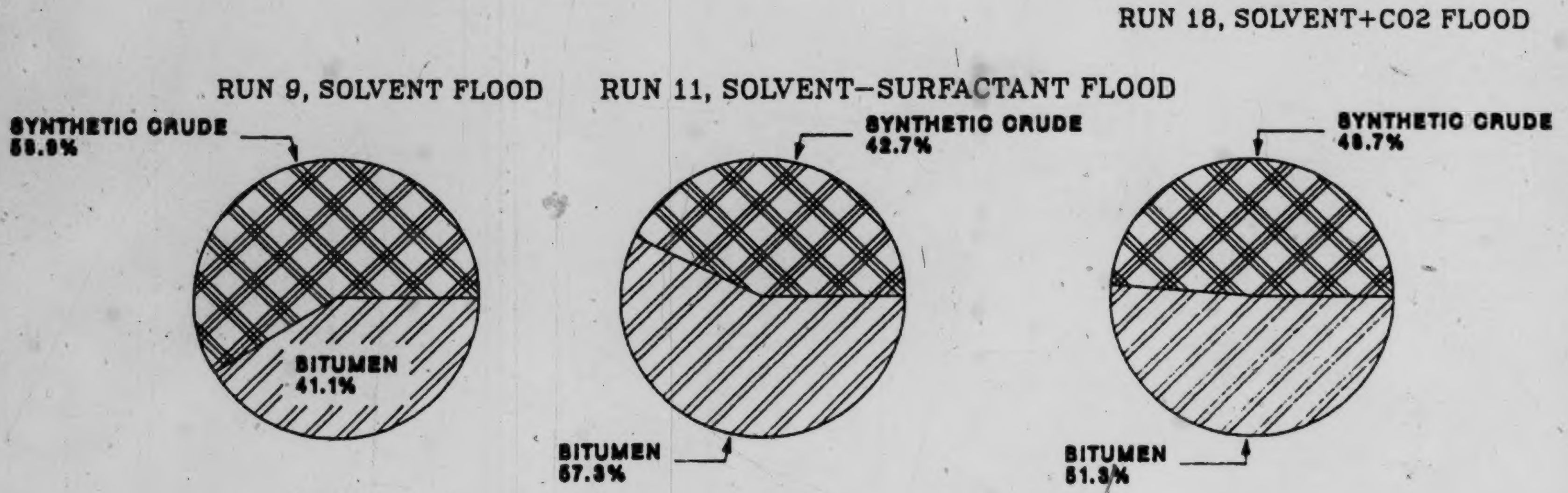

FIGURE 4.4 COMPARISON OF NORMALIZED BITUMEN RECOVERY VS SOLVENT USED BREAKDOWN

Table 4.6. Effect of Water Zone Permeability

Run No.	$\frac{h_b}{h_w}$	Capacity Ratio	Solvent Slug (% HCPV)	Bitumen Recovery (% IBIP)
9.	5.25	1.57	361.	82.1
17.	5.25	0.03	317.	25.1

The run was started with synthetic crude injection at a rate of 300 ml/h. The effluent bitumen concentration in the first sample was only 16% by volume. In contrast, the bitumen concentration was 69% in Run 9 where the bottom water zone had a permeability of 6 darcies. A production history of the run is given in Figure 4.5. The concentration fell to 6% by the time 1 HCPV of solvent was injected. It continued to drop gradually and it was decided to stop the solvent injection at 2.08 HCPV. At this point, the bitumen recovery was 10.7% of the bitumen in place. The sample taken showed a bitumen concentration value of only 4%. On the other hand, Run 9 had a bitumen recovery of 61.4% and a concentration value of 17% at the same point. Since both runs have similar features, the difference is due to the water zone permeability contrast. The mechanism resulting in such a low recovery in Run 17 could be that the injected solvent mobilized and transported the bitumen near the injection well. Subsequently, the solvent reached the bottom water zone without contacting bitumen in the unswept portions.

In an attempt to increase the effluent bitumen concentration, it was decided to stimulate the remaining bitumen by carbon dioxide in the second phase of this run. While studies involving combinations of gases and solvents were mentioned in the literature review, these were all combined with steam injection. Redford (1981) reported the use of solvents and gases with steam in the recovery of bitumen from oil sands. He found that there was a synergistic effect when carbon dioxide or ethane was used with naphtha in the recovery of

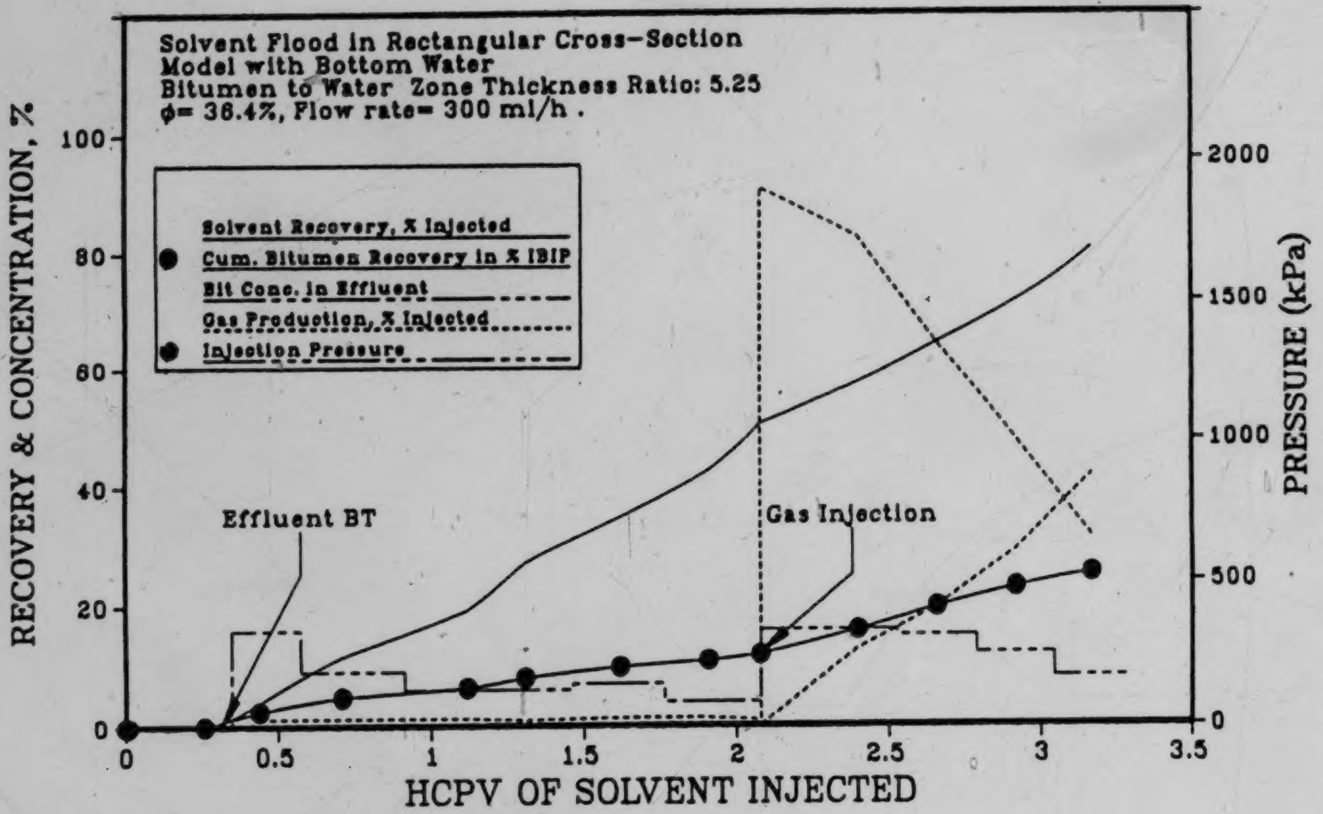

Figure 4.5 Production History of Run 17

bitumen. In such a process, the gas improves recovery on the drain portion of the cycle by viscosity and drive effects, and the naphtha improves recovery on the injection portion of the cycle by improved recovery in the water-swept zones.

In a similar process, where the solvent is used as an displacing agent instead of steam, the gas improves recovery by providing viscosity and drive effects, and the synthetic crude improves recovery by transporting the bitumen. Carbon dioxide, which has dissolved in the unswept portions of the core in the gas injection portion of the run, breaks out of solution and provides drive energy. The solvent lowers the viscosity of the bitumen and enables the drive energy of the carbon dioxide to be used more effectively.

The second phase of this run was performed to test the aforementioned effect of carbon dioxide with solvent displacing the bitumen. A slug of 50% HCPV carbon dioxide was injected after which the solvent injection was resumed. The bitumen concentration jumped to 16% from 4% in the next effluent sample (Figure 4.5). Decreasing gradually, it was 8% of the effluent at the conclusion of the run. It was also of importance that the drop in the bitumen concentration in this stage of the run was more gradual than the first phase when only solvent was displacing the bitumen. The interval of two hours during which the gas injection took place is unlikely to cause a sustained increase in bitumen concentration. Prior to that, over 2 HCPV of solvent dissolved and carried the bitumen it was able to contact. It is most likely that the gas came out of the solution with pressure decline and provided drive energy for the solvent.

The viscosity of live bitumen of 82.5 Pa.s after the gas injection at 1.9 MPa and 24° C is about 22.5 Pa.s using Figure 1.3. Although the bitumen might not be fully carbon dioxide-saturated, the reduction in viscosity is large. The actual viscosity was further reduced by the displacing solvent.

The effect of water zone permeability on recovery is evident from both bitumen concentration and recovery results. The bitumen and solvent recoveries of Run 17 were 25%

and 81% respectively. Before the gas injection, the run had a bitumen recovery of 11.7% and solvent recovery of 50.7%. On the other hand, Run 9 had bitumen and solvent recoveries of 61.7 and 24.9% at same injection point. The bitumen recovery of Run 9 was about 5 times as much as that of Run 17. of Run 9 was 6 darcies. A comparison of these two runs is given in Figure 4.6. As can be seen from the figure, very high permeability channels are detrimental to the mobilization and recovery of bitumen.

4.7 Surfactant Crumble Test

In the literature review section it was mentioned that the surfactants might promote the breakup of the oil sand matrix. It was observed in Run 12 that the surfactant, Stepanflo 80, was not able to mobilize the bitumen alone or in combination with carbon dioxide. Because of the presence of a bottom water zone, the effects of the water zone and surfactant were not isolated from each other. Hence Run 19 was carried out without a water zone.

Prior to this run, a beaker containing a known weight of oil sand was filled with Stepanflo 80 solution of 1% by volume at 25° C. The beaker was closed and kept at this temperature for 24 hours during which time the solution was occasionally stirred and agitated. At the end, no visible difference was observed in the surfactant solution. The oil sand sample taken out of the beaker was dried and extracted for the bitumen content. No significant change in the bitumen content of the sand was found. The beaker was then heated up to 60° C while it was being stirred. The colour of the solution slowly turned dark and with more agitation the bitumen started to break from the oil sand. Small droplets of bitumen were observed in the solution and the bitumen-free sand particles appeared. It was not however a complete separation, where the lighter bitumen was on top of the sand. The bitumen particles were dispersed among the sand particles which were still surrounded by bitumen. An accurate determination of the bitumen content could not be performed because of the bitumen still present in the remaining oil sand particles.

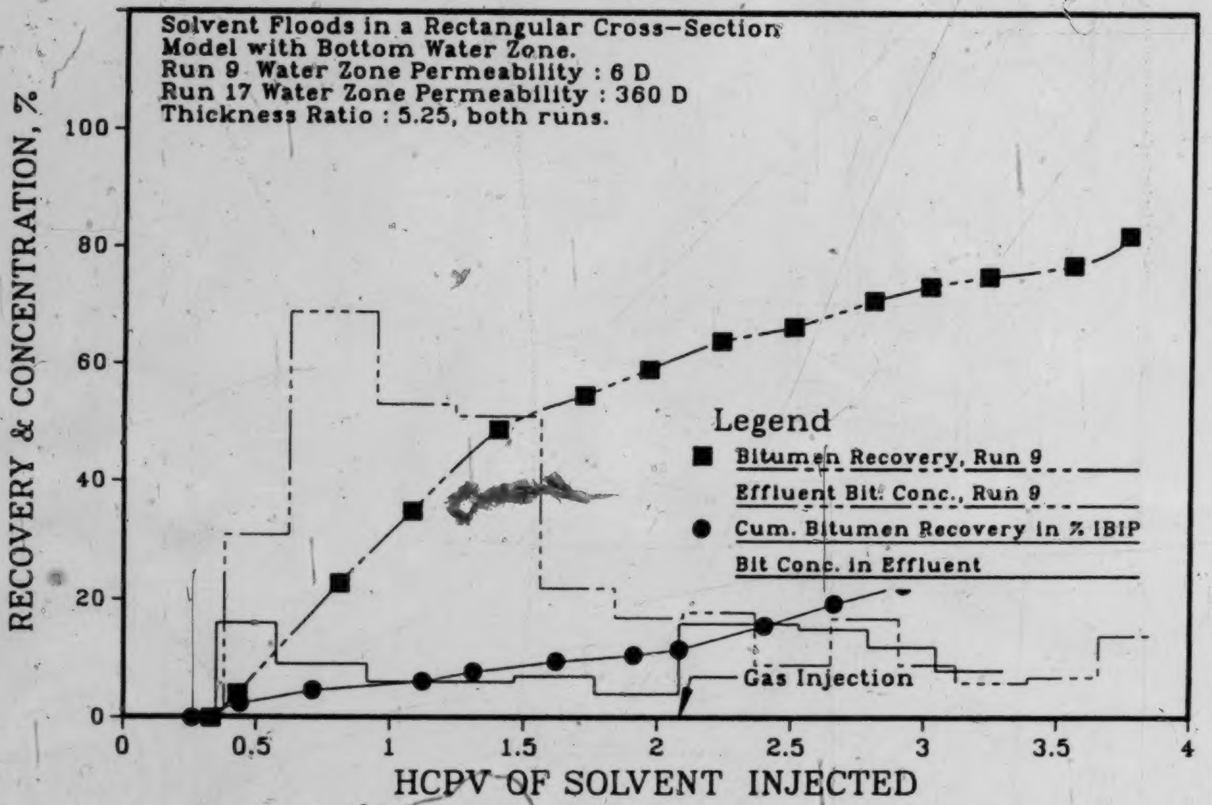

Figure 4.6 Comparison of Runs 9 and 17

Although the experiment above points out the necessity of viscosity reduction, such a surfactant solution flowing through the porous medium may help open flow paths under pressure gradients. Run 19 was performed to see if the surfactant solution prior to solvent injection would help injectivity and promote a breakup of the oil sand matrix.

The rectangular cross-section model was packed with oil sand and drawn a vacuum on. The 1% surfactant solution was injected at the production end of the model which was fully packed with oil sand. The injection continued until the pressure at the outlet end reached 1.9 MPa. The core was left closed at both ends until the pressure dropped by 0.4 MPa. The production well at this time was opened and the surfactant solution was allowed to flow out. The solution was visibly free of bitumen and about the same colour as it was injected. This procedure was repeated eight times and each time the solution was free of bitumen. It was intended that the surfactant solution injected and flowed out would open more flow paths.

Following above procedure, solvent injection was initiated at a rate of 300 ml/h. The bitumen concentration in the first effluent sample was 41% (Figure 4.7). It decreased with more injection of solvent and the bitumen recovery was 50% after about 2 HCPV of solvent injection. The concentration and hence the recovery of bitumen were lower than those of comparable runs where a substantial amount of solvent was used (Runs 9, 10, 11). In addition, those runs had bottom water layers. The significance of this run was that continuous solvent injection was achieved into a full sand pack without a bottom water layer. The run was continued with injection of carbon dioxide from the production well. At a pressure of 830 kPa, a 40% pore volume gas saturation was present in the core. After an interval of two hours, the surfactant injection was started and at the end of one pore volume, an incremental recovery of 6% was obtained. The total bitumen and solvent recoveries were 56.7 and 65.4% respectively. The process was however inefficient, since 70% HCPV of solvent was left in place. Carbon dioxide retention was 68.1%. Considering the incremental recovery and use of the surfactant solution, this part of the run was also inefficient. It was caused possibly by the

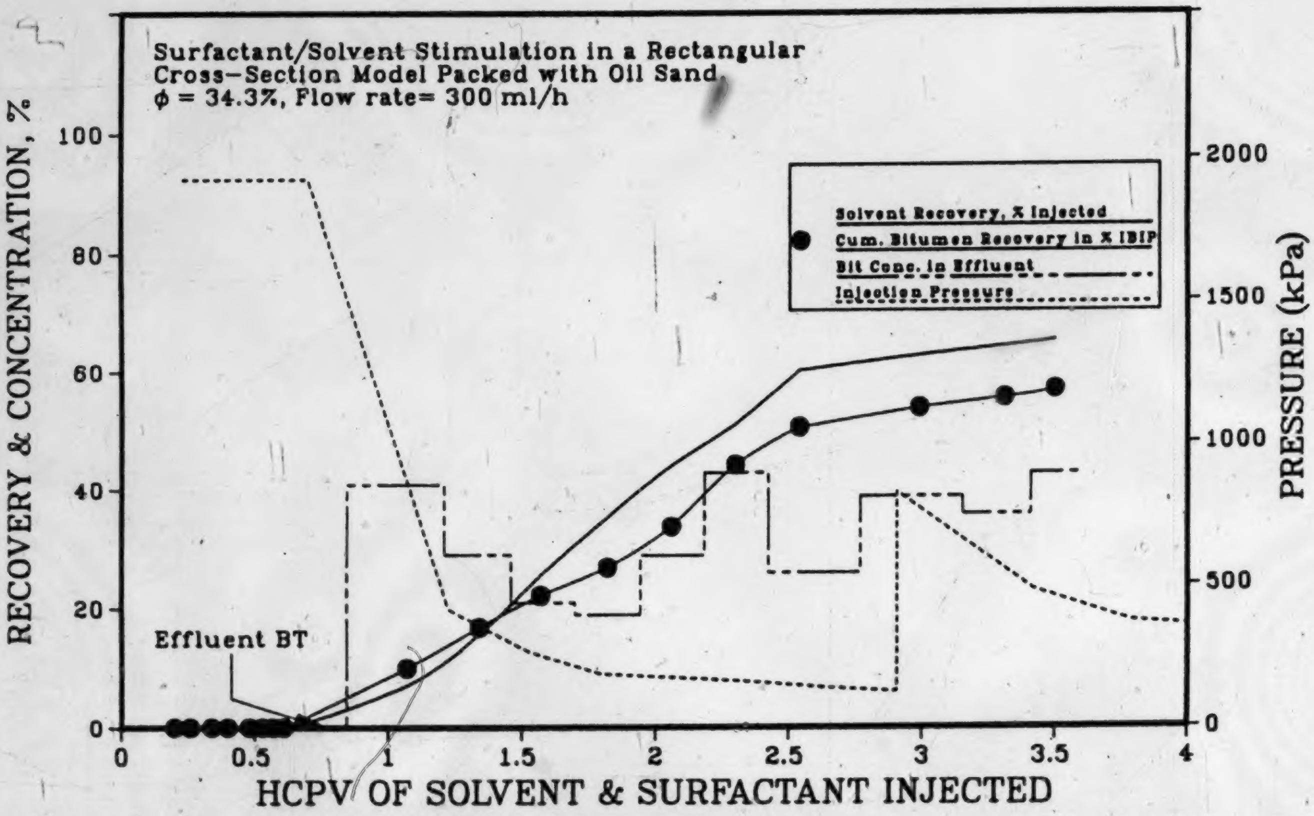

Figure 4.7 Production History of Run 19

flow paths which were near the walls of the model. The solvent tended to flow into these paths and did not contact some of the bitumen away from the walls. Continuous solvent injection was possible in this run whereas Run 13, for instance, had to be stopped when there was a bottom water zone present.

4.8 Visual Model Experiments

The visual model experiments were performed in an attempt to observe the flow patterns. It was not possible to inject the solvent at high pressures in this model (maximum working pressure is 400 kPag). As a result, it was not possible to inject enough solvent into the system. Another problem associated with the model was that the solvent tended to channel into the top of the model. The bottom of the model was pressurized by the rubber sheet connected to an air source. For this reason, solvent channelling did not present a problem at the bottom of the model.

Run 14 was performed to observe the effect of a small slug of solvent on bitumen mobilization in a five spot model. A total of 20% HCPV of solvent was injected in the beginning and middle of the run.

The visual model was packed tightly with oil sand and saturated with distilled water. A slug of 10% HCPV of synthetic crude was injected at a rate of 3.45 m/d. It was followed by water injection at the same rate. When the water broke through at the production end without mobilizing any bitumen, it was decided to inject another 10% slug of solvent, which was in turn followed by water again. The run was stopped when the effluent cut was less than 5% of the fluids produced (1.46 HCPV) (Figure 4.8). The total bitumen recovery was 4.1% of the bitumen in place. The highest bitumen concentration was 36% of the effluent. Compared to the bottom water runs in the rectangular model with the same slug size the visual model run in a five spot pattern gave somewhat better recovery (2% vs 4.1%). But the presence of the bottom water should be considered in the rectangular model runs. Samples were taken at

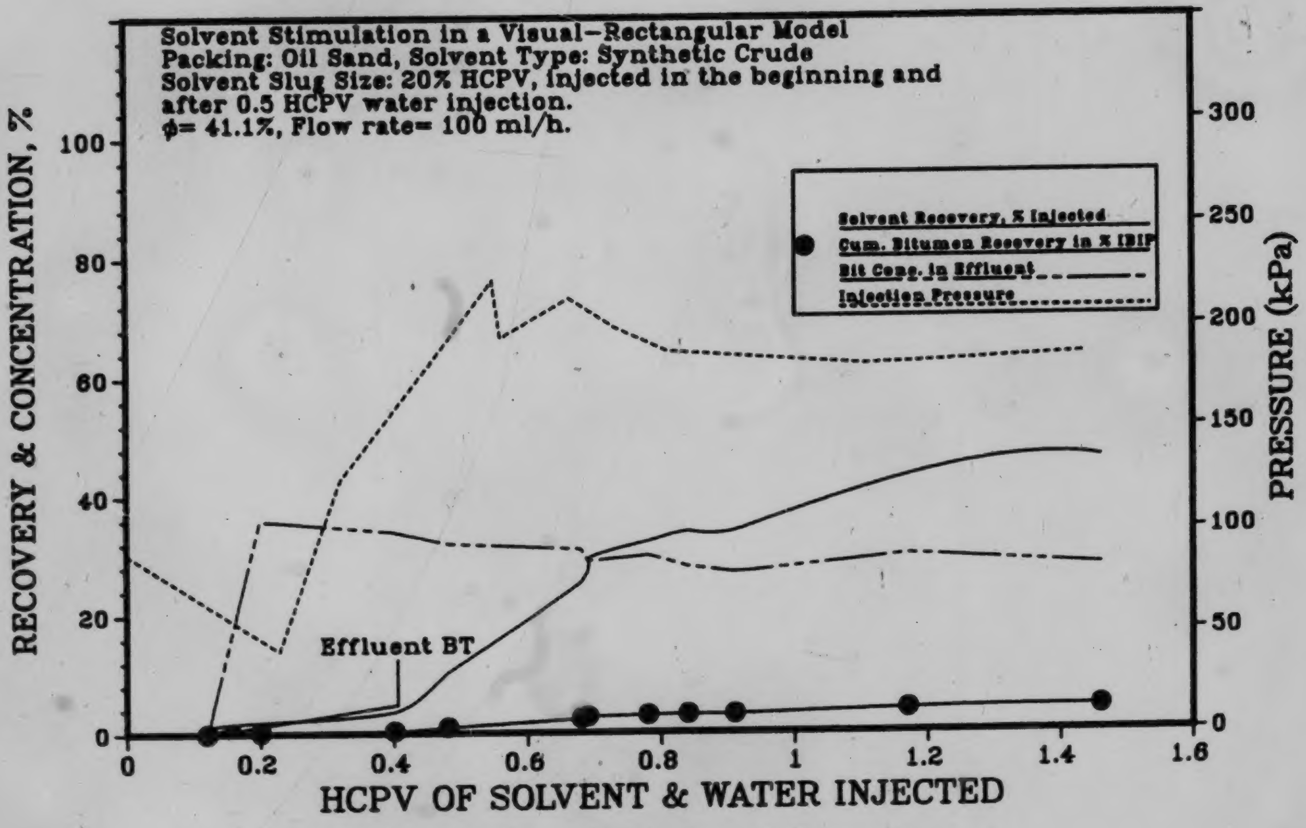

Figure 4.8 Production History of Run 14

different locations in the model and analyzed at the conclusion of the run. The residual saturations are shown in Figure 4.9. Note that most of the bitumen that was produced came from the area near the injection well. Very little bitumen near the production end and the corners was mobilized. This result is in accordance with those of the rectangular model runs. Upon visual inspection of the sand pack, it was observed that the bottom part of the pack was virtually unswept while the upper part was swept the most. This could perhaps be explained by the tighter packing in the bottom, and the small channels between the lid and the top of the sand.

In an attempt to solvent flood in a five spot pattern, Run 15 was performed. This time solvent was injected continuously in a similar packing to Run 14. The flow rate was 3.45 m/d. It was possible to inject solvent up to 55% HCPV when the pump had to be stopped because the pressure reached 400 kPa at that point. Lowering the flow rate and then switching to water injection did not prevent the pressure from going up. As a result, the run was terminated. At the conclusion, the bitumen recovery was 23.8% and 22.6% of solvent injected was recovered.

In both runs, it was observed that channelling of solvent took place in the top portion of the pack. The bottom portion of the pack was relatively unswept even though the injection points were close to the bottom of the model. One of the reasons could have been the damage to the bitumen formation during the packing. The wells were forced into the pack after the lid was closed. It was observed that the damage was most extensive between the lid and the top of oil sand pack. Combined with gravity segregation, the solvent injected tended to go towards the top, flowing in the small channels between the lid and the top of the sand.

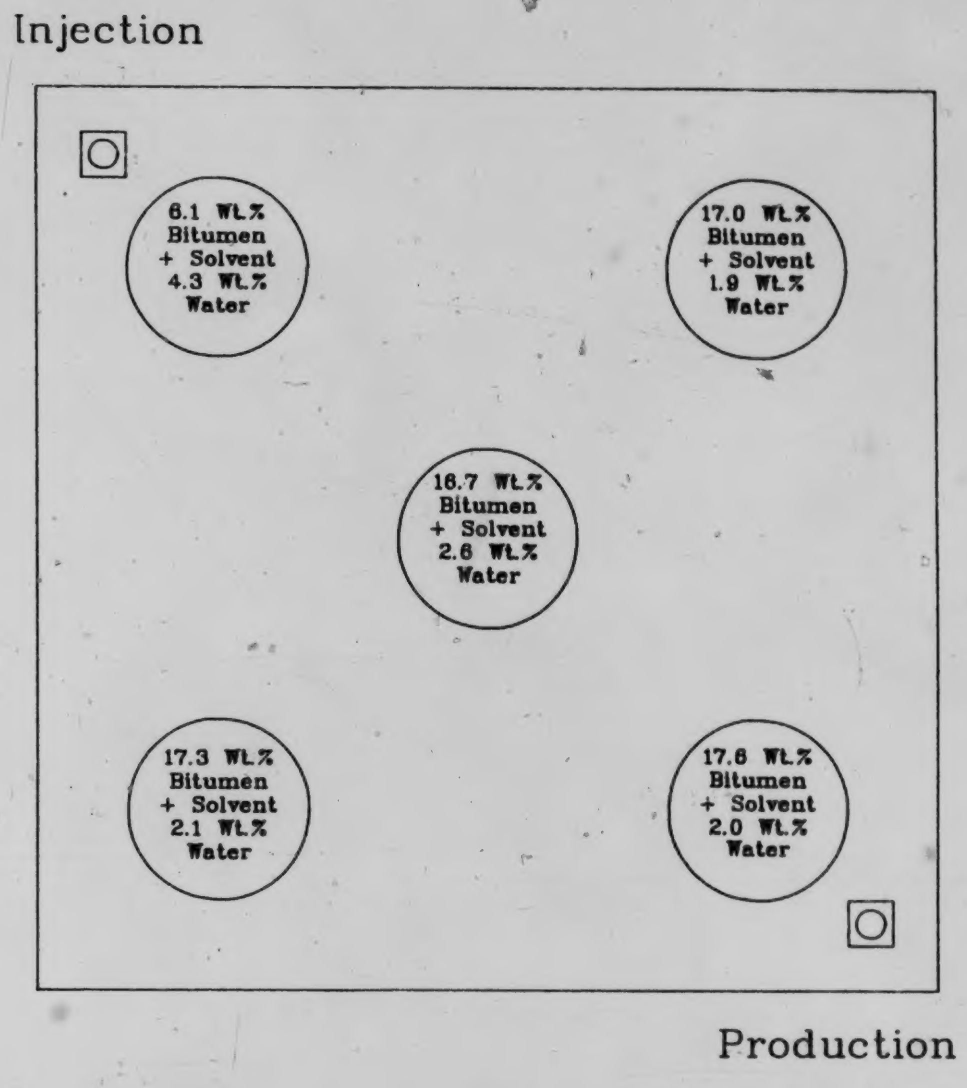
Injection
6.1 Wt.% Bitumen + Solvent 4.3 Wt.% Water
17.0 Wt.% Bitumen + Solvent 1.9 Wt.% Water
16.7 Wt.% Bitumen + Solvent 2.6 Wt.% Water
17.3 Wt.% Bitumen + Solvent 2.1 Wt.% Water
17.6 Wt.% Bitumen + Solvent 2.0 Wt.% Water
Production

Initial Bitumen Conc. : 17.2 Wt.%
Initial Water Conc. : 1.2 Wt.%

Figure 4.9 Bitumen and Water Content after Run 14

5. NUMERICAL SIMULATION

One of the objectives of this research is to compare the results of solvent floods obtained experimentally with those simulated numerically with a model for the simulation of solvent leaching of oil sands. Once the simulation of an actual run was achieved, it was possible to elaborate on the different model parameters and gain further insight into the process mechanism.

Numerical simulation of solvent leaching of oil sands was reported by Oguztoreli (1984). A two-dimensional mathematical model for the in situ isothermal solvent leaching of bitumen from oil sands was developed. The model was slightly modified in this work to account for the bottom water layer. For the basic model, the papers by Oguztoreli and Farouq Ali (1984, 1986) may be referred to. In the following sections the mathematical development of the model will be discussed briefly and the relevant parameters will be defined.

5.1 Porous Region

The liquid phase is a solvent-bitumen solution in which the constituents propagate by both convection and diffusion. The semi-solid phase is composed of discrete spherical particles confined to the pores of the matrix rock. Only diffusion occurs in this phase. The instantaneous porosity, ϕ, as defined by Oguztoreli (1984), is the volume fraction in which convection currents exist in the liquid phase. The constant matrix porosity, ϕ_m, is the volume fraction occupied by the combined solid-liquid mixture with the saturation, S, as the liquid fraction.

$$S = \frac{\phi}{\phi_m}$$

The average particle radius, r_p, is related to the liquid saturation using a particle number density, N_p, with the assumption of a uniform local size distribution.

$$S = 1 - \frac{4\pi}{3} \frac{N_p}{\phi} r_p^3$$

5.2 Radial Dissolution

Concentration gradients are established at the solute-solution contact of each particle as a result of the discontinuities in diffusive properties. These gradients create diffusion currents at the molecular level carrying bitumen from the solute particles into the streaming interstitial solution. As the bitumen desorbs from the solute, the spherical particles shrink in solid volume. The radial advance of the contact is the velocity of dissolution, r_p, in the model.

$$r_p = \frac{dr_p}{dt}$$

A uniform solvent concentration is assumed throughout the liquid phase with an initial non-zero saturation. All solid particles are initially bitumen and void of solvent. A critical concentration, C^*, determines the solidity of solid-liquid interface. The solvent concentration within the solid is less than or equal to this critical and the concentration at any external point in the liquid is greater.

A semi-solid molecular diffusion coefficent, D_s, determines the diffusion rate of solvent within the solid interior. Diffusion is governed by Fick's Law. Each sphere has an initial radius, $r_0(x,y)$, and is subject to radial dissolution with a moving boundary.

$$\frac{D_s}{r^2}\frac{\partial}{\partial r}\left(r^2\frac{\partial C_s}{\partial r}\right)=\frac{\partial C_s}{\partial t}\ ; \qquad 0 \le r \le r_p(t)$$

$$\left.\begin{aligned} r_p(0) &= r_0 \\ C_s(r_p, t>0) &= C^* \\ C_s(r, t=0) &= 0 \end{aligned}\right\}$$

The radial solvent concentration within the solid interior, C_s, is determined analytically using the method of Laplace transforms. The solvent mass within the solid sphere is obtained by spatially integrating the radial concentration.

The adsorption coefficient, α, governs the rate of solvent adsorption across the transition zone of the contact. Conservation of solvent mass equates the solvent transferred from the liquid to the accumulation within the solid spheres. This yields the the radial dissolution integro-differential equation for the sphere radius, r_p, as a function of the macroscopic liquid phase solvent concentration, C ,

$$\left.\begin{aligned} C^*\frac{\partial}{\partial t}\left\{r_0F(t)+\int_0^t \dot{r}_p(\tau)F(t-\tau)\,d\tau\right\} &= r_p^2\left[C\dot{r}_p+\alpha(C-C^*)\right] \\ F(t) &= r_p^2\left[\frac{1}{3}-\frac{2}{\pi^2}\sum_{k=1}^{\infty} e^{-k^2\pi^2D_st/r_p^2}\right] \end{aligned}\right\}$$

5.3 Convective-Diffusion with Adsorption

Solvent with constant density is transported in the liquid phase by convection and diffusion. In a flowing fluid, molecular diffusion is augmented by directional velocity dispersion.

For moderate flow rates, Perkins and Johnston (1963) found that the apparent longitudinal and transverse diffusion coefficients varied with the first power of the velocity magnitude, u. These apparent coefficients are determined in terms of total cross sectional areas.

$$D_\ell = \frac{D_0}{F_r} + \frac{1}{2}\sigma d_p u$$

$$D_t = \frac{D_0}{F_r} + 0.157\sigma d_p u$$

The constant liquid phase molecular diffusion coefficient, D_0, is adjusted by the formation resistivity factor, F_r, to account for the tortuosity of the capillary network. The average particle diameter, d_p, is the grain size and σ is a measure of packing inhomogeneity.

Conservation of solvent mass relates the net accumulation within the combined solute-solution system to the convective and diffusive transport fluxes in the macroscopic scale. Solvent accumulation in the solute to the interphase solvent transfer through adsorption, to give the convective-diffusion with adsorption equation.

$$\frac{\partial}{\partial x}\left[\frac{\rho k_x}{\mu}\frac{\partial}{\partial x}(p + \rho g h)\right] + \frac{\partial}{\partial y}\left[\frac{\rho k_y}{\mu}\frac{\partial}{\partial y}(p + \rho g h)\right]$$

$$= \phi_m\left(1 - \frac{4\pi}{3} N_p r_p^3\right)\frac{\partial \rho}{\partial t}$$

The matrix of the cartesian dispersion coefficient tensor is related to the longitudinal and transverse coefficients as a function of the velocity angle, θ

$$\begin{bmatrix} D_{xx} & D_{xy} \\ D_{yx} & D_{yy} \end{bmatrix} = \begin{bmatrix} D_\ell \cos^2\theta + D_t \sin^2\theta & (D_\ell - D_t)\cos\theta \sin\theta \\ (D_\ell - D_t)\cos\theta \sin\theta & D_\ell \sin^2\theta + D_t \cos^2\theta \end{bmatrix}$$

$$\theta = \tan^{-1}\left(\frac{u_y}{u_x}\right)$$

5.4 Darcy-Continuity Equation

The apparent velocity vector, u, is the rate of gross fluid flow through a unit area. Assuming sufficient capillarity and laminar flow rates, the velocity is related to the potential gradient by Darcy's law.

$$u_x = -\frac{k_x}{\mu}\frac{\partial \Phi}{\partial x}$$

$$u_y = -\frac{k_y}{\mu}\frac{\partial \Phi}{\partial y}$$

Assuming small changes in density, the force potential per unit volume, Φ, is the total of hydrodynamic pressure, P, and the hydrostatic gravity head, ρgh.

$$\Phi = P + \rho gh$$

The fluid density, ρ, is determined by the concentration weighted average of the component densities,

$$\rho = (\rho_s - \rho_0)C + \rho_0$$

and g is the acceleration due to gravity. It is assumed that solid phase dissolution will create a instantneous porosity increase resulting in capillary enlargement for the packed bed. The component permeabilities are related analytically to the porosity by the Kozeny-Carman equation.

$$k_i = k_{i0} \frac{(1-\phi_0)^2 \phi^3}{\phi_0^3 (1-\phi)^2}$$

The permeabilities, k_{i0}, are measured at the reference porosity, ϕ_0. The fluid viscosity, μ, is the fluid resistance to flow due to internal cohesive forces. The viscosity is assumed to be independent of fluid inertia for the flow rates in the laminar regime and dependent only on molecular interaction. For the solvent-bitumen system, the viscosity is related to the liquidity determined by the solvent concentration, component viscosities and densities using Cragoe's Method. The method defines a liquidity, L, based on the viscosity measured in mPa.s

$$L(\mu) = \frac{1000 \ell n 20}{\ell n \mu - \ell n (5x10^{-4})}$$

The fluid liquidity is calculated by the mass fractional weighted average of component liquidities,

$$L(\mu) = M_s L(\mu_s) + (1 - M_s) L(\mu_o)$$

with M_s as the solvent mass fraction.

$$M_s = \frac{\rho_s}{\rho} C$$

Although the individual fluid components are incompressible, there would be some fluid mass accumulation as a result of porosity changes by dissolution, and density variations due to mixing. Dissolution of solid bitumen generates fluid as a result of nonreversible phase changes. Conservation of fluid mass determines the rate of mass accumulation to that generated by dissolution and the fluid fluxes within the porous medium.

$$\frac{\partial}{\partial x}\left(D_{xx}\frac{\partial C}{\partial x} + D_{xy}\frac{\partial C}{\partial y} - u_x C\right) + \frac{\partial}{\partial y}\left(D_{yx}\frac{\partial C}{\partial x} + D_{yy}\frac{\partial C}{\partial y} - u_y C\right)$$

$$= \left(\phi_m - \frac{4\pi}{3} N_p r_p^3\right)\frac{\partial C}{\partial t} + 4\pi N_p r_p^2[\alpha(C-C^*)]$$

5.5 Leaching

The mechanisms that govern dissolution kinetics are solvent adsorption and solvent absorption. Adsorption is the surface phenomenon responsible for the driving force behind dissolution. Absorption is internal, solid phase, solvent accumulation in the solid interior, and may produce an initial swelling. The leaching process is first dominated by dissolution, followed by a miscible drive.

The system void of solvent sources and pressure gradients can be modelled by the radial dissolution equation coupled with the adsorption equation. The equations in dimensionless form will give rise to the Damkohler number, N_{Da}, which is the characteristic ratio of the solvent adsorption rate from the liquid phase to the diffusion rate in the solid interior.

$$N_{Da} = \frac{\alpha r_0}{D_0}$$

The accumulation term in the radial dissolution equation determines solvent absorption from the liquid phase with the critical concentration, C^*, as the capacitance. In the absence of adsorption (N_{Da}), solvent absorption will increase the solid mass as a result of internal solvent diffusion bounded by the critical concentration ($C_s < C^*$). A maximum swell capacitance is determined from the lower bound to the equilibrium saturation, S_e.

$$C^* = \frac{S_0 - S_e}{1 - S_e} C_0$$

above which, pore space is not available to accommodate solid expansion.

Adsorption is the driving mechanism for the dissolution process. As solvent is adsorbed into the solid, local concentrations about the contact are forced above the critical. That portion above the critical undergoes an irreversible phase change resulting in the dissolution of solid material. As dissolution proceeds, the liquid concentration drops indicating bitumen desorption. When the solid phase is completely dissolved, an equilibrium concentration is reached. Adsorption decreases rapidly as the liquid concentration approaches the critical, leaving absorption to elevate internal concentration levels to the critical.

Dissolution and miscible displacement are the two phenomena that are concurrently involved in the solvent leaching process. Constricted flow within the bitumen saturated sands allows rapid solvent absorption into the solid. Absorption is followed by a dissolution driven irreversible phase change. The upstream constrictions are gradually relieved, as the liquid pore space increases. A dissolution wave trails the sluggish displacement, creating a high porosity zone with increased mobility. Upstream dissolution is driven by adsorption while absorption increases downstream solid-phase concentration levels.

Solid bitumen downstream responds to the fresh upstream solvent with rapid dissolution. A burst of dissolved bitumen appears in the effluent, and dissolution ceases with the completion of total phase inversion. A miscible drive follows to displace the remaining bitumen in solution. Injection pressures peak high initially as a consequence of low injectivity. As dissolution proceeds, pressures drops exponentially raising the injectivities by several orders of magnitude. The time scaling of dissolution with displacement is crucial for resolution of the saturation history. The dimensionless time ratio,

$$\frac{t_d}{PV} = \frac{D_s \phi_m L W \Delta Z}{r_0^2 \, q_{in}}$$

relates the dissolution time, t_d, to pore volumes of injected solvent, PV.

5.6 Simulation

The laboratory scale rectangular model in which the solvent flood runs with bottom water were performed was chosen as a basis for simulation. Among the solvent flood runs, Run 9, gave the best match with simulation. Geometric equality in both the physical model and the simulation was maintained. Fluid and formation properties used in the simulation were the same as those in the experimental run. The permeabilities were taken different in x and z direction for the oil sand formation. It was believed that the packing in the vertical direction was tighter thus resulting in lower permeability in z direction. The value of 0.5 darcy was estimated based on the permeability of the lateral direction. Dimensionless numbers and adsorption coefficents were chosen to give the best history match with the experimental results. Simulation data is given in Table 5.1. The resistivity factor, F_r, and the inhomogeneity factor, σ, were the average values taken from Perkins and Johnston (1963).

In order to avoid the infinite pressures required to move the solid bitumen in the mathematical model, the simulation assumed an initial solvent saturation. Invasion time of the pore space by solvent was small compared to the total injection period. The experimental run, on the other hand, started with zero solvent saturation. At first, water was displaced by the solvent in the bottom layer. Effluent breakthrough occurred after 0.33 HCPV of solvent injection. At this point, the solvent was assumed to occupy the pore space, and any additional injection resulted in bitumen production. The initial amount of solvent in the bitumen zone was calculated to be the difference between the solvent injected and the water produced at the effluent breakthrough point. Since both are immiscible and incompressible, the solvent

TABLE 5.1 Leaching Simulation Data

Model Dimensions

$L = 60$ cm

$W = 3.75$

$\Delta Z = 6.25$ cm

Bitumen Zone

$k_{x0} = 1.8$ darcy

$k_{z0} = 0.5$ darcy

$\Delta Z = 5.25$ cm

Water Zone

$k_x = 6$ darcy

$k_z = 6$ darcy

$\Delta Z = 1.0$ cm

Fluid Properties

$q_{in} = 0.0833$ ml/s

ρ_o(oil sand) = 1.03 g/ml

ρ_s(solvent) = 0.845 g/ml

μ_o(bitumen) = 80,000 mPa.s
at 25 °C

Parameters

$D_0 = 10^{-4}$ cm^2/s

$F_{ro} = 4$

$\sigma = 3.5$

$r_p = 0.2$ cm

$C^* = 0.10$

$S_0 = 0.20$

$\alpha = 2.7 \times 10^{-5}$ cm/s

$D_s = 10^{-8}$ cm^2/s

r_0(particle diameter) = 0.1 cm

$N_{Da} = 270.0$

LL

displaced water volumetrically. The total injection was 120 ml and the water produced was 30 ml. The difference of 90 ml solvent was presumed to occupy the bitumen zone. The saturation was then obtained by dividing the solvent in place by the total bitumen and solvent in place.

The simulation starting point thus corresponded to the effluent breakthrough in the experimental run (0.33 HCPV). The results of both runs are shown in Figure 5.1. The bitumen concentration increases rapidly until it peaks at 69%. The values are all volumetric percentages. Bitumen concentration by weight is higher due to the smaller density of the solvent.

At about 1 HCPV injection, dissolution is completed and a rapid drop in concentration is observed. The concentration declines gradually as more solvent is injected and produced in the effluent. There are a few local maximums in the experimental data. These are thought to be caused by the intervals during which the run had to be stopped in order to refill the pump. During these intervals, which were about five minutes each, diffusion had time to contact bitumen in the absence of displacement. The relatively bitumen rich effluent was observed in the very next effluent samples. The small peaks which occur after about 1.5 HCPV injection in the simulation curve were caused by numerical dispersion.

The results of both simulation and experimental runs seem to match each other well. It should be remembered that the experimental data were taken at a small number of points. Hence they represent the average values between two subsequent data points. The overall trend is very similar in both, and the later recoveries tend to match better.

Although the fluids are incompressible, there is mass transfer taking place between the solid and fluid phase. In the beginning of the run the volumetric production rate was less than the injection rate. This is observed both in the experimental run and the simulation. At this stage, the solvent is absorbed by the solid bitumen phase. On the other hand, the mass flow rates were the same. In the later stages of the run the volumetric production rate approaches the injection rate due to the completion of the leaching process. In general a greater volume

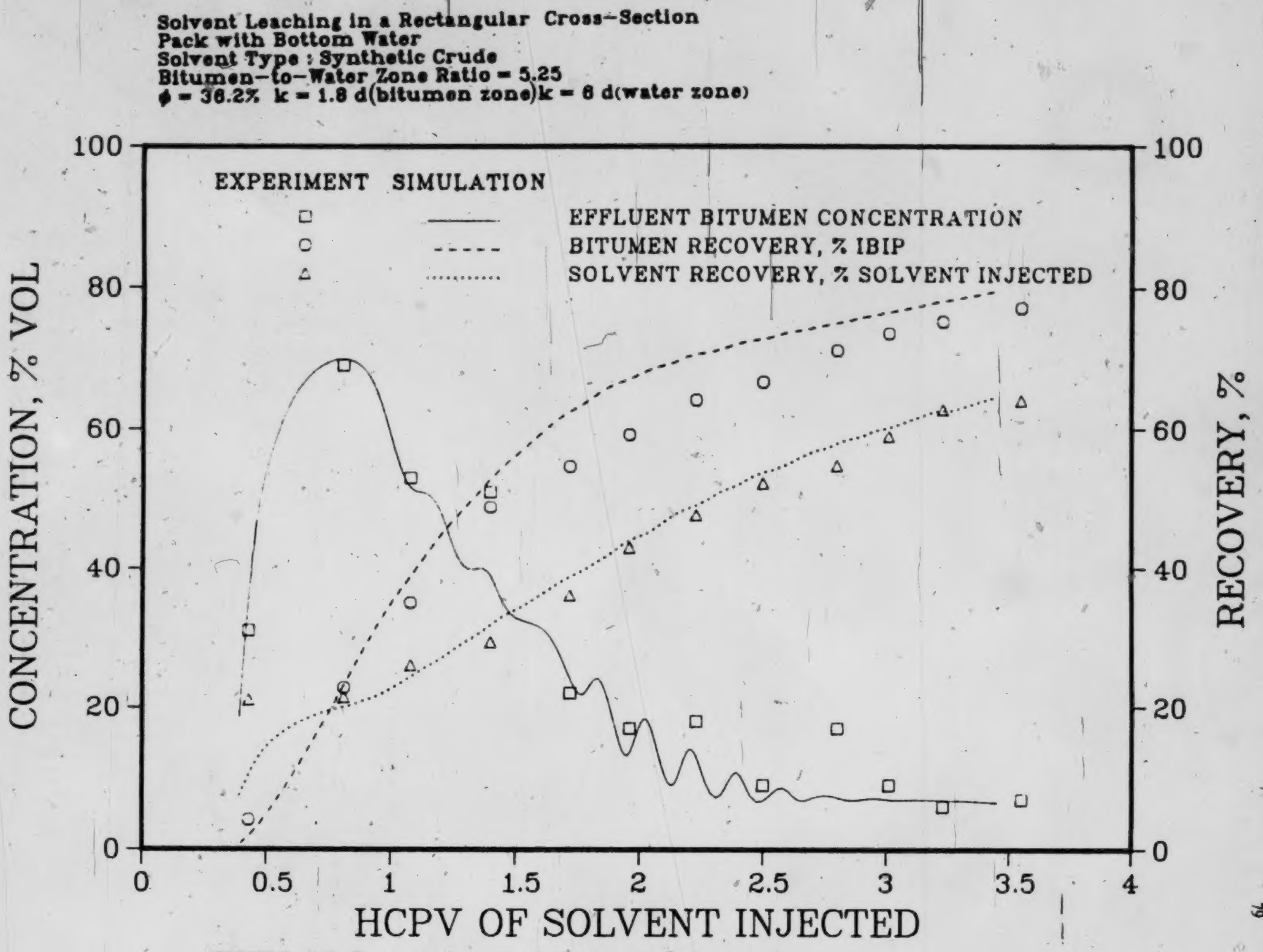

FIGURE 5.1 Concentration and Recovery Profiles

of a relatively lighter solvent is needed to displace the denser bitumen. This must be taken into account in a field scale application. A material balance check was made for the experiment and found to be very acceptable. The simulation checked the material balance at the end of each iteration. The maximum overshoot in the concentration profiles was 9% during miscible displacement.

5.7 Effect of Bottom Water on Leaching

As was discussed in the previous chapter concerning the bottom water runs, the relative thickness of the water zone played an important role in the process. In order to evaluate the extreme cases, two more simulation runs were made to isolate the effect of bottom water zone thickness. This way physical experiments restricted to a smaller range of paramaters would be extended from the ones at hand. The simulation runs were performed for three different water zone thicknesses. Figures 5.2 through 5.4 give the concentration profiles for each run. A summary of these runs is given in Table 5.2.

TABLE 5.2. Effect of Bottom Water Thickness

Thickness Ratio	**Bitumen Recovery, %**	**Solvent Recovery, %**
3.33	71	58
5.25	80	65.5
12.0	85	64

The highest recovery as seen from the above table and the respective figures was obtained from the run with the thinnest water zone(ratio=12). On the other hand, the run with a ratio of 3.33, 23 % of the total thickness, gave the lowest recoveries of solvent and

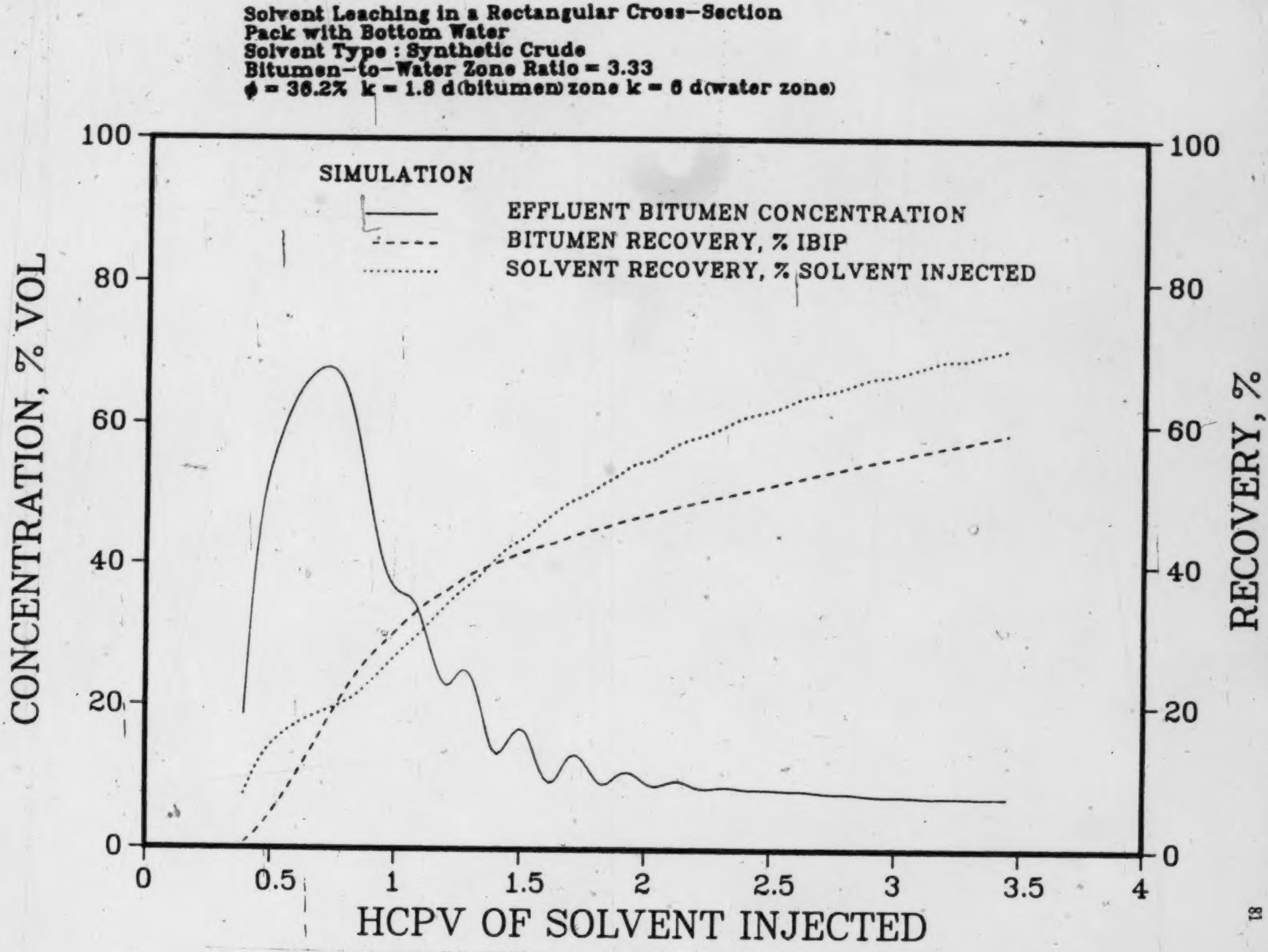

Solvent Leaching in a Rectangular Cross−Section
Pack with Bottom Water
Solvent Type : Synthetic Crude
Bitumen−to−Water Zone Ratio = 3.33
ϕ = 36.2% k = 1.8 d(bitumen) zone k = 6 d(water zone)

FIGURE 5.2 Concentration and Recovery Profiles

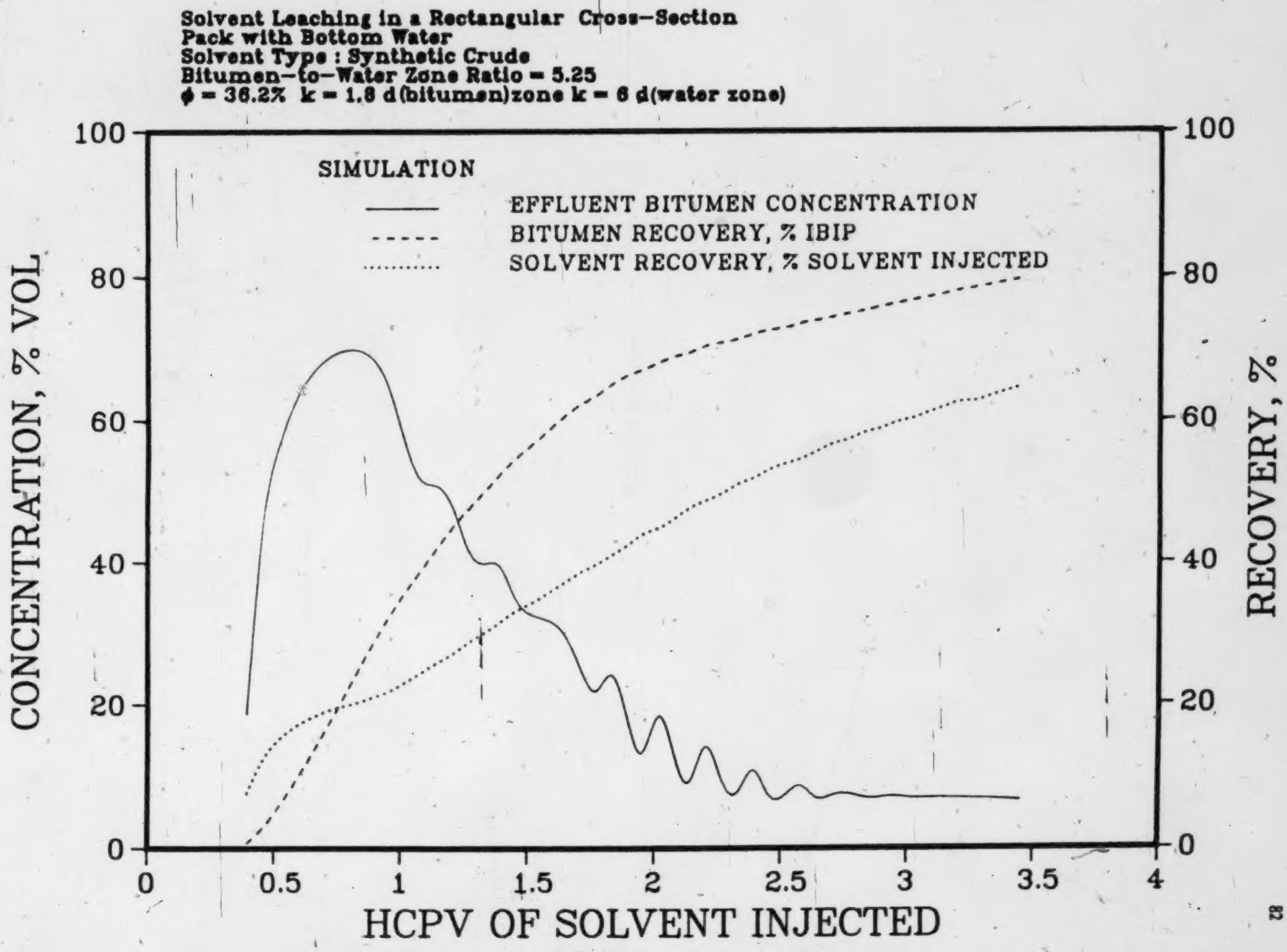

FIGURE 5.3 Concentration and Recovery Profiles

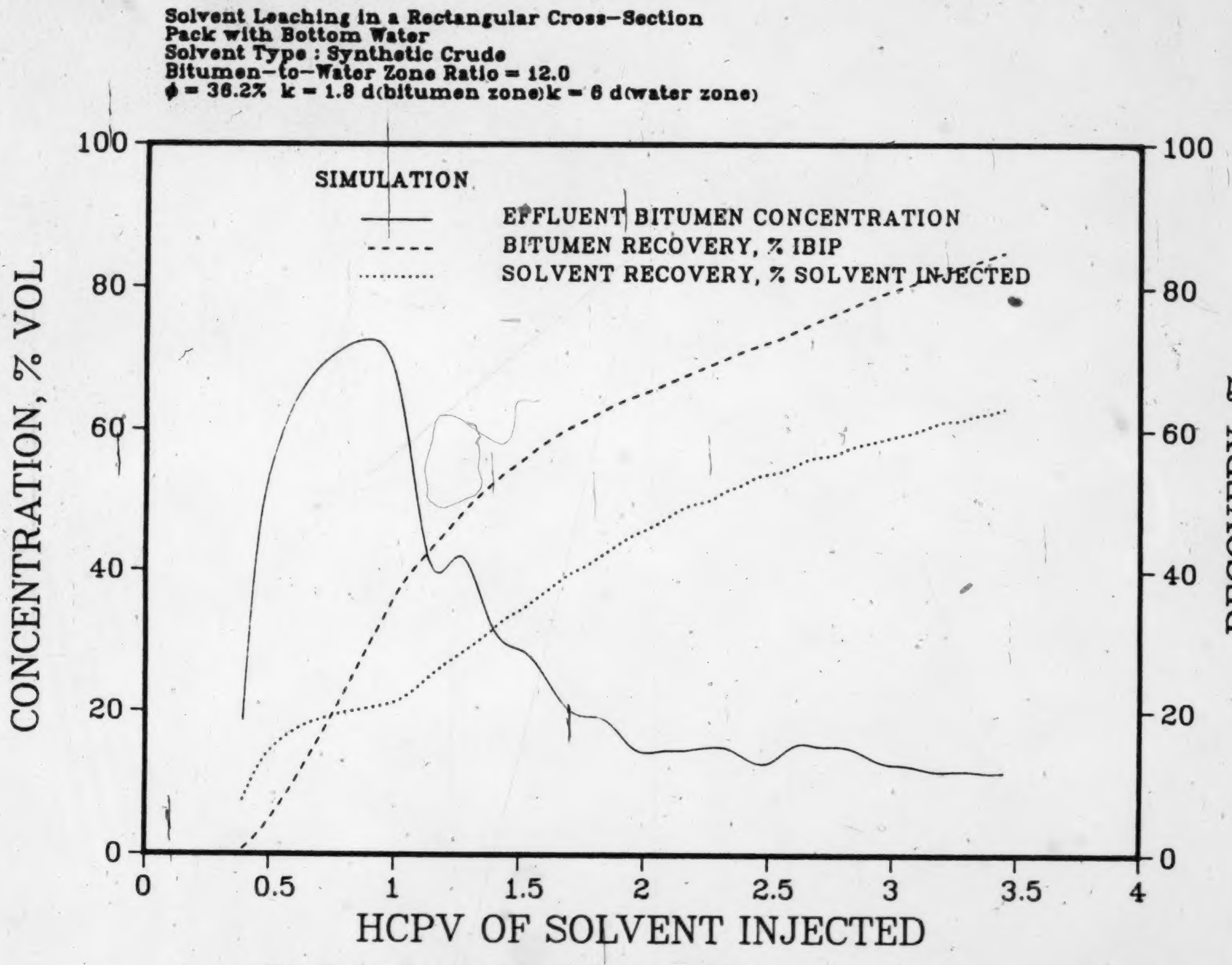

FIGURE 5.4 Concentration and Recovery Profiles

bitumen. The run with the ratio of 5.25 was the simulation of the actual run, which was discussed earlier.

The movement of the solvent through the core is important in the evaluation of the recovery performance. It is apparent that the relative thickness and permeability of the water zone play decisive roles. If the water zone is thick and very permeable, the solvent will channel into the more permeable water zone and will be produced relatively free of bitumen. The points of injection and production are also of importance. In the experiments, the solvent was injected in the middle of the oil sand zone and the production was from the lower portion of the bitumen zone close to the water zone. It was intended that in such an arrangement the effluent would be transported through the bottom zone. In order to monitor this, the solvent concentrations throughout the flood and along the core were plotted in Figures 5.5 through 5.10 for the three different thickness ratios.

From Figure 5.5 for the run with a ratio of 3.33, it can be seen that solvent channels into the water zone quickly. Consequently the solvent which follows goes into the producing well without contacting much of the bitumen. At the end there is still a high bitumen concentration zone towards the production end. On the other hand, the solvent in the run with a thickness ratio of 5.25, channels into the production end later than the previous one. It is evident that the effluent is carried through the bottom water zone, where the permeability is higher. Towards the end of the run, much of the bitumen in the core is swept and produced. In the case of a very thin water zone, ratio of 12, the solvent channels through the top of the bitumen layer. ~~The~~ thickness of the water layer is not enough to divert the solvent and the bitumen recovery is the highest due to the unswept water zone.

An optically produced gray scales of the concentration profiles in Figure 5.8 for each run at different injection times clearly shows how the solvent travelled in the core. Note that the solvent was not much affected by the bottom zone in the run with ratio of a 12. Instead it preferentially moved to the top of the core. This could be merely a result of numerical tendency but it nevertheless shows the importance of a high permeability channel in carrying a highly viscous effluent. Incidentally, a similar observation was made in the experimental Run 13. The thickness ratio was 7 for that run. Upon post-run inspection, it was found that the top of the bitumen layer was soft and contacted by the solvent. As in Run 13, the injection pressures required were higher than the previous runs. It is thus difficult to perform such a run in a laboratory core. This may also be true in a field scale application in shallow oil sand formations.

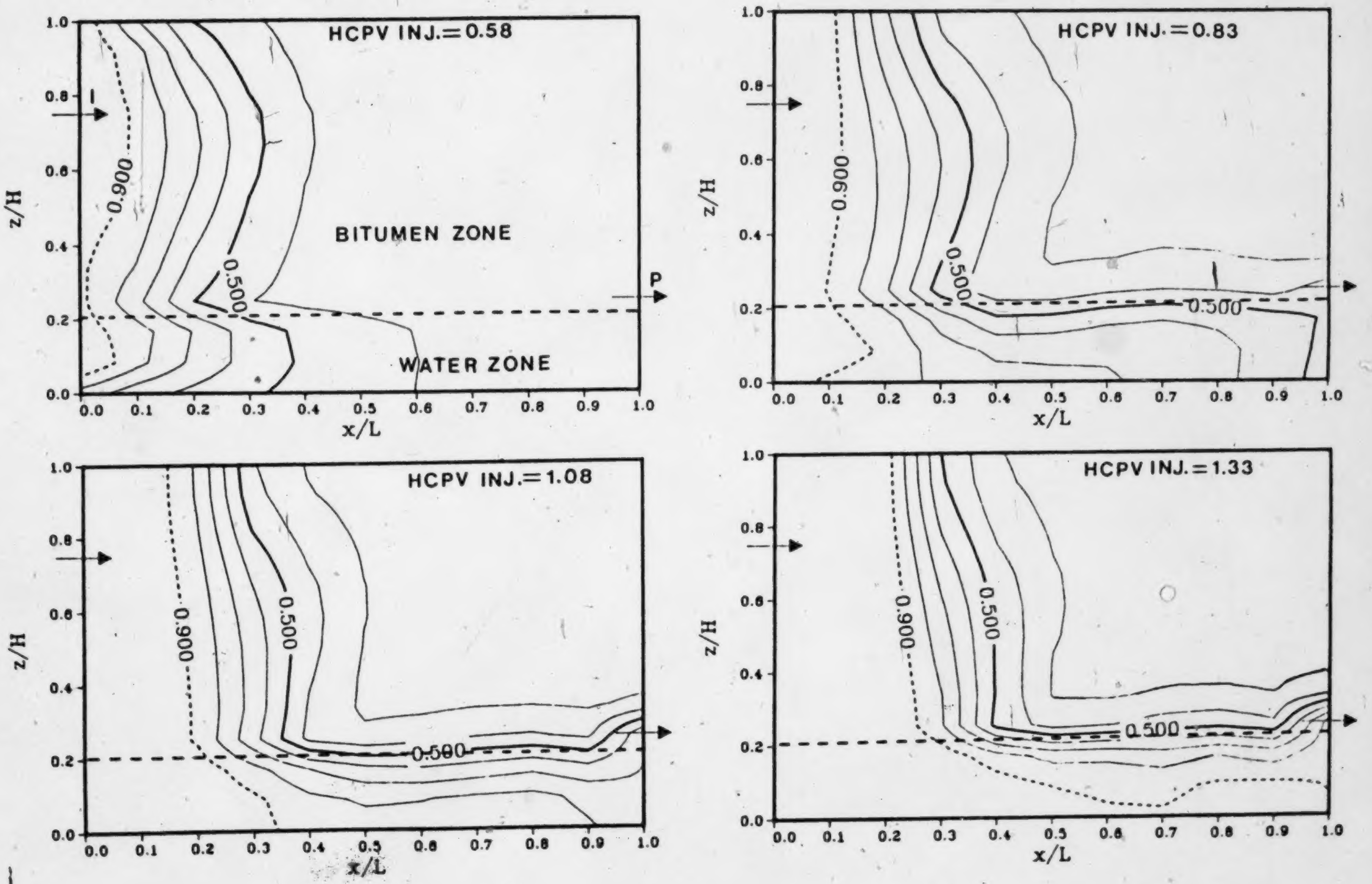

FIGURE 5.5 Solvent concentrations along the core at different injection times

Bitumen-to-Water Zone Ratio = 3.33

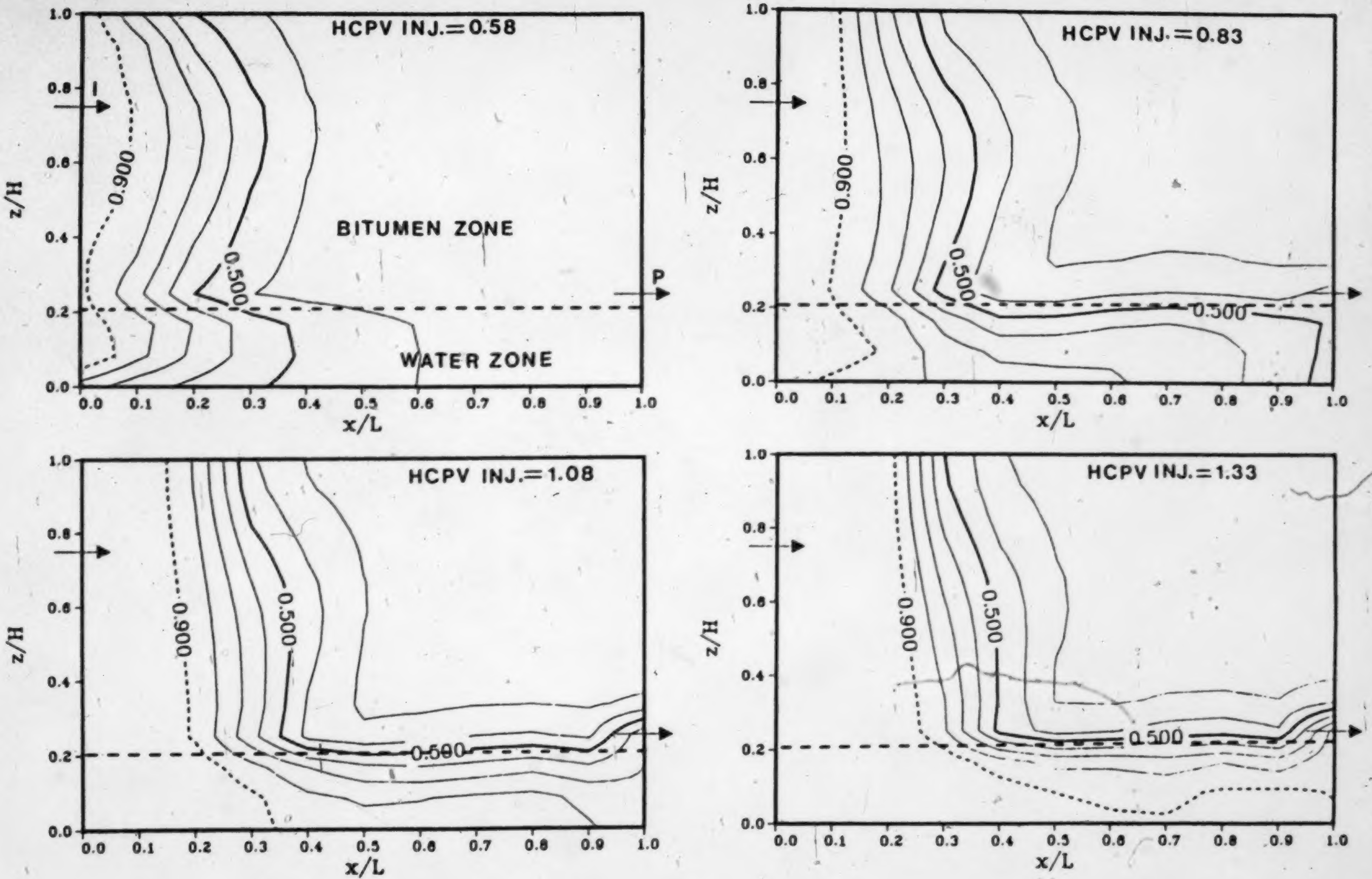

FIGURE 5.5 (CONTINUED)

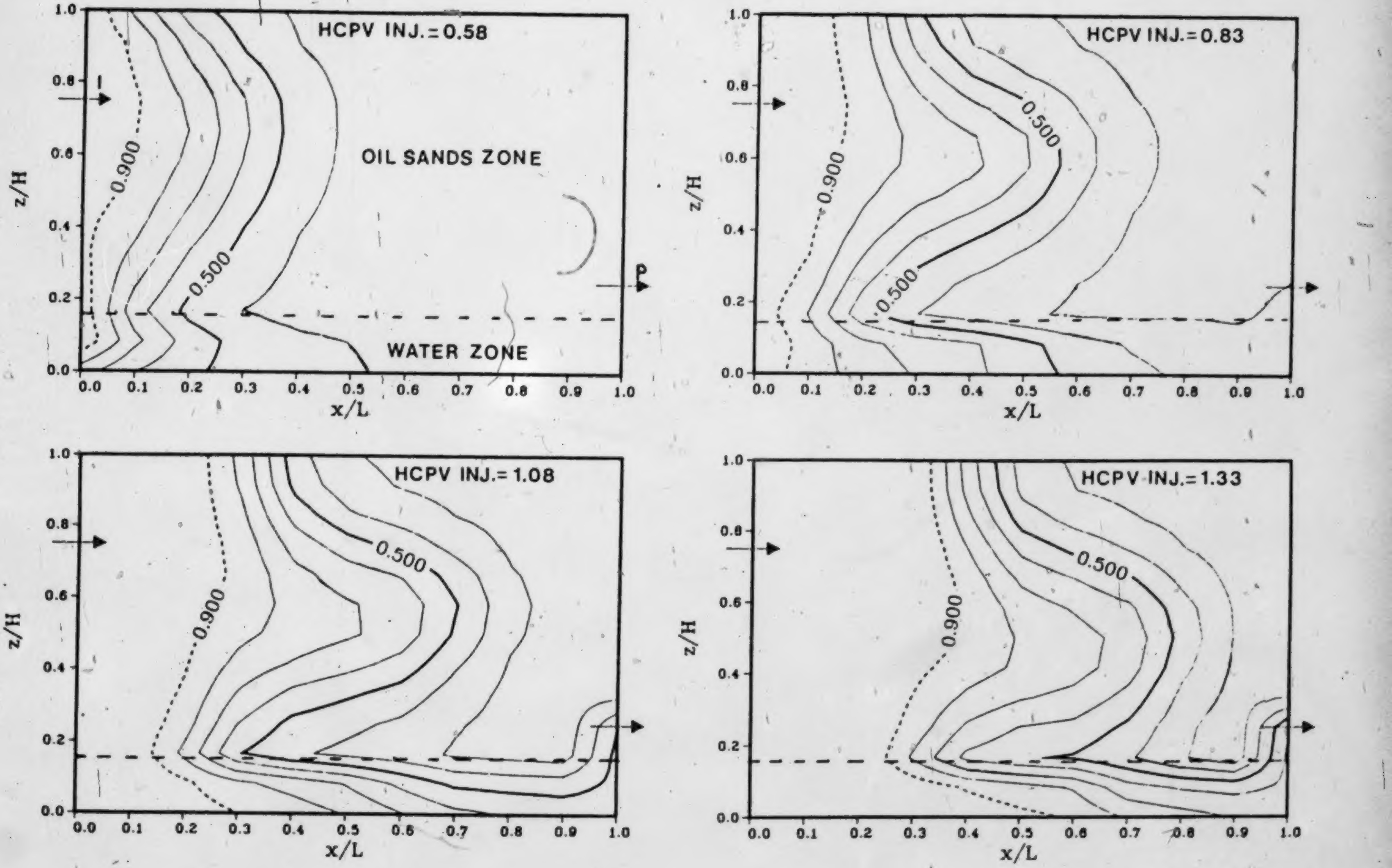

FIGURE 5.6 Solvent concentrations along the core at different injection times
Bitumen-to-Water Zone Ratio = 5.25

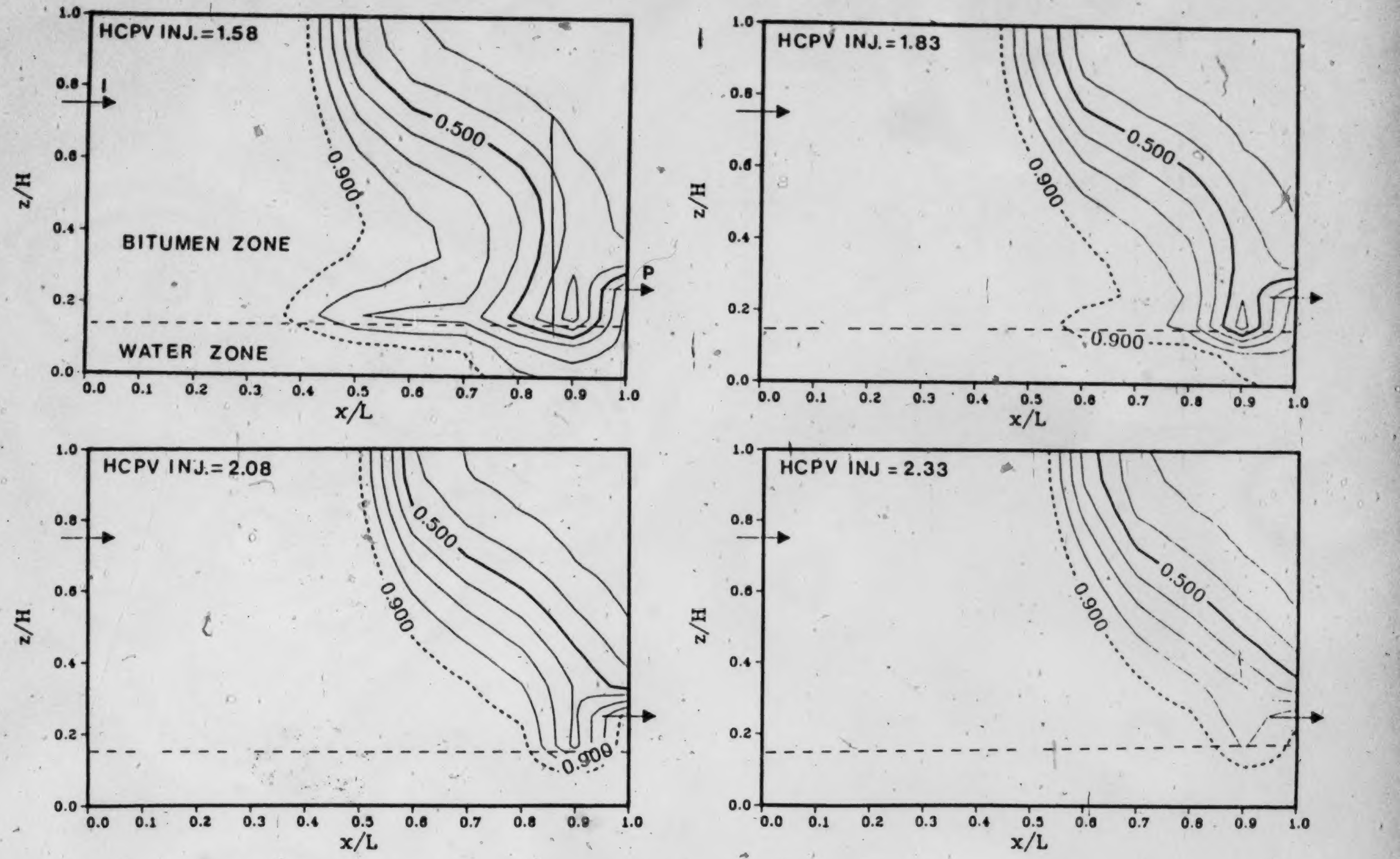

FIGURE 5.6 (CONTINUED)

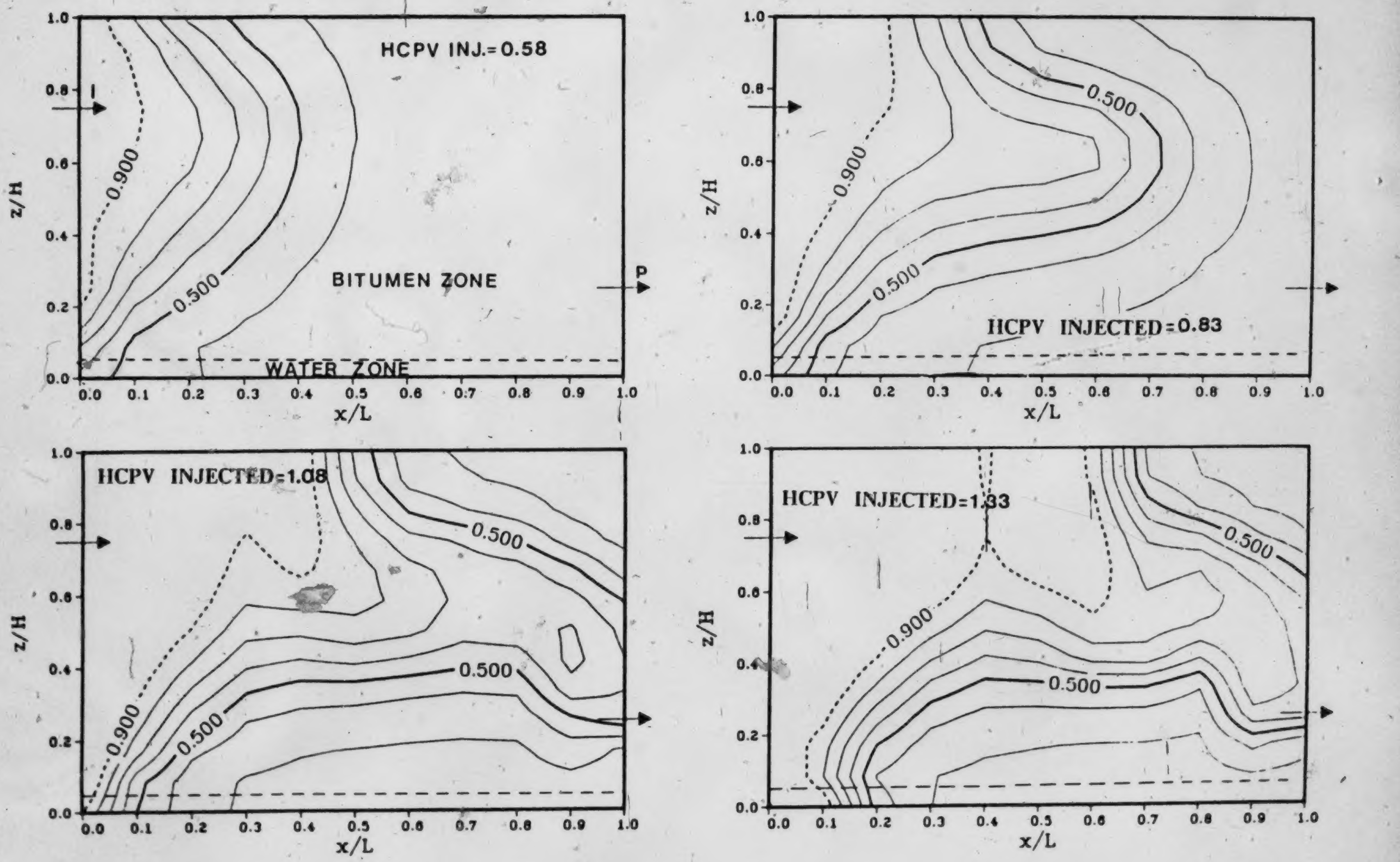

FIGURE 5.7 Solvent concentrations along the core at different injection times

Bitumen-to-Water Zone Ratio = 12.0

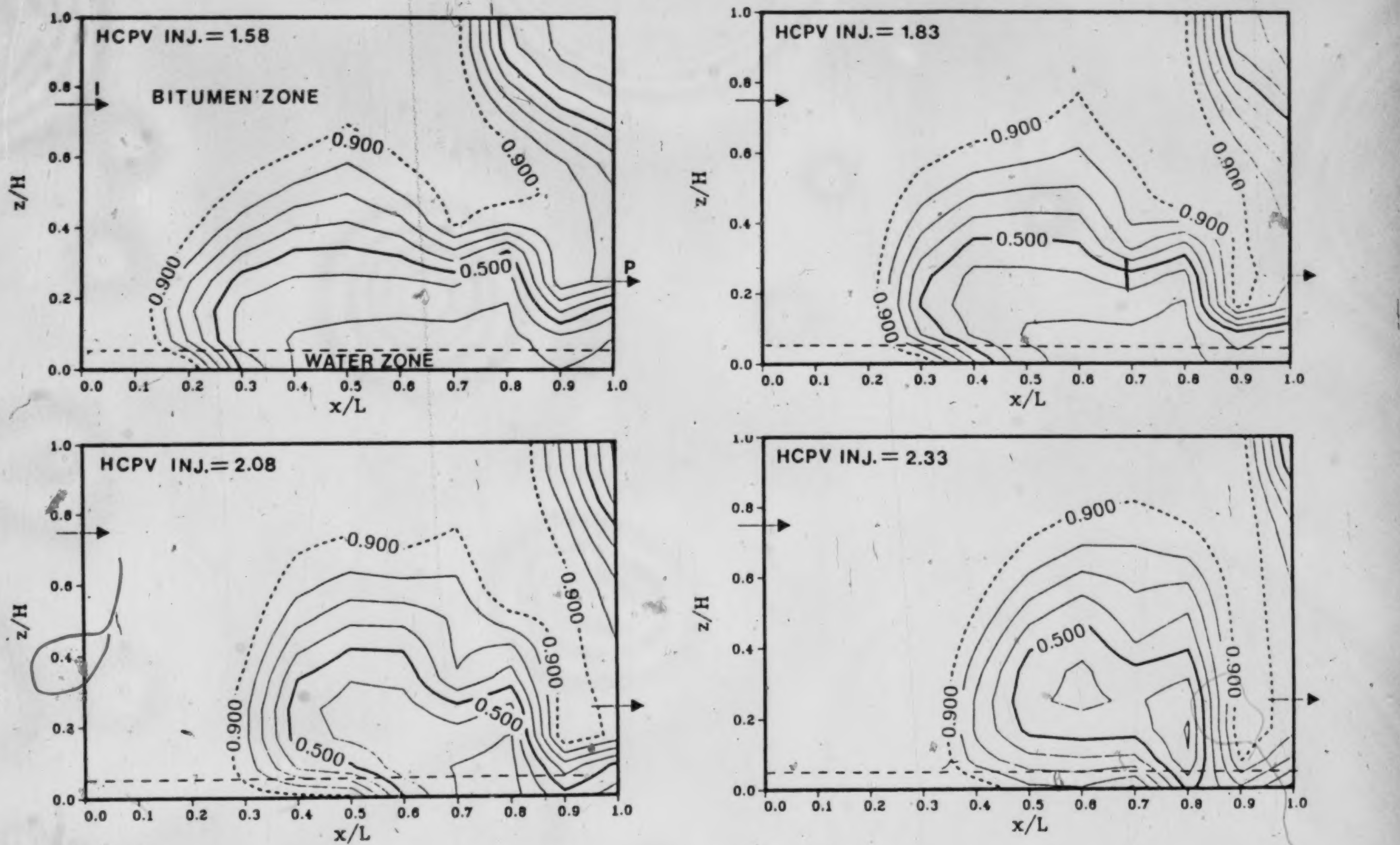

FIGURE 5.7 (CONTINUED)

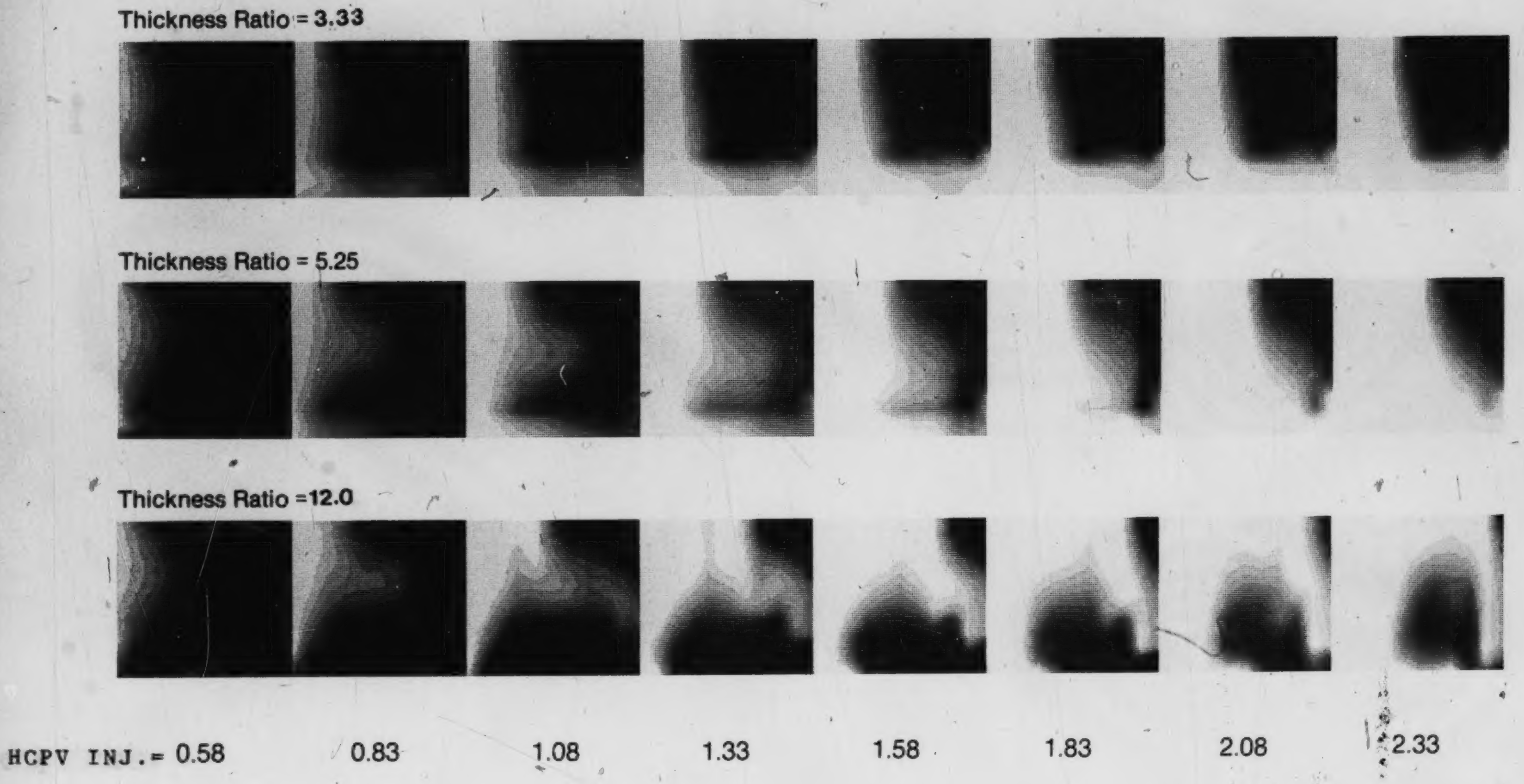

Figure 5.8. Solvent Concentrations along the core at different injection times.

6. LEACHING MODEL

6.1 Analytical Formulation

One of the objectives of this research was to correlate the results of the rectangular model experiments with those predicted by other *in situ* recovery techniques used in leaching of various minerals. Leaching originally referred to the percolation of the liquid through a bed of the solid, and is now used to describe the operation generally by whatever means it may be accomplished.

Current interest in leaching from the reservoir engineering view is in the area of *in situ* recovery of uranium ore, which is adopted to solvent leaching of bitumen in this investigation. Uranium ore found at shallow depths is not rich enough to warrant surface operations, yet it may be economic to recover by an *in situ* technique. It is usually in oxidized form and its recovery requires chemical reactions.

Use of streamlines in predicting recovery performances was first used by Muskat (1937), Higgins and Leighton (1962, 1964) for secondary recovery and Wang *et al* (1979) for tertiary oil recovery. For solution mining, Bommer and Schechter (1979) and Kabir(1982) used the streamlines. Two important assumptions are generally made in streamline models: time independent well conditions so that the streamlines are fixed with time, and no cross flow occurs among streamlines. A pictorial representation of a streamline is shown in Figure 6.1A.

In this study an attempt was made to combine the material balance and streamline equations and derive a scaling criterion for solvent leaching of oil sand. With scaling criterion on hand, the results of rectangular core experiments were used to predict the concentrations for various flood patterns. The equations to predict the well effluent concentrations are derived in Appendix A. The effluent bitumen history of the well is computed from the

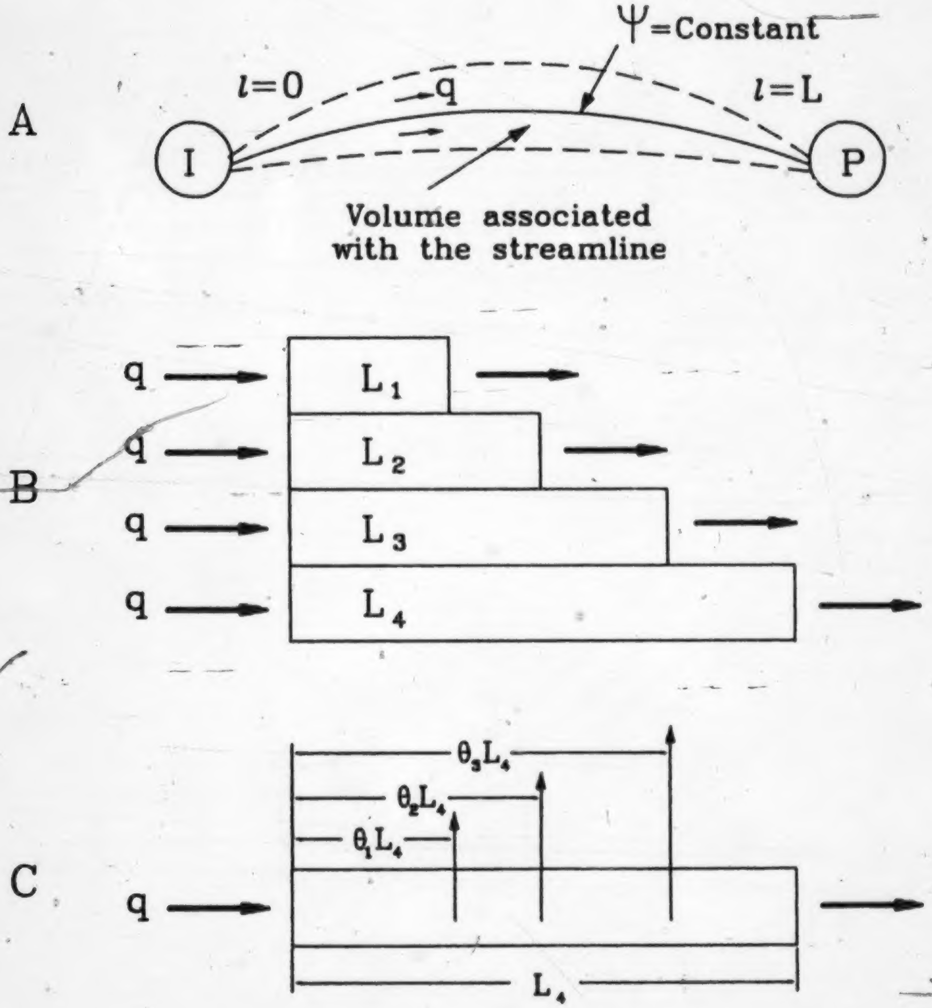
A
Ψ=Constant
l=0
q
l=L
I
P
Volume associated with the streamline
B
q
L 1
q
L 2
q
L 3
q
L 4
C
θ3L4
θ2L4
θ1L4
q
L4

Figure 6.1 Layered Presentation of Streamlines

summation

$$C_D(t_D^P) = \frac{1}{N_s} \sum_{j=1}^{N_s} \{C_D(\theta_j, \theta_j t_D)\}_\ell \tag{6.1}$$

The effluent solvent concentrations are given by a similar equation:

$$C_{sD}(t_D^P) = \frac{1}{N_s} \sum_{j=1}^{N_s} \{C_{sD}(\theta_j, \theta_j t_D)\}_\ell \tag{6.2}$$

These equations indicate that concentrations are required as function of both time and position. The concentrations can be calculated by a numerical scheme if the relevant data are available or they can be the results of laboratory experiments. The data are obtained by sampling along the length of a laboratory core at various times. However this can be difficult in a model packed with oil sand in the absence of a high permeability channel. If the proper sampling is achieved, the results can then be scaled to field conditions.

The above equations can be interpreted in another fashion. The bundle of streamlines associated with a producer can be taken as non-communicating layers. The layers have equal thickness and cross-sectional areas but different lengths. Thus they have unequal pore volumes. For such a system,

$$\theta_j = \frac{L_j}{L_\ell} \quad j=1,\dots N_s \tag{6.3}$$

This representation is shown in Figure 6.1B. The stack of layers can also be represented as a single layer of length L, with observation points at distances from the injector $\theta_j L_\ell$. Such a presentation is shown in Figure 6.1C. The mathematical expression of this relationship is:

$$C(1,t) = \{ C(\theta_j L, t) \}_\ell \tag{6.4}$$

Equation (6.4) means that the concentration at a streamline can be obtained from a corresponding observation point at the longest streamline. The interpretation of θ is that θ is the ratio of the arrival time of the jth streamline to the longest streamline. Equations (6.1) and (6.4) are identical while equations (6.1) and (6.2) are expressed in dimensionless time and distance.

The dimensionless distances in equations (6.1) and (6.2) are related by the equation:

$$t_D^P = \beta_j t_{D,j} \tag{6.5}$$

where

$$\beta_j = \frac{N_s V_{p,j}}{V_p^P}$$

The β_j values can be calculated by a computer program for desired N_s values. The β_j values in this study are taken from Kabir(1984). These values for five spot and line drive patterns are given in Table 6.1.

Using equation (6.3), it is possible to predict the streamline and well effluent concentrations from the history of a single streamline. Before applying this method, the validity of the procedure was checked. In a carefully designed experimental run in the rectangular model, the prediction of well concentrations was tested by taking samples along the model at corresponding arrival times. The sampling distances were determined by the parameter θ_j. The reference streamline having the largest volume or the largest N_{Da} was

Table 6.1 β_j **Values for Line Drive and Five Spot Patterns**

Line Drive[*]		Five Spot	
j	β_j	j	β_j
1	0.61659	1	0.73104
2	0.62489	2	0.7400
3	0.63946	3	0.75904
4	0.65680	4	0.78904
5	0.67857	5	0.83296
6	0.70498	6	0.89496
7	0.73680	7	0.98304
8	0.65680	8	1.14400
9	0.81966	9	1.33000
10	0.87300	10	1.82600
11	0.93639		
12	1.01136		
13	1.01593		
14	1.21209		
15	1.34978		
16	1.45845		
17	1.63912		
18	1.75120		
19	1.81424		
20	1.89876		

[*] Injector-injector distance= producer-producer distance

represented by the entire core. Note that θ_j does not depend on the bitumen and is between 0 and 1. Its values can be calculated from the ratio of the β values.

The rectangular model was equipped with additional observation wells. The relative distances of the wells from the inlet were calculated from the ratio of the β's. The largest β_j value for the line drive pattern is 1.89876 and the smallest value is 0.61659 (Table 6.1) Their ratio, 0.3247, gives the relative distance of the first observation well from the injector. All of remaining observation points can then be determined in the same manner by the ratio of each β_j value to the maximum β_j. In a short laboratory core, however, the implementation of all the points was not possible. For this reason only three observation wells were drilled along the core(later, six wells). These points were j= 1, 11, and 16 from the line drive pattern. By choosing the scattered points along the core, it was hoped to obtain a better average of all the points.

6.2 Experimental Runs

A total of three runs were conducted to test the model. In the first of these runs (Run 20), the rectangular model was packed with oil sand without any bottom water. After drawing a vacuum on the pack, the model was saturated with the solvent (Synthetic Crude), just before the run was started. The solvent, which was injected at a rate of,300 ml/h, failed to reach the production end even at the maximum working pressure of the core. After only 18% HCPV of solvent injected it was decided to take samples. It was possible to take samples from all three observation wells. Following sampling of the wells, the injection was restarted at 100 ml/h but it had to be stopped because of the high injection pressure(3800 kPa). This procedure was repeated twice without producing any fluid at the production well.

In a last attempt, the nitrogen gas from a high pressure cylinder was forced to the third observation well. All the other the wells were closed except the production one. Still no fluid was produced at the open end. The run was then converted to an inject and produce test to see whether such a procedure could be employed to recover the mobilized bitumen around the injection point. This way the effluent was produced from the observation well, and the run was terminated. Upon inspection of the core, it was observed that the solvent had failed to reach the observation well. In a second attempt, Run 21 was performed in a little different manner.

In order to be able into inject solvent continuously, water was injected to the core to establish communication between the wells. This was similar to Run 19 where the surfactant solution was injected at the producing end and a solvent flood was subsequently achieved without the presence of a water zone. The water injection was stopped when it broke through at the production end. Subsequently, solvent injection was started. Effluent samples were taken from the observation and producing points at predetermined intervals. Each time, about 3-4 ml of sample were taken from each observation well. The amount of bitumen obtained from the observation points was not accounted for in recovery calculations. In Table 6.2, an example of calculations is given for two different dimensionless time values. The concentrations from the streamline and the observation points are within 10% of each other for these two times. The concentrations compare well up to 1.5 HCPV(Dimensionless time = 1.25) injection. Then they deviate as much as 25%. A comparison of the concentrations is given in Figure 6.2. The deviation could be explained by the fact that the leaching part of the displacement is by and large completed by 1.5 HCPV solvent injection. The dissolved bitumen

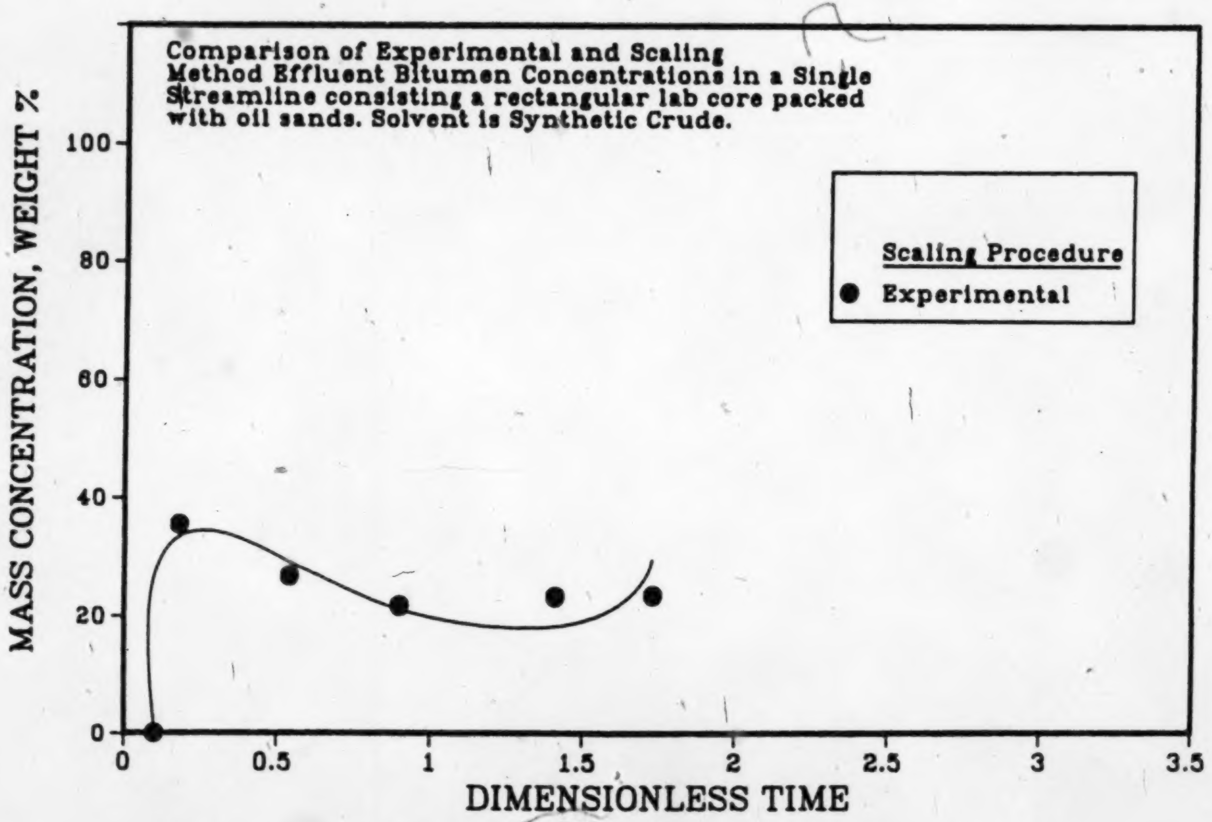

Figure 6.2. Effluent Concentration History

is then carried by miscible displacement.

Table 6.2 Example Calculation for Leaching in Line Drive

	$t_D^P = 0.18$		$t_D^P = 0.90$	
j	$t_{D',j}$	C	$t_{D',j}$	C
1	0.2919	0.21751	1.4141	0.0781
11	0.1939	0.1894	0.9611	0.2648
16	0.1241	0.5886	0.6170	0.2760
		+		+
	Equation 6.1	0.3318		0.2063
	Experimental	0.3538		0.2150

Encouraged by the comparison, it was then attempted to predict the well effluent concentrations in five spot and line drive patterns. Using the equation 6.1 and the data from the experiment and the Table 6.1, the concentrations in a solvent flood were predicted. Figure 6.3 shows the profile for five spot solvent flooding. Similarly, Figure 6.4 is for the line drive. In both figures, the well concentrations are lower than the single streamline bitumen ones.

6.3 Limitations of the Model

The data points were taken from only 3 observation wells. Although more data points are desirable, this might not be practical as well as improper. The volume of effluent samples taken certainly influences the concentration measured at the producing end, and this, in turn, affects the reliability of the predictions.

The scaling technique assumes that the bitumen is uniformly distributed initially. Although the laboratory tests can be conducted with fairly uniform oil sand packs, the bitumen saturations may vary considerably in field conditions. The dispersion gradients normal to the streamlines are assumed negligible in the derivation of the material balance equations.

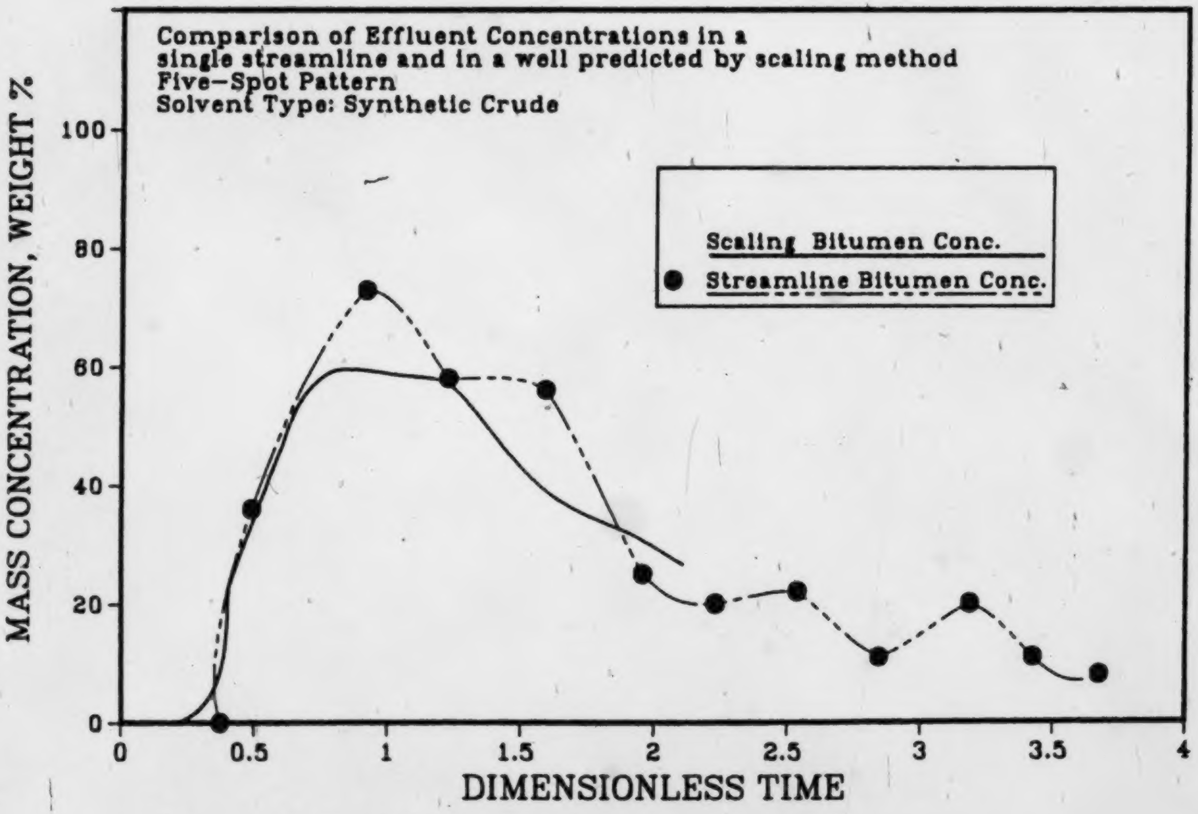

Figure 6.3 Effluent Concentration History

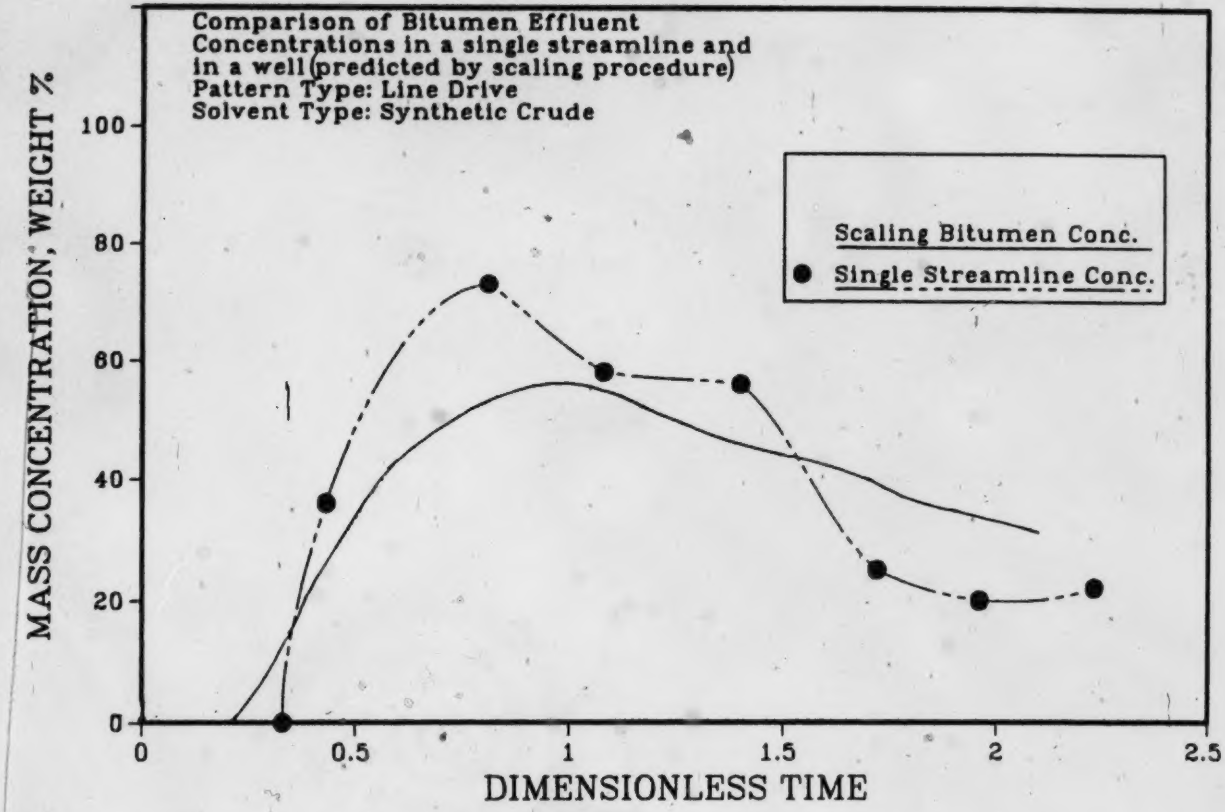

Figure 6.4. Effluent Concentration History

The recovery of bitumen from oil sands is not entirely governed by the leaching process. As was discussed in the numerical simulation chapter, the recovery is dominated by miscible displacement at the conclusion of the dissolution of the semi-solid bitumen. According to both simulation results and results of this chapter, the leaching part of the displacement is completed by 1.5 HCPV solvent injection. The Peclet number governing the miscible displacement is ignored for the sake of the scaling in the material balance equations derived in Appendix A. In the leaching dominated part of the process, the omission of the Peclet number does not seem to affect the predictions significantly. It should be noted that only the liquid phase diffusion coefficients are ignored. The solid phase diffusion coefficient, D_s, is included in the dimensionless Damkohler number.

This procedure does not take the porosity changes into account. But it is still valid since the porosity changes are the same in each streamline with uniform distribution. The viscosity of the solvent used was 4.56 mPa.s while there was water in the formation. The densities of solvent and water were 0.845 g/ml and 1.00 g/ml, respectively. Although it is assumed that they are equal, the differences in the viscosities and densities are not great.

7. CONCLUSIONS

This chapter presents the main conclusions drawn from this experimental and theoretical study on mobilization of bitumen/heavy oil. The conclusions are outlined in the approximately same order as the list of objectives in Chapter 2. They may be valid for the sand fluid system and injection strategies used herein.

1. Small solvent slugs can mobilize bitumen/heavy oil but fail to transport it to the producers, in the absence of a high permeability channel.

2. Continuous solvent injection with the presence of a bottom water zone resulted in bitumen recoveries as high as 80% of bitumen in place. The water zone served as a transporting medium for the mobilized bitumen. The relative thickness of the water zone was the crucial factor in bitumen mobilization. Thick zones were detrimental to mobilization. However, very thin zones required high injection pressures. A bitumen-to-water thickness ratio of 5 gave the optimum results in the experiments conducted.

3. Carbon dioxide and surfactant are less effective than solvent in mobilizing bitumen/heavy oil, whether alone or in combination with each other. Carbon dioxide, when used with synthetic crude, further improves recovery. The gas provides drive energy, helping the displacing agent.

4. Surfactant, in combination with solvent, improves the bitumen and solvent recovery. It is particulary effective after the viscosity of bitumen is reduced by the solvent.

5. A modified numerical simulator designed to simulate the water zone adequately predicted the concentration and recovery profiles for solvent leaching of bitumen. From the residual saturations analyzed and the numerical simulation, it can be concluded that the

dissolved bitumen is carried through the bottom water zone from the start. As the leaching process continues, the permeability of the swept zone increases due to bitumen dissolution.

6. An analytical treatment of the leaching problem was developed using a streamline model to determine the well effluent concentrations for the various flood patterns using the rectangular model results. The concentrations predicted by the model and those obtained from experimental runs were in good agreement, until the dissolution process was largely completed. The streamline model, which only considered the leaching process, was not effective when dispersion started to dominate. The numerical simulation which took both leaching and miscible displacement into account showed that the the miscible displacement started to influence the process at around 1.5 HCPV solvent injection, which was confirmed by the deviation of the streamline model predicted concentrations.

8. RECOMMENDATIONS

The experiments in this work were performed at room temperature. Although the high bitumen/heavy oil recoveries can be achieved employing solvent, surfactants and gases, the amount of solvent required is substantial. A large amount of solvent is left in the formation. Some of the future experiments should be repeated at elevated temperatures in an attempt to decrease the amount of solvent and its loss. The influence of the surfactants could also be more pronounced at elevated temperatures. In addition, the gas injection was performed at low pressures to prevent the corrosion of the model. If coating of the model is accomplished, carbon dioxide injection could be performed at higher pressures.

Besides the general suggestion with respect to use of heat, some future runs should be conducted to observe the effects of heterogeneity of the bottom water zone. Such experiments are of academic interest since they help in understanding the process. Specifically, the situations where the high permeability zone is not present around the injection well or production well and the effects of injecting and producing from the same well in order to increase the permeability and porosity around the injection well in the absence of a bottom water zone.

Since the thermal methods are mostly employed in heavy oil formations, use of steam with solvent and surfactant should be considered to assess the economic feasibility of the process in the presence of a bottom water zone.

REFERENCES

Abad Guerra ,B.P., "Thermal Miscible Displacement Studies in Athabasca Tar Sands," M.S. Thesis,The Pennslyvania State University (March 1975).

Alban, G.L.I., "Recovery of Bitumen from Athabasca Tar Sand by Miscible Processes", M.S. Thesis, The Pennsylvania State University, May 1975.

Alikhan, A.A., and Farouq Ali, S.M., " Oil recovery by hydrocarbon slugs drive by a hot water bank", Soc. Pet. Eng. J.,1971 **11**, 342-50.

Alikhan, A.A. and Farouq Ali, S.M., "Heavy oil recovery by steam-driven hydrocarbon slugs from linear porous packs", Journal of University of Kuwait (Science)8, 1981.

Blackwell, R. J., and Terry, W. M., "Factors Influencing the Efficiency of Miscible Displacement", Trans. AIME, *216*, 1 (1959).

Bommer, P.M. and Schechter, R.S, "Optimization of Uranium Leach Mining" Soc. Pet. Eng. J., 1982 22, 132-140.

Briggs, J. P. and Puttagunta, V. R., "The effect of Carbon Dioxide on the Viscosity of Lloydminster Aberfeldy Oil at Reservoir Temperature", Alberta Research Council, Oil Sands Department, Edmonton, Alberta, Jan. 1984.

Briggs, J.P., Redford, D.A., and Harris, P., "Core sized physical experiments to study the effect of naphtha and CO_2 addition to steam in the recovery of bitumen from oil sands", CIM Paper No. 82-33-84, 33rd Annual Technical Meeting of the Petroleum Society of CIM, Calgary, June 6-9, 1982.

Cashdollar, C.H., The effect of Viscosity Ratio and Path Length on Miscible Displacement in Porous Media, M.S. Thesis, The Pennslyvania State University (1959).

Cragoe, C.S., "Changes in the Viscosity of Liquids with Temperature, Pressure and Composition," Proc. World Petroleum Congress, Vol.II (1963), pp 529-541.

Currie, D.J., Hathaway, A.P., Isaacs, E.E., Mar, A., Morrison, and D.N., Richmond, C., "The potential of the crumble test as a tool for oil sands research", paper presented at the 30th Can. Chem. Eng. Conf., October, 19-22 1980, Edmonton.

Davies, G.A., Ponter, A.B., and Craine, K. "The Diffusion of Carbon Dioxide in Organic Liquids" The Canadian Journal of Chemical Engineering, Vol.45, December,1967.

Denoyelle, L. and Bardon, C., "Diffusivity of Carbon Dioxide into Reservoir Fluids", Paper CIM 115-15: 30 presented at the 86th CIM Annual General Meeting, Ottawa, April 17, 1984.

Diaz, M. T., " Asphaltene Precipitation", M.S. Thesis, Pennslyvania State University, May 1978.

Ehrlich, R., "Laboratory Investigation of Steam Displacement in the Wabasca Grand Rapids "A" Sands", Oil Sands of Canada Venezuela, CIM (1977), 364-379.

Farouq Ali, S.M., Look Yee, K.C., Cordero, F.J., Figueroa, J.M., "Role of injection-production strategy in the solvent-steamflooding of the Athabasca Oil Sands" J. Can. Pet. Tech. (October-December, 1979).

Farouq Ali and Snyder, S.G., "Miscible Thermal Methods Applied to a Two-Dimensional, Vertical Tar Sand Pack, with Restricted Fluid Entry", Journal of Canadian Petroleum Technology, October-December, 1973.

Graue, D.J. and Zana, E.T., "Study of a Possible CO_2 Flood in Rangely Field," Jour. Pet. Tech., July 1981, 1312-1318.

Handy, L., and Ziegler, V., " The Effect of Temperature on Surfactant Adsorption in Porous Media", SPE No. 8264, Las Vegas, Nevada, Sept. 23-26, 1979.

Handy, L., El Gassier, M., and Ershaghi, I., "Interfacial Tension Properties of Surfactant-Oil Systems Measured by a Modified Spinning Drop Method at High Temperatures", SPE Paper No. 9003, Stanford, California, May 28-30, 1980.

Hekim, Y and Fogler, H.S., "On the Movement of Multiple Reaction Zones in Porous Media", AIChE Journal(Vol.26, No.3) May, 1980.

Higgins, R.V. and Leighton, A.J., "A Computer Method to Calculate Two-Phase Flow in Any Irregularly Bounded Porous Medium", Jour. Pet. Tech. (June, 1962) 679.

Higgins, R.V., Boley, D.W. and Leighton, A.J. " Aids to Forecasting the Performance of Water Floods", Journal of Petroleum Technology, September 1964, 1076-1082.

Huygen, H.H.A., and Lowry, W.E., Jr., "Steamflooding Wabasca Tar Sand Through the Bottom Water Zone - Scaled Lab Experiments", Paper SPE 8398, presented at the 54th Annual Fall Meeting of SPE, Las Vegas, Sept. 23-26, 1979.

Isaacs, E., McCarthy, C., and Smolek, K., 2^{nd} Eur. Sym. on Enhanced Oil Recovery, Paris, 11/8-10/1982.

Islam, M. R. and Farouq Ali, S. M., "Mobility Control in Waterflooding Oil Reservoirs with a Bottom Water Zone" to be presented at the 38th Annual Technical Meeting of the Petroleum Society of CIM, June 7-10, 1987.

Jacobs, F.A., Donnely, J.K., Stanislav, J. and Svrcek, N.Y., "Viscosity of Gas Saturated Bitumen", Jour. Can. Pet. Tech., Oct-Dec. 1980, 46-50.

Kabir, M.I., Lake, L. W., and Schechter, R.S., 1982a "Uranium Leaching Test: Restoration," Society of Petroleum Engineers Journal, Vol 22, No. 1, February, 141-150.

Kabir, M. I., Lake, L. W., and Schechter, R. S., 1982b, "A Minitest of In Situ Uranium Leaching: Practical Problems in the Interpolation of Test Data," In Situ Journal, Vol. 6, No. 4, 181-327.

Kabir, M. I., Schechter, R. S., and Lake, L.W., "Novel Scaling Methods for Modeling In Situ Leaching", Minerals and Metallurgical Processing, May 1985, 127-136.

Kasraie, M and Farouq Ali, S.M., " Heavy Oil Recovery in the Presence of Bottom Water", Paper No. 84-35-122 Presented at the 35th Annual Technical Meeting of the Petroleum Society of CIM, June 10-13, 1984.

Kasraie, M., Farouq Ali, S.M., "Application of Thermal Recovery Techniques to Marginal

Reservoirs", Proc. of 3rd European Meeting on Improved Oil Recovery, Vol 1, Rome 379-389 (1985).

Lake, L.W., Pope, G.A., Carey, G.F., and Sepehrnoori, "Isothermal, Multiphase, Multicomponent Fluid-Flow in Permeable Media. Part I: Description and Mathematical Formulation," Center for Enhanced Oil and Gas Recovery Research, The University of Texas at Austin.

Mehrotra, A.K. and Svrcek, W.Y., "Gas solubility, viscosity and density measurements for Athabasca bitumen", Canadian Journal of Petroleum Technology", July-August 1982.

Mehrotra, A.K. and Svrcek, W.Y., "Measurement and Correlation of Viscosity, Density and Gas Solubility for Marguerite Lake Bitumen Saturated with Carbon Dioxide", AOSTRA Journal of Research, Volume 1 Number 1, September 1984.

Mehrotra, A.K. and Svrcek, W.Y., "Viscosity , Density and Gas Solubility Data for Oil Sand Bitumens. Part I: Athabasca Bitumen Saturated with CO and C_2H_6", AOSTRA Journal of Research, Volume 1, Number 4 June, 1985.

Mehrotra, A.K. and Svrcek, W.Y., "Viscosity , Density and Gas Solubility Data for Oil Sand Bitumens. Part II: Peace River Bitumen Saturated with N_2, CO, CH_4, CO_2 and C_2H_6", AOSTRA Journal of Research, Volume 1, Number 4 June, 1985.

Miller, J.S. and Jones, R.A., "Physical Characteristics of Heavy Oil After CO_2 Saturation are studied in DOE Tests.", The Oil and Gas Journal, July 6, 1981, 135-145.

Mitchell, D.L. and Speight, J.G., "The solubility of Asphaltenes in Hydrocarbon Solvents", Fuel, (1973), Vol. 52, p. 149-152.

Muskat, M., *The Flow of Homogeneous Fluids through Porous Media*, McGraw-Hill, New York, 1937; 2nd printing by Edwards, Ann Arbor, Mich., 1946.

Oguztoreli, M., " The Solvent Leaching of Tar Sands " Master of Science of Thesis, University of Alberta, February 1984.

Oguztoreli, M.,and Farouq Ali, S.M., "A Mathematical Model for the Solvent Leaching of Tar Sand", SPE Journal, Reservoir Engineering, November 1986, Volume 1, Number 16, 545-555.

Perkins, T. K., Johnston, O. C., " A Review of Diffusion and and Dispersion " SPE Journal, March 1963, 70-84.

Prats, M., "Peace River Steam Drive Scaled Model Experiments", Oil Sands of Canada-Venezuela (1977) 346-363

Pursley, S.A., "Experimental Studies of Thermal Recovery Processes", Proc. of Heavy Oil Symp., Maracaibo (1974).

Raplee, G. B., Cottrell, F., Cottrell, S., Raab, J. "Evaluation of Additives to enhance the in-situ steam Processes Applied to U.S and Canadian Tar Sand and Heavy Oil Reservoirs" Final Report, December 1984, DOE/TRW.

Redford, D.A. " The use of Solvents and Gases with Steam in the Recovery of Bitumen for oil sands" Jour. Can. Pet. Tech. Jan-Feb 1982, 45-53.

Redford, D.A., McKay, A.S., "Hydrocarbon Steam Process for Recovery of Bitumen from Oil Sands", Symposium on Enhanced Oil Recovery, SPE/DOE Oklahoma (April 20-23, 1980)

Rodriguez, H.M. "An Investigation of the Mechanics of Miscible Fluid Displacement in Natural Porous Media", M.S. Thesis, The Pennslyvania State University (1957).

Rojas, G.A., "Scaled Model Studies of Immiscible Carbon Dioxide Displacement of Heavy Oil" Ph.D Thesis, University of Alberta (Spring, 1985).

Schechter, R.S and Bommer, P.M., "Mathematical Modelling of *In-Situ* Uranium Leaching," Soc. Pet. Eng. J. (Dec. 1979), 393-400.

Schmidt, T.R., Leshchyshyn, T.H., and Puttagunta, V.R., "Diffusivity of Carbon Dioxide into Athabasca Bitumen", CIM Paper No. 82-33-100, presented at the 33rd Annual Technical Meeting of the Petroleum Society of CIM, Calgary, June 6-9, 1982.

Schmidt, T.R., Ridley, R. and Heidrick, A. "Dispersion of a Solvent Slug Injected Into a Communication Path", SPE Paper No. 13602, presented at SPE California Regional Meeting, Bakersfield, CA, March 27-29, 1985.

Shu, W. R. and Hartman, K. J. " Effect of Solvent on Steam Recovery of Heavy Oil" SPE Paper No. 14223 presented at the 60th Annual Technical Conference of the Society of Petroleum Engineers, Las Vegas, NV September 22-25, 1985.

Starling, K. E.: "Fluid Thermodynamic Properties for Light Petroleum Systems," Gulf Publishing Co., 1973

Stegemeier, G.L. et al.,"Representing Steam Processes with Vacuum Models", Society of Petroleum Engineering Journal, (June 1980), 151-174.

Scheidegger, A.E., "The Physics of Flow Through Porous Media" The MacMillan Co., New York City (1957).

Sievert, J. A., Dew, J. N., and Conley, F. R., "The Deterioration of Miscible Zones as Applied to Recovery Process", Paper SPE 904-G, presented 32nd Annual Fall Meeting of SPE of AIME, Dallas, Texas (Oct., 1957).

Snyder, S.G., "Miscible Thermal Methods Applied to a two-dimensional Vertical Tar Sand Pack with Restricted Fluid Entry", M.S. Thesis, The Pennslyvania State University, December, 1972.

Treybal, R.E., *Mass-Transfer Operations,* McGraw-Hill Book Company, Third Edition, 1980.

Wang, B., Lake, L.W., and Pope, G.A., "Development and Application of a Streamline Micellar/Polymer Simulator," SPE 10290 presented at the 55th Annual Fall Technical Conference, San Antonio, TX, October, 5-7, 1981.

APPENDIX A

Derivation of Scaling Equations

In order to derive the equations used in Chapter 6, a mathematical description of a streamline model coupled with a material balance is needed. The following sections provide a combined derivation of the scaling equations.

Streamline Model

The following assumptions are made in the streamline model.

(a) Single phase flow

(b) Incompressible flow

(c) Viscosities and densities of formation and injected fluids are equal and constant.

(d) Time independent boundary and well conditions.

(e) Homogeneous porosity and permeability but permeability can be anisotropic.

The travel time T of a fluid particle along a streamline is:

$$T = \sum_{k=1}^{M} \Delta t_k \tag{1}$$

where Δt_k is the travel time over a finite increment

$$\Delta t_k = \frac{\Delta \ell}{v(x_k, y_k)} \tag{2}$$

and M is the total increments required for the streamline to traverse from injector to producer.

Thus, the length of the streamline is

$$L = M\Delta\ell \tag{3}$$

Since the boundary conditions are time independent, the streamlines are fixed in time and space.

Since mobilities are constant, the volumetric flow rate associated with each streamline is constant and given as:

$$q = \frac{Q^P}{N_s} \tag{4}$$

where Q^P is the production well flow rate and N_s is the number of streamlines associated with each producer. Since streamlines are traced backward, the production rate, instead of the injection rate, is used in computing the streamline flow rate.

The pore volume associated with each streamline is

$$V_p = qT \tag{5}$$

The travel time T varies from streamline to streamline. Thus, a temporarily omitted subscript should appear on T and V_p.

Material Balance

The material balance equation in Cartesian coordinates for incompressible, single phase, 2-D flow is (Lake, Pope, Carey, and Seperhnoori (1981)):

$$- v_x \frac{\partial C}{\partial x} - v_y \frac{\partial C}{\partial y} + \frac{\partial}{\partial x} (K_{xx} \frac{\partial C}{\partial x}) + \frac{\partial}{\partial x} (K_{xy} \frac{\partial C}{\partial y}) + \frac{\partial}{\partial y} (K_{yx} \frac{\partial C}{\partial x}) + \frac{\partial}{\partial y} (K_{yy} \frac{\partial C}{\partial y}) = \frac{\partial C}{\partial t} + R \tag{6}$$

where C is the concentration (mass per unit pore), R is a source term, and K_{xx}, K_{xy}, K_{yx} and K_{yy} are components of the dispersion tensor. If dispersion gradients normal to the streamline are assumed negligible, (the above equation can be transformed to curvilinear (potential Φ and stream function Ψ) coordinates (Kabir, 1982; Wang *et al* ., 1981)

$$(\frac{\mu v^2}{\bar{k}_a} \frac{\partial C}{\partial \Phi})_{\Psi,t} + \frac{\mu \varphi v^2}{\bar{k}_a} \frac{\partial}{\partial \Phi} (\frac{\mu k_\ell}{\bar{k}_a} \frac{\partial C}{\partial \Phi})_{\Psi,t} = (\frac{\partial C}{\partial t})_{\Psi,\Phi} + R \tag{7}$$

where $\bar{k}_a$ is the absolute permeability given as (Muskat, 1937)

$$\bar{k}_a = [\frac{1}{k_x} (\frac{v_x}{v})^2 + \frac{1}{k_y} (\frac{v_y}{v})^2]^{-1} \tag{8}$$

and k_ℓ, the longitudinal dispersion coefficient, is (Perkins and Johnston (1963)) is given by:

$$k_\ell = \frac{D_0}{F_r} + \alpha_\ell v \tag{9}$$

In the above equation, D_o is the molecular diffusion coefficient, F_r the formation resistance factor, and α_L the longitudinal dispersivity. The (Ψ,Φ) coordinates are orthogonal only if the flow field is isotropic. The method nevertheless is valid if this requirement is not met.

Neglecting the streamline-normal concentration gradient in this development means that $(\frac{\partial C}{\partial \Psi})_{\Phi,t}$ is small. The magnitude of a velocity vector is v. Its components are v_x and v_y. Equation 7 is a material balance equation along a streamline(Ψ or j=constant) and is similar to a 1-D material balance equation. It can be solved for each streamline in a bundle to obtain the producer's effluent history (Kabir, 1982; Wang *et al*., 1981). For the scaling procedure, Equation (7) is further simplified in the following way:

The interstitial velocity $v(\ell)$ and cross-sectional area $A(\ell)$ along a streamline are given by Equations (10) and (11)

$$v(\ell) = -\left(\frac{\phi \bar{k}_a}{\mu} \frac{\partial \Phi}{\partial \ell}\right)_\Psi \tag{10}$$

and

$$A(\ell) = \left(\frac{q}{\phi v(\ell)}\right)_\Psi \tag{11}$$

Using equations (10) and (11), Equation (7) can be simplified to:

$$- v(\ell) \frac{\partial C}{\partial \ell} + \frac{1}{A(\ell)} \frac{\partial}{\partial \ell} \left[\phi A(\ell) k_\ell \frac{\partial C}{\partial \ell}\right] = \frac{\partial C}{\partial t} + R \tag{12}$$

where the subscripts Ψ,Φ were dropped and t indicated the constant variable values in Equation (7). Note that Equation (12) is the concentration balance equation for a 1-D, variable cross section system.

The above mentioned equation can be written in dimensionless form using dimensionless distance ℓ_D and time t_D defined as:

$$\ell_D = \frac{\int_0^{\ell} A(\xi)d\xi}{\int_0^{L} A(\xi)d\xi} = \text{fractional volume measured along a streamline}$$

$$t_D = \frac{\int_0^{\ell} q dt}{\phi \int_0^{L} A(\xi)d\xi} = \frac{qt}{V_p}$$

$$= \text{cumulative flow in fractional streamline pore volumes}$$

In terms of the above dimensionless variables, and neglecting molecular diffusion, D_o, equation (12) becomes

$$-\frac{\partial C}{\partial \ell_D} + \frac{\partial}{\partial \ell_D}\left(\frac{1}{N_{Pe}(\ell_D)}\frac{\partial C}{\partial \ell_D}\right) = \frac{\partial C}{\partial t_D} - \frac{V_p}{q} R \tag{13}$$

where $N_{Pe}(\ell_D)$, the Peclet number, can be defined as:

$$N_{Pe}(\ell_D) = \frac{V_p}{\phi \alpha_\ell A(\ell_D)} \tag{14}$$

If $A(\ell_D)$ does not vary with position, as in a linear system, $N_{Pe}(\ell)$ becomes the constant Peclet number $\frac{L}{\alpha_L}$. Equation (14) shows that N_{Pe} varies along the length of a streamline and from streamline to streamline since V_p will be different for each. Hence, equation (13) should carry a subscript j (for the jth streamline) which is again omitted for clarity.

Equation (13) can be used for the displacement of bitumen by solvent leaching or surfactant solution. Here, the case of solvent leaching will be considered. The concentration balance equation for solvent in the mobile phase (Eq. 13) is:

$$-\frac{\partial C_s}{\partial \ell_D} + \frac{\partial}{\partial \ell_D}\left(\frac{1}{N_{Pe}(\ell_D)}\frac{\partial C_s}{\partial \ell_D}\right) = \frac{\partial C_s}{\partial t_D} + \frac{V_p}{q} R \tag{15}$$

The rate at which solvent dissolves the bitumen is given by R. The reaction rates between the bitumen and the solvent can be expressed as a function of the solvent concentration and the accessible bitumen content. If the reaction rates are kinetically controlled, Kabir *et al.*, 1982b) gave the rate of reaction in a general form for mineral leaching in terms of order of the reaction. While for most other leaching problems involve some kind of chemical reaction, it is the dissolution of the bitumen from the oil sand in this study. The rate of dissolution of bitumen from the oil sand is given by:

$$R = \frac{D_s C W \rho_0 (1-\phi)}{r_0^2 \rho_b \phi} \tag{16}$$

where ρ_o, oil sand density, ρ_b, bitumen density, r_o, particle diameter, C, solvent concentration, and W is the leachable bitumen concentration where W is the weight percentage of bitumen. It is assumed that the solvent can leach all of the bitumen leaving the sand particles bitumen free.

The material balance equation for the bitumen in the mobile phase is

$$-\frac{\partial C}{\partial \ell_D} + \frac{\partial}{\partial \ell_D}\left(\frac{1}{N_{Pe}(\ell_D)}\frac{\partial C}{\partial \ell_D}\right) = \frac{\partial C}{\partial t_D} + \frac{V_p}{q} R \tag{17}$$

The stationary phase material balance equation is

$$\frac{\rho_0 (1-\phi)}{\phi}\frac{\partial W}{\partial t_D} = \frac{V_p}{q} R \tag{18}$$

Substituting Equation (16) in Equations 15, 16, 17 and introducing the following dimensionless variables

$$C_{sD} = \frac{C_s}{C_{si}} \; ; \qquad W_D = \frac{W}{W_i}$$

$$C_D = \frac{C}{C_i} \quad \text{where} \quad C_i = W_i \rho_0 \frac{(1-\phi)}{\phi} \tag{19}$$

(i stands for initial concentrations)

Therefore, Equation (15) for solvent becomes

$$-\frac{\partial C_{sD}}{\partial \ell_D} + \frac{\partial}{\partial \ell_D}\left(\frac{1}{N_{Pe}(\ell_D)}\frac{\partial C_{sD}}{\partial \ell_D}\right) = \frac{\partial C_{sD}}{\partial t_D} + N_{Da} V_i W_D \tag{20}$$

The concentration balance equation for the bitumen in the liquid phase,

$$-\frac{\partial C_D}{\partial \ell_D} + \frac{\partial}{\partial \ell_D}\left(\frac{1}{N_{Pe}(\ell_D)}\frac{\partial C_D}{\partial \ell_D}\right) = \frac{\partial C_D}{\partial t_D} - N_{Da} C_{sD} W_D \tag{21}$$

for the bitumen in the solid phase,

$$\frac{\partial W_D}{\partial t_D} = - N_{Da} C_{sD} W_D \tag{22}$$

where N_{Da}, the dimensionless Damkohler number,

$$N_{Da} = \frac{D_s V_p}{r_0^2 q}$$

and

$$V_i = \frac{W_i \rho_0 (1-\phi)}{\phi \rho_b}$$

The Damkohler number is the ratio of dissolution to the rate of convective transport. The parameter V_i is the solvent requirement for a unit volume of bitumen.

Leaching

When dispersion is neglected, the Peclect number term is dropped and Equations (20) and (21) reduce to

$$\frac{\partial C_{sD}}{\partial \ell_D} + \frac{\partial C_{sD}}{\partial t_D} = - N_{Da} V_i C_{sD} W_D \tag{23}$$

$$\frac{\partial C_D}{\partial \ell_D} + \frac{\partial C_D}{\partial t_D} = N_{Da} C_{sD} W_D \tag{24}$$

The solid phase material balance equation is unchanged. The solvent dissolution requirement factor is the same for all the streamlines since the bitumen is assumed to be distributed uniformly. The injected solvent concentration does not vary from injector to injector. Since it is a function of V_p, the Damkohler number changes from streamline to streamline. Hence, effluent histories of each streamline are not identical. A solution to each equation will be needed to obtain the well effluent histories. However, this will not be necessary by introducing the following procedure.

Let us take a bundle of streamlines associated with a producer and define a parameter θ_j for the j^{th} streamline

$$\theta_j = \frac{N_{Da,j}}{N_{Da,\ell}} \qquad j = 1 \ \ldots \ N_s \tag{25}$$

where $N_{Da,\ell} = \max\{ N_{Da,1} \ldots N_{Da,n} \}$. Equation (22) using the Damkohler number definition and equation can be written as

$$\theta_j = \frac{V_{p,j}}{V_{p,\ell}} \tag{26}$$

The subscript ℓ refers to a reference streamline having the largest pore volume or largest N_{Da}. The ratio, θ, does not depend on the properties of the bitumen and is always less than or equal to one.

Using Equation (25), the material balance Equations (23), (24), and (22) are modified as, for bitumen,

$$\frac{\partial C_D}{\partial(\theta t_D)} + \frac{\partial C_D}{\partial(\theta \ell_D)} = N_{Da,\ell} V_i C_{sD} W_D \qquad \text{(27}$$

for solvent,

$$\frac{\partial C_{sD}}{\partial(\theta t_D)} + \frac{\partial C_{sD}}{\partial(\theta \ell_D)} = N_{Da,\ell} V_i C_{sD} W_D \tag{28}$$

and for the solid phase bitumen,

$$\frac{\partial W_D}{\partial(\theta t_D)} = - N_{Da} C_{sD} W_D \tag{29}$$

The significance of these equations is such that if the solutions for Equations (27) through

(29) can be obtained for the reference streamline($\theta_j = 1$), the solution for the other streamlines can be found from:

$$\{C_{sD}(\ell_D, t_D)\}_j = \{C_{sD}(\theta_j \ell_D, \theta_j t_D)\}_\ell \tag{30}$$

$$\{C_D(\ell_D, t_D)\}_j = \{C_D(\theta_j \ell_D, \theta_j t_D)\}_\ell$$

The well effluent concentrations are then computed by summation:

$$C_D(t_D^P) = \frac{1}{N_s} \sum_{j=1}^{N_s} \{C_D(\theta_j, \theta_j t_D)\}_\ell \tag{31}$$

A similar relationship can be written for the solvent.

The dimensionless times of the well and a streamline can be found in the following fashion. The pore volume associated with a producer V_p^P is

$$V_p^P = \sum_{j=1}^{N_s} V_{p,j} \tag{32}$$

where $V_{p,j}$ is the pore volumes associated with the jth streamline, evaluated by Equation (5). The subscript j refers to a streamline which was omitted earlier for simplicity. If the number of streamlines approaches infinity, the streamline pattern V_p^P approaches the pattern volume for confined streamline patterns.(Kabir (1985). From Equation (4) the streamline production rate is obtained. The dimensionless production time for a producer t_D^P is then:

$$t_D^P = \frac{Q^P t}{V_p^P} \tag{33}$$

The ratio of dimensionless time of the jth streamline to that of the pattern is:

$$\frac{t_D^P}{t_{D,j}} = \frac{Q^P V_{p,j}}{qV_p^P} \tag{34}$$

or

$$t_D^P = \beta_j t_{D,j}$$

where

$$\beta_j = \frac{Q^P V_{p,j}}{qV_p^P} = \frac{N_s V_{p,j}}{V_p^P} \tag{35}$$

β values can be calculated for various symmetric patterns using a computer program. The higher the value of N_s the the more accurate the representation of the pattern volume will be.

APPENDIX B

PRODUCTION HISTORIES OF RUNS IN GRAPHICAL FORM

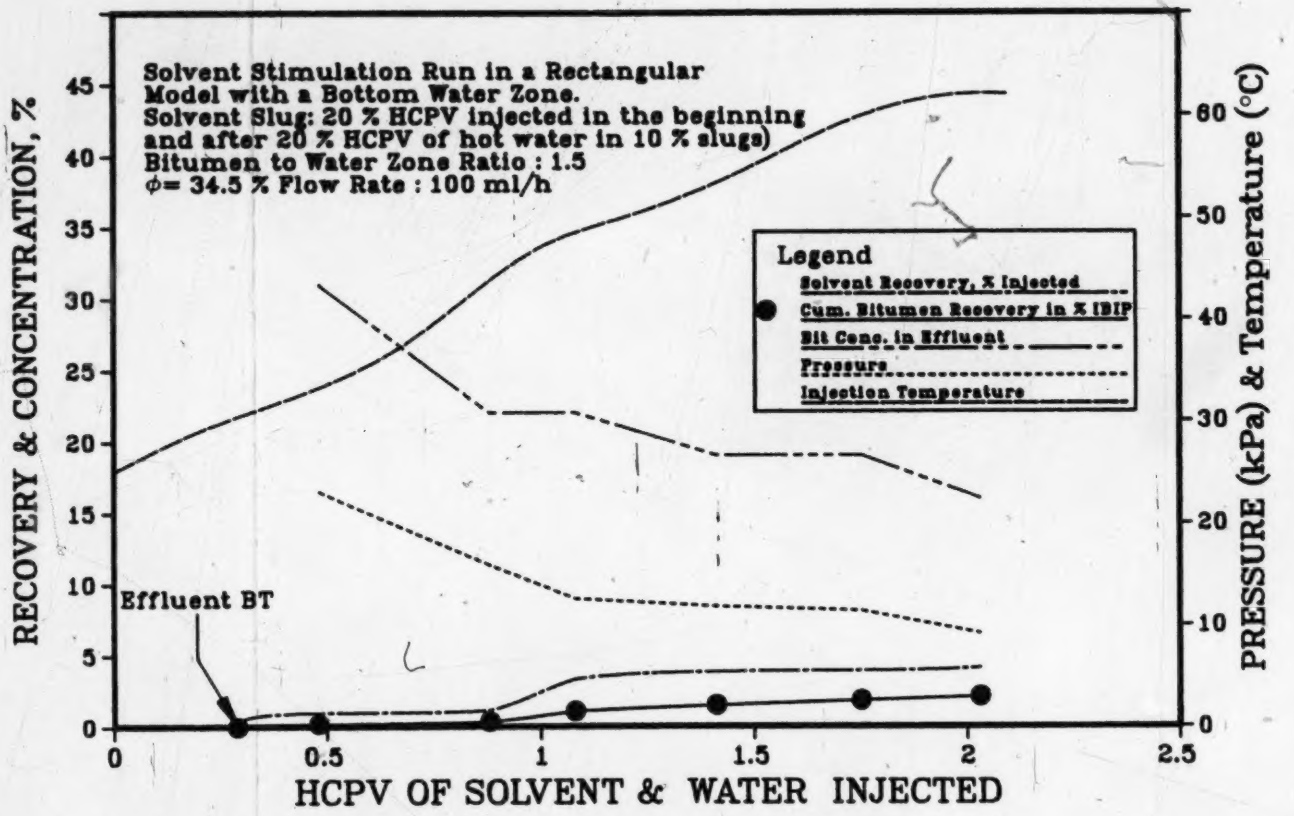

Figure B.1 Production History of Run 4

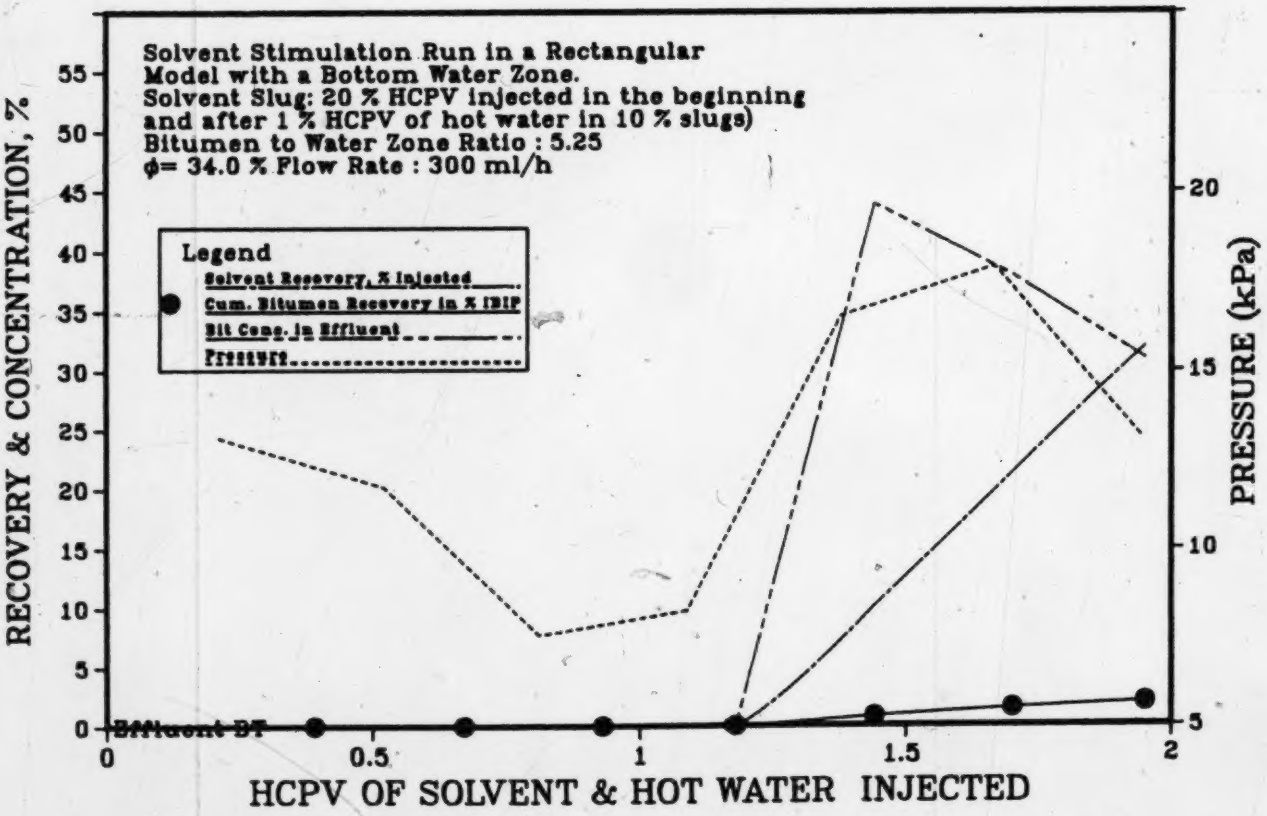

Figure B.2 Production History of Run 5

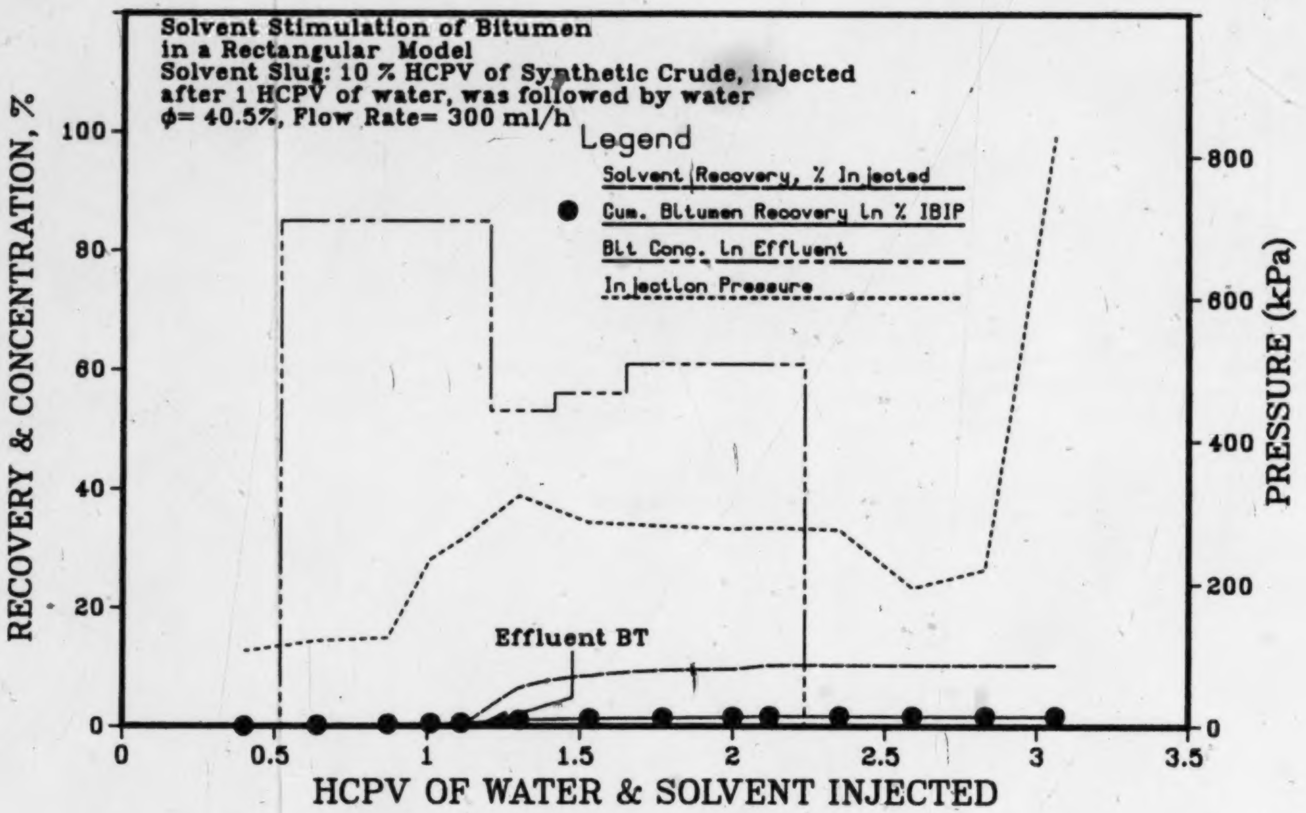

Figure B.3 Production History of Run 6

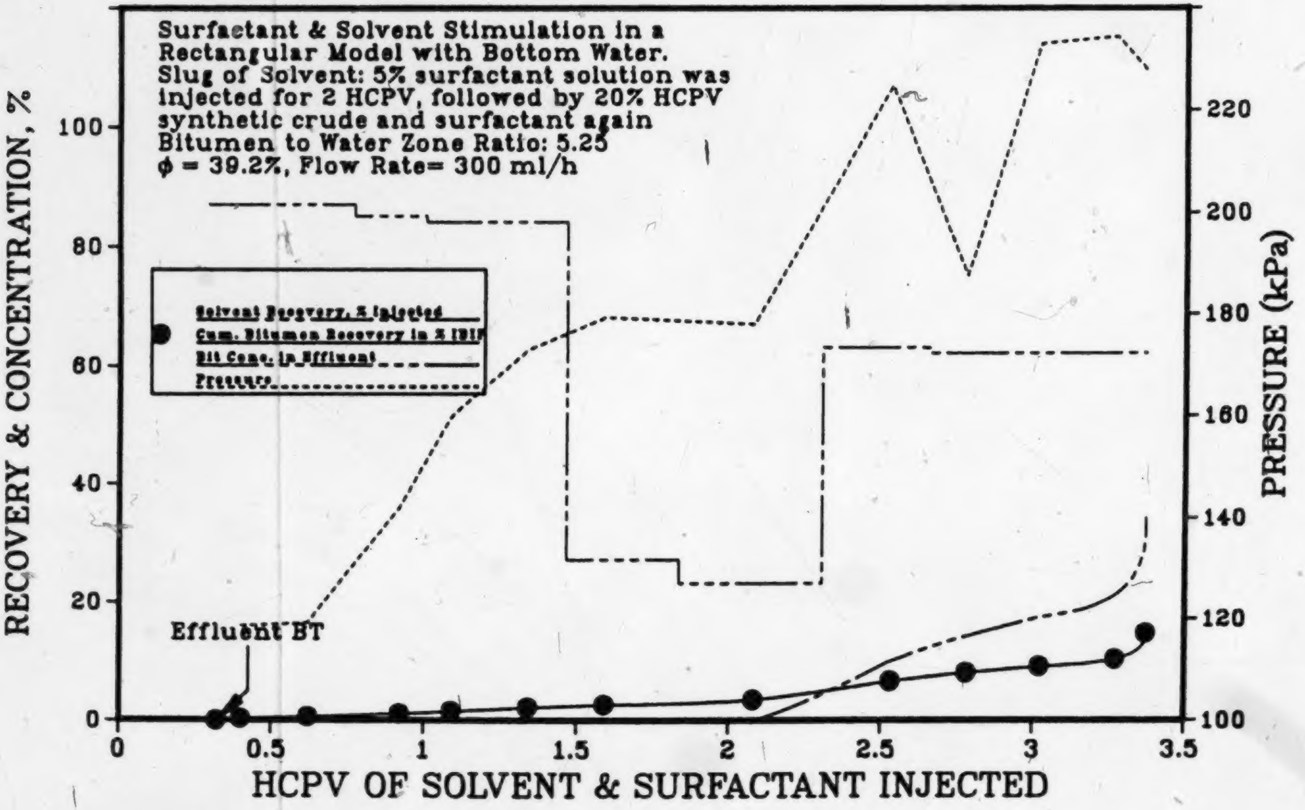

Figure B.4 Production History of Run 7

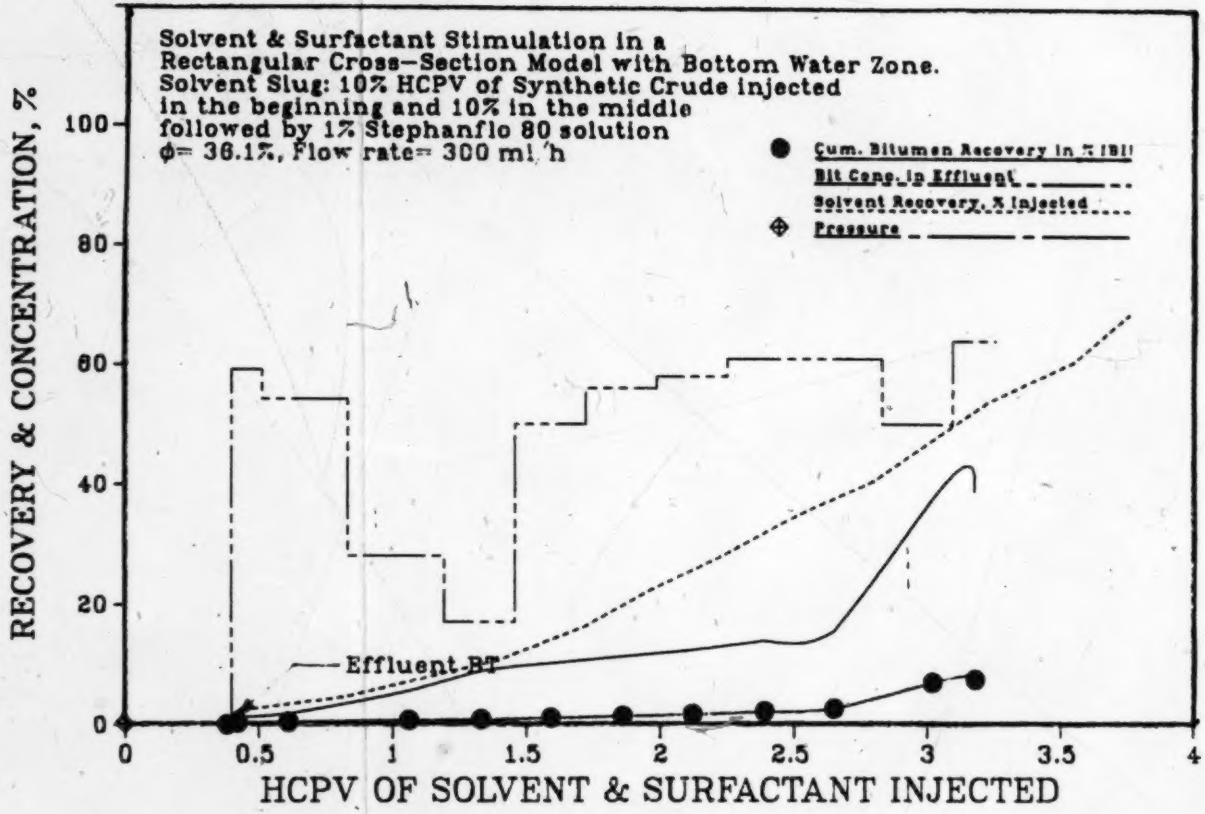

Figure B.5 Production History of Run 8

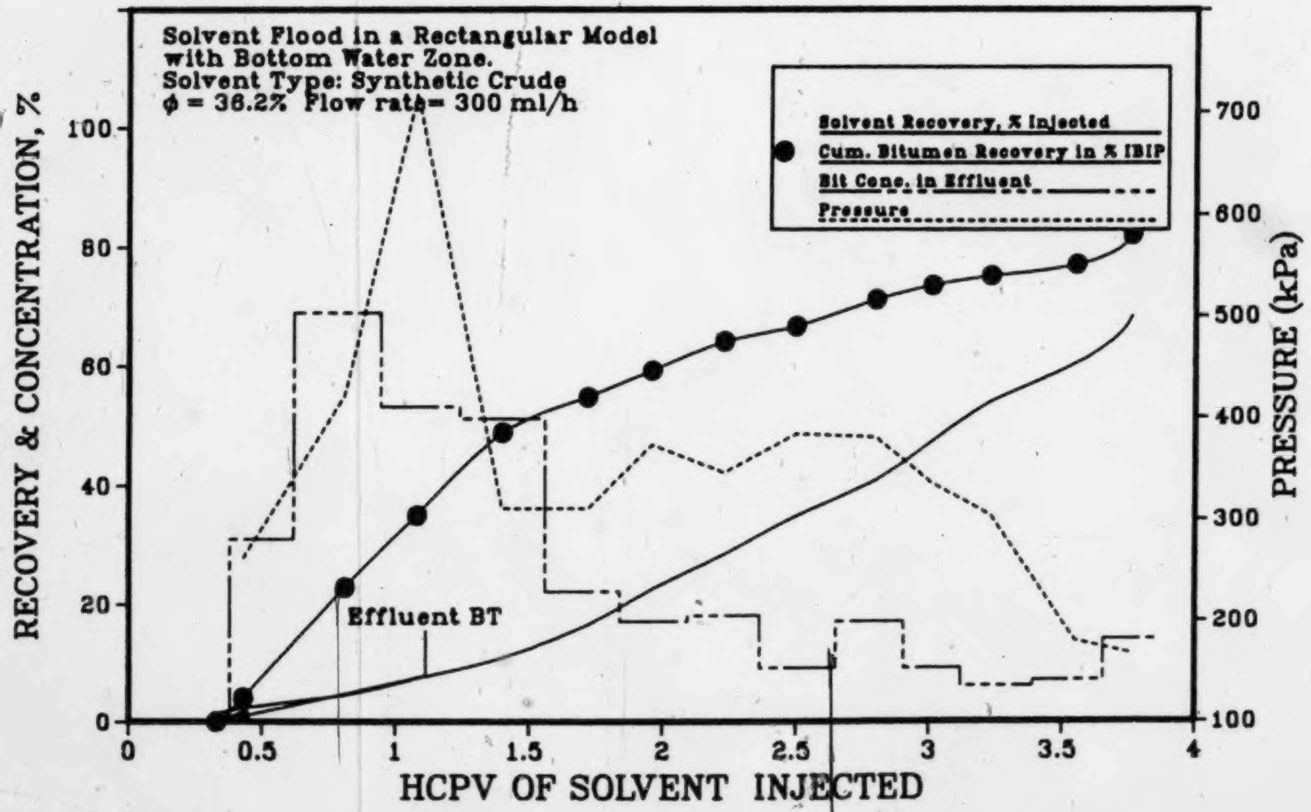

Figure B.6 Production History of Run 9

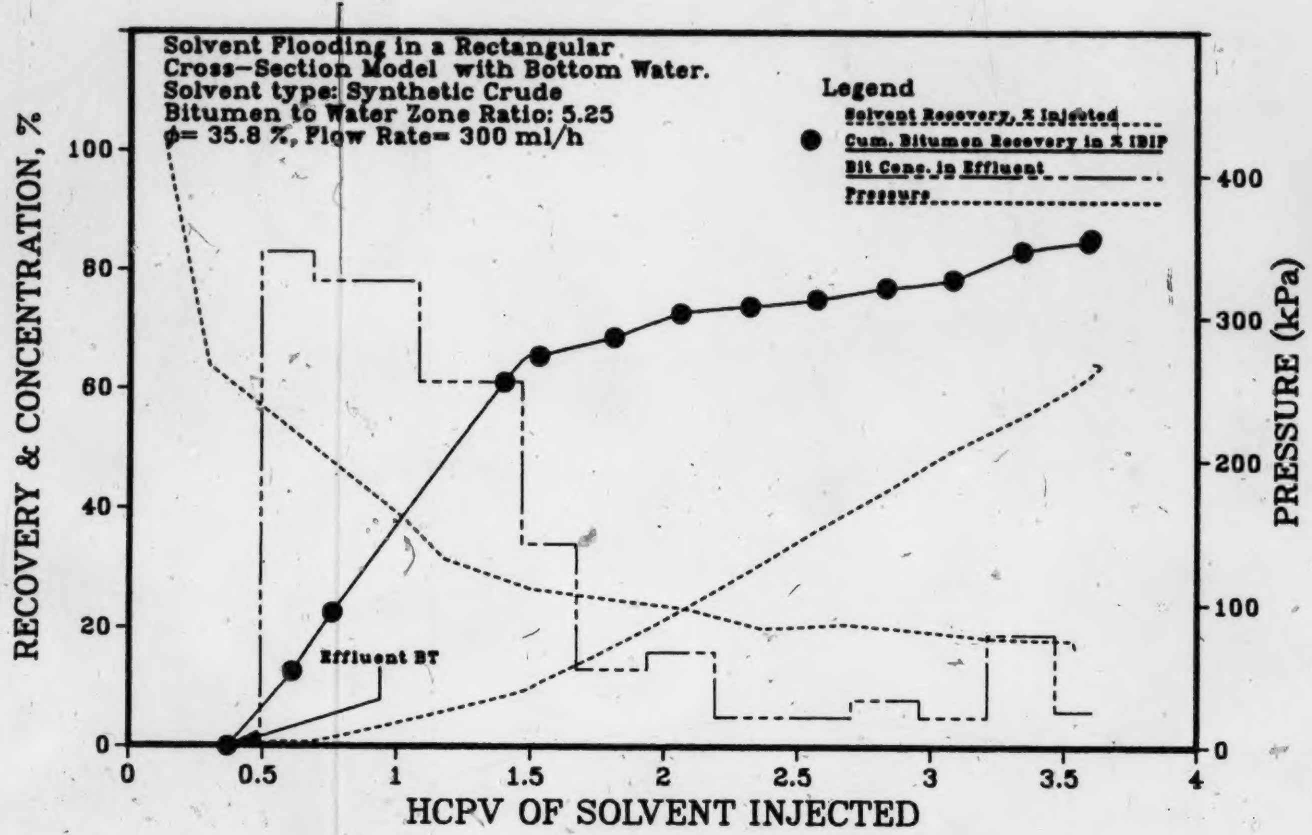

Figure B.7 Production History of Run 10

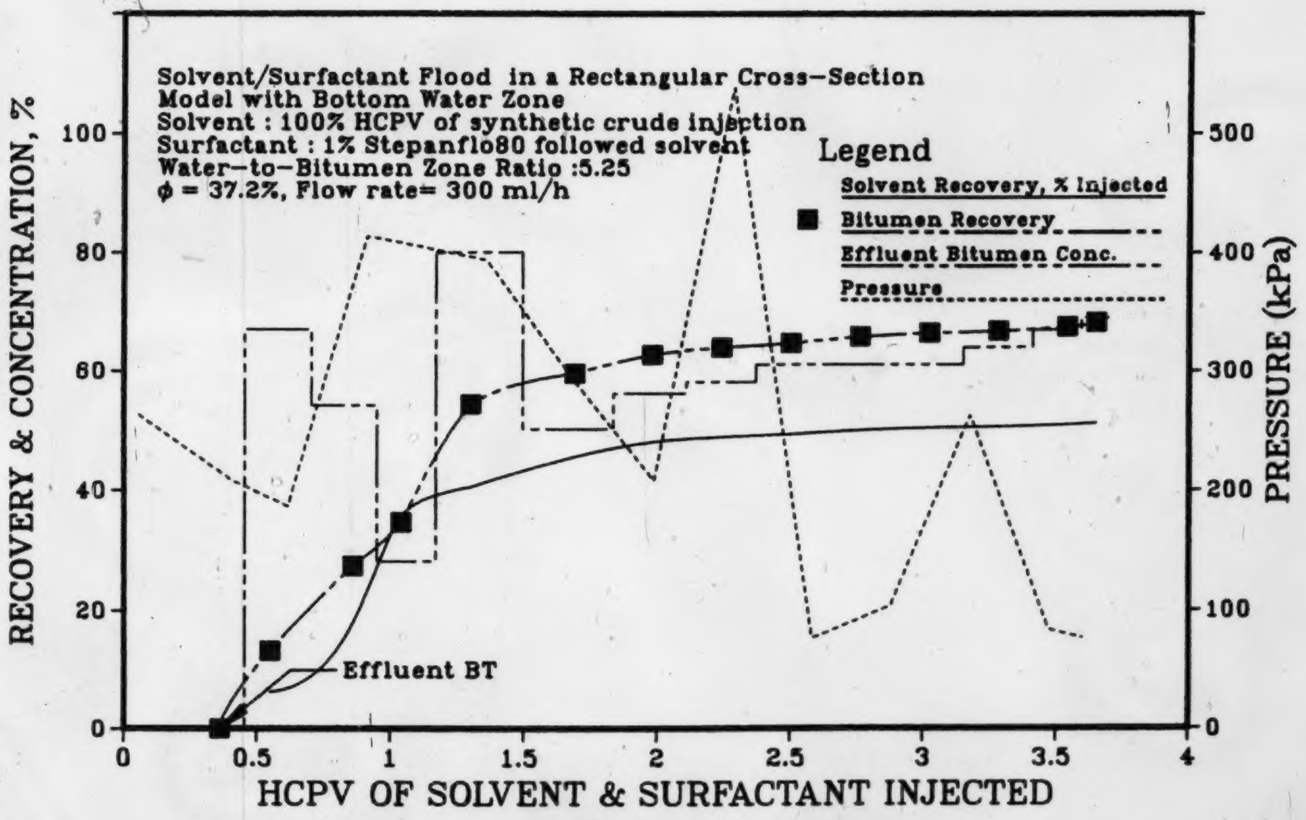

Figure B.8 Production History of Run 11

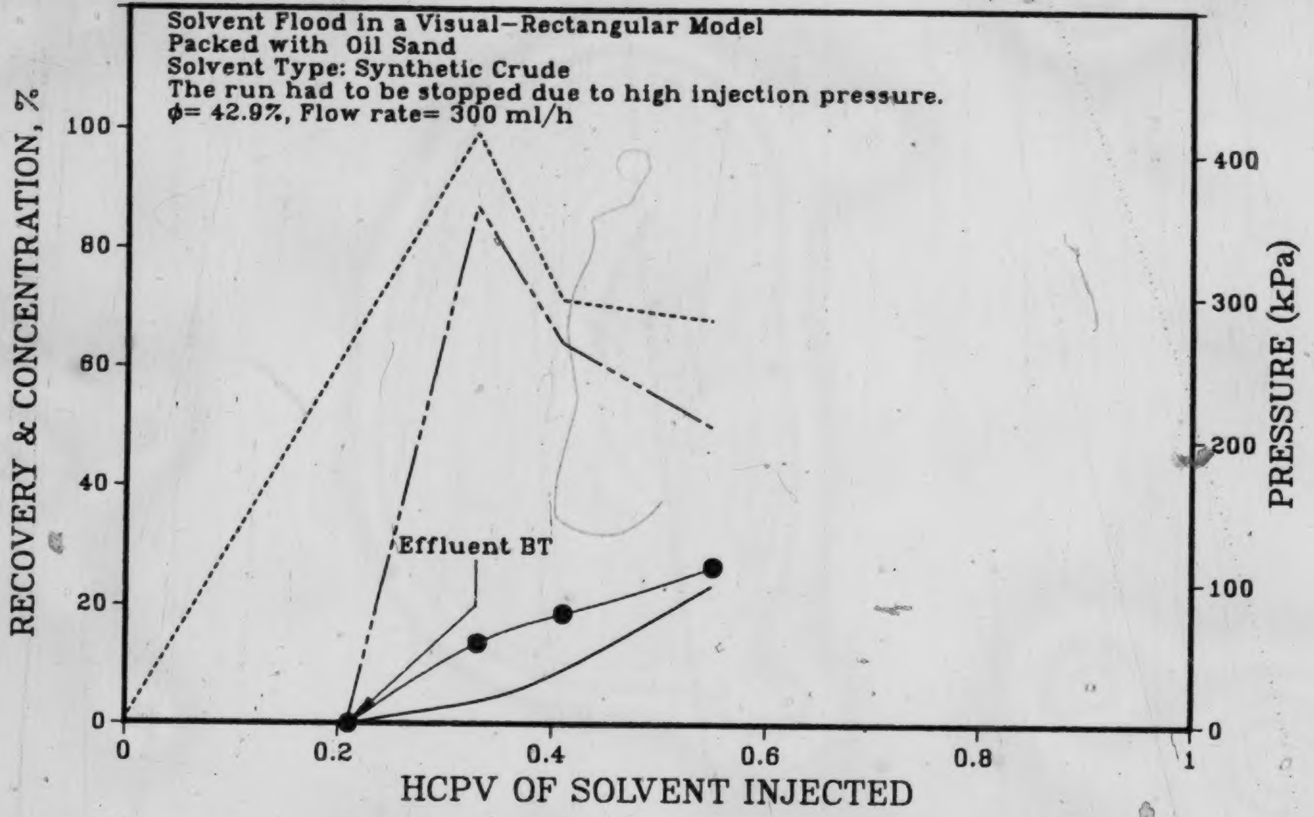

Figure B.9 Production History of Run 15

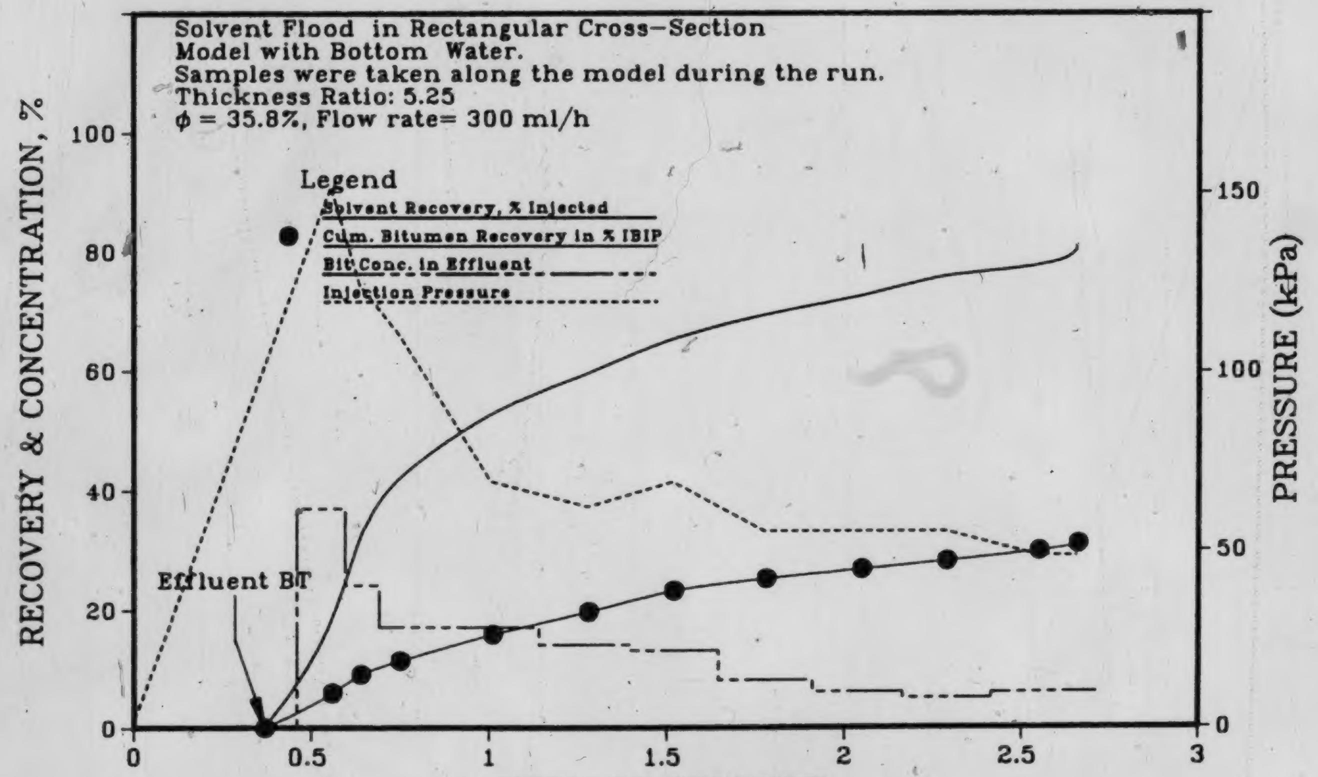

Figure B.10 Production History of Run 16

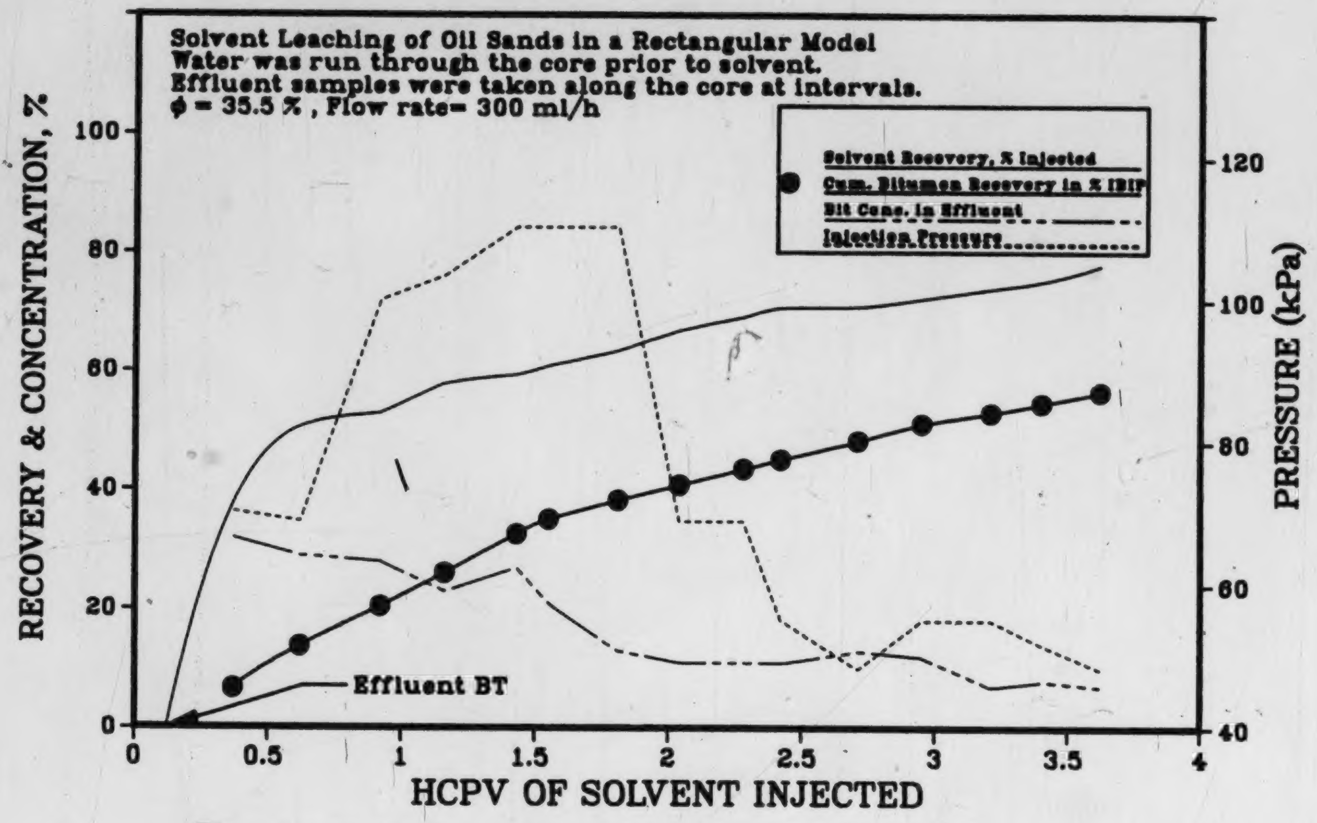

Figure B.11 Production History of Run 20

APPENDIX C

PRODUCTION HISTORIES OF ALL RUNS IN TABULATED FORM

Table C.1 Summary of Run 1

Weight of oil sand (g)	6552
Bitumen Content(weight%)	15.7
Bitumen Density (g/ml)	1.03
Bitumen Volume (ml)	998.7
Porosity (%)	33.89
Slug Size	36% HCPV
Hot Water Injected	60% HCPV
Bitumen Recovery	10% OBIP

Table C.2 Summary of Run 2

Weight of Sand Pack (g)	7059
Bitumen Content by weight(%)	15.2
Oil Sand Density (g/ml)	1.95
Bitumen Density (g/ml)	1.03
Bitumen Volume (ml)	1041.7
Porosity (%)	31.3
Solvent Injected(% HCPV)	10
Water Injected at 80°C (ml)	30
Bitumen Recovery (%)	Nil

Table C.3 Summary of Run 3

Viscosity of Oil at 25°C	50827 mPa.s
Density of Oil (g/ml)	0.8517
Permeability (mm²)	22.8
Porosity (%)	0.38
Initial Water Saturation (%)	9.09
Solvent Injected	0.46 HCPV
Hot Water Injected	0.60 HCPV
Solvent Recovered (ml)	410
Solvent Inj-Recovered Ratio	0.713
Oil Recovery(%)	17% IOIP

HISTORY OF RUN 4

WEIGHT OF OIL SAND: 1710.00 g

WEIGHT % OF BITUMEN: 16.50

SLUG SIZE: 20.00 % HCPV

FLOW RATE: 100.0 ml/h

DETAILS : A 10% SOLVENT SLUG WAS INJECTED AT THE START OF THE EXPERIMENT, FOLLOWED BY 20% HCPV OF HOT WATER. WHEN ONLY THE WATER BROKE THROUGH, AN ADDITONAL SLUG OF 10% WAS ADDED. FOR THE BOTTOM WATER ZONE

80-120 SIZE GLASS BEADS WERE USED. THE RATIO OF BITUMEN TO WATER ZONE THICKNESSES WAS 1.5.

PRESSURE,KPa	CUM.INJ.,CM3	FLUID PROD.	EFF. PROD.	SOL. REC.,%	BIT. REC.,%	WOR	SOR	BIT. CONC.	HCPV INJ.
29.45	31.00	0.00	0.0	0.0	0.00	0.0	0.0	0.0	0.11
23.09	132.00	100.00	2.00	1.04	0.23	50.00	2.20	0.31	0.48
15.86	240.00	200.00	4.00	1.22	0.39	50.00	3.57	0.22	0.88
12.55	295.00	300.00	13.00	3.38	1.11	11.11	3.57	0.22	1.08
11.79	385.00	400.00	19.00	3.86	1.52	16.67	4.33	0.19	1.41
11.38	480.00	500.00	24.00	3.94	1.86	20.00	4.33	0.19	1.75
9.17	557.00	575.00	29.00	4.15	2.14	15.00	5.40	0.16	2.03

PRESSURE: INJECTION PRESSURE
CUM. INJ: CUMULATIVE FLUID INJECTED
FLUID PROD.: CUMULATIVE FLUIDS PRODUCED
EFF. PROD.: BITUMEN-SOLVENT MIXTURE PRODUCED
SOL.& BIT. REC.: SOLVENT & BITUMEN RECOVERED
WOR = INSTANTENOUS WATER OIL RATIO
SOR = INSTANTENOUS SOLVENT OIL RATIO

TABLE C.5 HISTORY OF RUN 5

WEIGHT OF OIL SAND: 2428.00 g

WEIGHT % OF BITUMEN: 16.50

SLUG SIZE: 10.00 % HCPV

FLOW RATE: 300.0 ml/h

The pack consisted of an oil sands zone and a bottom water zone. Bitumen to water zone thickness ratio was 5.25. 10 % of synthetic crude slug was injected at the injection well. This was followed by 1 HCPV of water. Another 10 % slug of solvent was injected; succeeded by water flooding.

PRESSURE,kPa	CUM.INJ.,CM3	FLUID PROD.	EFF. PROD.	SOL. REC.,%	BIT. REC.,%	WOR	SOR	BIT. CONC.	HCPV INJ.
13.10	150.00	105.00	0.00	0.00	0.00	98.00	0.00	0.00	0.39
11.72	260.00	205.00	0.00	0.00	0.00	98.00	0.00	0.00	0.67
7.58	360.00	305.00	0.00	0.00	0.00	98.00	0.00	0.00	0.93
8.27	460.00	405.00	0.00	0.00	0.00	98.00	0.00	0.00	1.18
16.55	560.00	505.00	7.00	11.25	0.67	35.43	1.67	0.38	1.44
17.92	660.00	605.00	13.00	21.85	1.16	50.13	2.20	0.31	1.70
13.10	760.00	705.00	18.00	31.49	1.48	76.00	3.00	0.25	1.95

PRESSURE: INJECTION PRESSURE
CUM. INJ: CUMULATIVE FLUID INJECTED
FLUID PROD.: CUMULATIVE FLUIDS PRODUCED
EFF. PROD.: BITUMEN-SOLVENT MIXTURE PRODUCED
SOL.& BIT. REC.: SOLVENT & BITUMEN RECOVERED
WOR = INSTANTENOUS WATER OIL RATIO
SOR = INSTANTENOUS SOLVENT OIL RATIO

TABLE C.6 . HISTORY OF RUN 6

WEIGHT OF OIL SAND: 2700.00 g

WEIGHT % OF BITUMEN: 16.20

SLUG SIZE: 10.00 % HCPV

FLOW RATE: 300.0 ml/h

PRESSURE,kPa	CUM.INJ.,CM3	FLUID PROD.	EFF. PROD.	SOL. REC.,%	BIT. REC.,%	WOR	SOR	BIT. CONC.	HCPV INJ.
104.79	170.00	100.00	0.00	0.00	0.00	98.00	0.00	0.00	0.40
119.96	270.00	200.00	1.00	0.34	0.20	115.84	0.17	0.85	0.64
124.09	370.00	300.00	2.00	0.68	0.40	115.84	0.17	0.85	0.87
234.40	428.00	360.00	2.60	0.89	0.52	115.84	0.17	0.85	1.01
261.97	470.00	400.00	3.00	1.03	0.60	115.84	0.17	0.85	1.11
324.02	550.00	500.00	7.00	5.47	1.10	45.47	0.89	0.53	1.30
286.10	650.00	601.00	9.00	7.57	1.36	89.10	0.80	0.56	1.53
281.28	750.00	701.00	10.00	8.48	1.51	162.00	0.64	0.61	1.77
277.14	850.00	801.00	11.00	9.40	1.65	162.00	0.64	0.61	2.00
279.21	900.00	841.00	12.00	10.32	1.79	63.82	0.64	0.61	2.12
275.76	1000.00	941.00	12.00	10.32	1.79	98.00	0.00	0.00	2.35
194.41	1100.00	1041.00	12.00	10.32	1.79	98.00	0.00	0.00	2.59
220.61	1200.00	1141.00	12.00	10.32	1.79	98.00	0.00	0.00	2.83
827.28	1300.00	1241.00	12.00	10.32	1.79	98.00	0.00	0.00	3.06

PRESSURE: INJECTION PRESSURE
CUM. INJ: CUMULATIVE FLUID INJECTED
FLUID PROD.: CUMULATIVE FLUIDS PRODUCED
EFF. PROD.: BITUMEN-SOLVENT MIXTURE PRODUCED
SOL.& BIT. REC.: SOLVENT & BITUMEN RECOVERED
WOR = INSTANTENOUS WATER OIL RATIO
SOR = INSTANTENOUS SOLVENT OIL RATIO

TABLE C.7 HISTORY OF RUN 7

WEIGHT OF OIL SAND:	2549.00 g
WEIGHT % OF BITUMEN:	16.30
SLUG SIZE:	20.00 % HCPV
FLOW RATE:	300.0 ml/h

DETAILS : BOTTOM WATER ZONE THICKNESS IS ONE FIFTH OF OIL SAND THICKNESS (RATIO IS 5:1). THE FLOOD STARTED WITH INJECTION OF 5% STEPANFLO 80 SURFACTANT SOLUTION. AT 2.08 HCPV OF INJECTION, 20 % SOLVENT SLUG WAS INJECTED AT THE INJECTION WELL & FOLLOWED BY THE SURFACTANT SOLUTION AGAIN.

PRESSURE,kPa	CUM.INJ.,CM3	FLUID PROD.	EFF. PROD.	SOL. REC.,%	BIT. REC.,%	WOR	SOR	BIT. CONC.	HCPV INJ.
118.58	160.00	100.00	1.50	0.27	0.32	76.83	0.17	0.85	0.40
119.27	250.00	200.00	3.00	0.54	0.64	76.83	0.17	0.85	0.62
142.02	370.00	300.00	5.50	0.99	1.17	45.63	0.17	0.85	0.92
159.94	440.00	370.00	7.50	1.35	1.59	39.78	0.17	0.85	1.09
173.04	540.00	470.00	10.50	1.89	2.22	37.83	0.17	0.85	1.34
179.24	640.00	570.00	17.50	8.20	2.70	48.75	2.67	0.27	1.59
177.87	840.00	795.00	31.50	20.83	3.64	55.31	2.67	0.27	2.08
224.74	1020.00	895.00	51.50	30.18	6.73	6.42	0.61	0.62	2.53
187.52	1120.00	995.00	60.50	34.39	8.12	16.24	0.61	0.62	2.78
233.02	1220.00	1095.00	67.50	37.66	9.20	21.33	0.61	0.62	3.02
234.40	1320.00	1195.00	75.50	41.40	10.44	18.46	0.60	0.62	3.27
227.50	1360.00	1300.00	103.50	54.49	14.76	4.42	0.61	0.62	3.37

PRESSURE: INJECTION PRESSURE
CUM. INJ: CUMULATIVE FLUID INJECTED
FLUID PROD.: CUMULATIVE FLUIDS PRODUCED
EFF. PROD.: BITUMEN-SOLVENT MIXTURE PRODUCED
SOL.& BIT. REC.: SOLVENT & BITUMEN RECOVERED
WOR = INSTANTENOUS WATER OIL RATIO
SOR = INSTANTENOUS SOLVENT OIL RATIO

TABLE C.8 HISTORY OF RUN 8

WEIGHT OF OIL SAND:	2459.00 g
WEIGHT % OF BITUMEN:	15.80
SLUG SIZE:	20.00 % HCPV
FLOW RATE:	300.0 ml/h

PRESSURE,kPa	CUM.INJ.,CM3	FLUID PROD.	EFF. PROD.	SOL. REC.,%	BIT. REC.,%	WOR	SOR	BIT. CONC.	HCPV INJ.
[illegible]6.52	160.00	100.00	2.00	1.10	0.31	83.60	0.71	0.59	0.42
97.89	230.00	200.00	3.00	1.70	0.45	182.77	0.85	0.54	0.61
93.07	400.00	430.00	7.00	5.52	0.75	200.89	2.56	0.28	1.06
224.05	500.00	530.00	10.00	8.83	0.88	195.22	5.04	0.17	1.33
259.21	600.00	630.00	12.00	10.16	1.15	98.00	1.00	0.50	1.59
286.10	700.00	730.00	14.00	11.34	1.44	88.20	0.80	0.56	1.86
277.14	800.00	820.00	16.00	12.44	1.75	75.43	0.71	0.58	2.12
261.97	900.00	920.00	19.00	13.99	2.24	52.91	0.64	0.61	2.39
275.76	1000.00	1020.00	22.00	15.54	2.73	52.91	0.64	0.61	2.65
172.35	1140.00	1120.00	55.00	37.41	7.10	4.06	1.00	0.50	3.02
137.88	1200.00	1177.00	58.00	38.84	7.61	28.17	0.57	0.64	3.18

PRESSURE: INJECTION PRESSURE
CUM. INJ: CUMULATIVE FLUID INJECTED
FLUID PROD.: CUMULATIVE FLUIDS PRODUCED
EFF. PROD.: BITUMEN-SOLVENT MIXTURE PRODUCED
SOL.& BIT. REC.: SOLVENT & BITUMEN RECOVERED
WOR = INSTANTENOUS WATER OIL RATIO
SOR = INSTANTENOUS SOLVENT OIL RATIO

TABLE C.9 HISTORY OF RUN 9

WEIGHT OF OIL SAND: 2425.00 g
WEIGHT % OF BITUMEN: 15.80
SLUG SIZE: 376.00 % HCPV
FLOW RATE: 300.0 ml/h

PRESSURE,KPa	CUM.INJ.,CM3	FLUID PROD.	EFF. PROD.	SOL. REC.,%	BIT. REC.,%	WOR	SOR	BIT. CONC.	HCPV INJ.
207.43	90.00	30.00	0.00	0.0	0.0	--	--	--	0.33
261.97	160.00	100.00	49.00	2.41	4.12	2.04	2.20	0.31	0.43
420.53	300.00	200.00	149.00	4.59	22.78	1.00	0.44	0.69	0.81
716.98	400.00	285.00	234.00	7.43	34.97	1.00	0.87	0.53	1.08
310.23	520.00	385.00	334.00	10.90	48.79	1.00	0.95	0.51	1.40
310.23	640.00	485.00	434.00	16.49	54.67	1.00	3.57	0.22	1.72
372.28	730.00	585.00	534.00	22.43	59.20	1.00	4.93	0.17	1.96
344.70	830.00	685.00	634.00	28.26	64.16	1.00	4.42	0.18	2.23
382.62	930.00	785.00	734.00	34.74	66.68	1.00	9.67	0.09	2.50
379.17	1040.00	885.00	834.00	40.69	71.22	1.00	4.93	0.17	2.80
334.36	1120.00	985.00	934.00	47.19	73.65	1.00	10.03	0.09	3.01
303.34	1200.00	1085.00	1034.00	53.89	75.33	1.00	15.00	0.06	3.23
179.24	1320.00	1185.00	1134.00	60.53	77.26	1.00	12.91	0.07	3.55
166.83	1400.00	1315.00	1264.00	68.49	82.29	1.00	5.96	0.14	3.76

PRESSURE: INJECTION PRESSURE
CUM. INJ: CUMULATIVE FLUID INJECTED
FLUID PROD.: CUMULATIVE FLUIDS PRODUCED
EFF. PROD.: BITUMEN-SOLVENT MIXTURE PRODUCED
SOL.& BIT. REC.: SOLVENT & BITUMEN RECOVERED
WOR = INSTANTENOUS WATER OIL RATIO
SOR = INSTANTENOUS SOLVENT OIL RATIO

TABLE C.10 HISTORY OF RUN 10

WEIGHT OF OIL SAND: 2560.00 g
WEIGHT % OF BITUMEN: 15.80
SLUG SIZE: 360.00 % HCPV
FLOW RATE: 300.0 ml/h

PRESSURE,KPa	CUM.INJ.,CM3	FLUID PROD.	EFF. PROD.	SOL. REC.,%	BIT. REC.,%	WOR	SOR	BIT. CONC.	HCPV INJ.
427.43	240.00	100.00	60.00	0.74	12.61	1.67	0.21	0.83	0.61
265.42	300.00	150.00	110.00	1.52	22.53	1.00	0.28	0.78	0.76
158.56	550.00	400.00	360.00	8.50	61.08	1.00	0.65	0.61	1.40
130.99	600.00	450.00	410.00	10.82	65.46	1.00	1.91	0.34	1.53
110.30	710.00	550.00	510.00	17.01	68.64	1.00	7.00	0.13	1.81
103.41	810.00	650.00	610.00	22.95	72.70	1.00	5.27	0.16	2.06
96.52	910.00	750.00	710.00	29.70	73.90	1.00	20.33	0.05	2.32
82.73	1010.00	850.00	810.00	36.44	75.09	1.00	20.33	0.05	2.57
86.17	1110.00	950.00	910.00	42.96	77.08	1.00	11.80	0.08	2.83
81.35	1210.00	1050.00	1010.00	49.66	78.43	1.00	17.82	0.05	3.08
75.83	1310.00	1150.00	1110.00	55.40	83.21	1.00	4.33	0.19	3.34
74.46	1410.00	1250.00	1210.00	62.03	84.80	1.00	15.00	0.06	3.59
68.94	1414.00	1285.00	1245.00	64.36	85.36	1.00	15.00	0.06	3.60

PRESSURE: INJECTION PRESSURE
CUM. INJ: CUMULATIVE FLUID INJECTED
FLUID PROD.: CUMULATIVE FLUIDS PRODUCED
EFF. PROD.: BITUMEN-SOLVENT MIXTURE PRODUCED
SOL & BIT. REC.: SOLVENT & BITUMEN RECOVERED
WOR = INSTANTENOUS WATER OIL RATIO
SOR = INSTANTENOUS SOLVENT OIL RATIO

TABLE C.11 HISTORY OF RUN 11

WEIGHT OF OIL SAND:	2470.00 g
WEIGHT % OF BITUMEN:	16.00
SLUG SIZE:	104.00 % HCPV
FLOW RATE:	300.0 ml/h

PRESSURE,KPa	CUM.INJ.,CM3	FLUID PROD.	EFF. PROD.	SOL. REC.,%	BIT. REC.,%	WOR	SOR	BIT. CONC.	HCPV INJ.
261.97	210.00	100.00	76.00	6.30	13.26	1.32	0.49	0.67	0.55
206.82	330.00	200.00	176.00	17.78	27.38	1.00	0.85	0.54	0.86
186.14	400.00	300.00	276.00	35.79	34.71	1.00	2.56	0.28	1.04
413.64	500.00	400.00	370.00	40.51	54.31	1.06	0.25	0.80	1.30
392.96	650.00	500.00	410.00	45.52	59.52	2.50	1.00	0.50	1.69
289.55	760.00	600.00	432.00	47.97	62.70	4.55	0.80	0.56	1.98
206.82	860.00	700.00	440.00	48.80	63.92	12.50	0.71	0.58	2.24
537.73	960.00	800.00	445.00	49.29	64.72	20.00	0.64	0.61	2.50
75.83	1060.00	900.00	452.00	49.97	65.83	14.29	0.64	0.61	2.76
103.41	1160.00	1000.00	456.00	50.36	66.47	25.00	0.64	0.61	3.02
261.97	1260.00	1100.00	458.00	50.54	66.80	50.00	0.57	0.64	3.28
82.73	1360.00	1200.00	462.00	50.88	67.50	25.00	0.50	0.67	3.54
75.83	1400.00	1278.00	466.00	51.18	68.22	19.50	0.44	0.69	3.65

PRESSURE: INJECTION PRESSURE
CUM. INJ: CUMULATIVE FLUID INJECTED
FLUID PROD.: CUMULATIVE FLUIDS PRODUCED
EFF. PROD.: BITUMEN-SOLVENT MIXTURE PRODUCED
SOL.& BIT. REC.: SOLVENT & BITUMEN RECOVERED
WOR = INSTANTENOUS WATER OIL RATIO
SOR = INSTANTENOUS SOLVENT OIL RATIO

TABLE C.12 RUN 12

WEIGHT OF OIL SAND:	2540.00 g
WEIGHT % OF BITUMEN:	15.50
SLUG SIZE:	1.50 % HCPV
FLOW RATE:	300.0 mL/h

PRESSURE,KPa	CUM.INJ.,CM3	FLUID PROD.	EFF. PROD.	GI, CM3	GP, CM3	SOL. REC.%	BIT. REC.%	WOR	SOR	BIT. CONC.
3805.49	295.00	0.00	0.00	1414.00	0.00	0.00	0.00	100.00	0.00	0.77
3805.49	295.00	100.00	0.00	1414.00	635.00	0.00	0.00	100.00	0.00	0.77
3584.88	410.00	200.00	0.00	1414.00	650.00	0.00	0.00	100.00	0.00	1.07
1275.39	510.00	300.00	0.00	1414.00	664.00	0.00	0.00	100.00	0.00	1.33
1061.68	600.00	400.00	0.00	1414.00	678.00	0.00	0.00	100.00	0.00	1.57
34.47	700.00	500.00	0.00	1414.00	683.00	0.00	0.00	100.00	0.00	1.83
41.36	790.00	600.00	0.00	1414.00	685.00	0.00	0.00	100.00	0.00	2.07
27.58	890.00	700.00	0.00	1414.00	685.00	0.00	0.00	100.00	0.00	2.33
55.15	990.00	800.00	0.00	1414.00	685.00	0.00	0.00	100.00	0.00	2.59

PRESSURE: INJECTION PRESSURE
CUM. INJ: CUMULATIVE FLUID INJECTED
FLUID & EFF. PROD.: FLUID AND EFFLUENT PRODUCED
SOL.& BIT. REC.: SOLVENT & BITUMEN PRODUCED
WOR = INSTANTENOUS WATER OIL RATIO
SOR = INSTANTENOUS SOLVENT OIL RATIO
GI= CO2 INJECTED GP= CO2 PRODUCED

University of Alberta

TABLE C.13 HISTORY OF RUN 13

WEIGHT OF OIL SAND: 2580.00 g

WEIGHT % OF BITUMEN: 15.60

SLUG SIZE: 39.00 % HCPV

FLOW RATE: 300.0 ml/h

PRESSURE,kPa	CUM.INJ.,CM3	FLUID PROD.	EFF. PROD.	SOL. REC.,%	BIT. REC.,%	WOR	SOR	BIT. CONC.	HCPV INJ.
310.23	100.00	20.00	0.00	0.00	0.00	99.00	63.00	--	0.26
1089.25	120.00	24.00	0.00	0.00	0.00	99.00	63.00	--	0.31
2068.20	136.00	26.00	0.00	0.00	0.00	99.00	63.00	--	0.35
4136.40	153.00	27.00	0.00	0.00	0.00	99.00	63.00	--	0.39

PRESSURE: INJECTION PRESSURE
CUM. INJ: CUMULATIVE FLUID INJECTED
FLUID PROD.: CUMULATIVE FLUIDS PRODUCED
EFF. PROD.: BITUMEN-SOLVENT MIXTURE PRODUCED
SOL.& BIT. REC.: SOLVENT & BITUMEN RECOVERED
WOR = INSTANTENOUS WATER OIL RATIO
SOR = INSTANTENOUS SOLVENT OIL RATIO

TABLE C.14 HISTORY OF RUN 14

WEIGHT OF OIL SAND:	3680.00 g
WEIGHT % OF BITUMEN:	17.20
SLUG SIZE:	20.00 % HCPV
FLOW RATE:	100.0 ml/h

PRESSURE,kPa	CUM.INJ.,CM3	FLUID PROD.	EFF. PROD.	SOL. REC.,%	BIT. REC.,%	WOR	SOR	BIT. CONC.	HCPV INJ.
88.24	122.00	100.00	4.00	2.18	0.22	72.45	2.02	0.33	0.20
40.67	247.00	200.00	7.00	3.82	0.37	99.49	2.08	0.33	0.40
124.78	297.00	250.00	19.00	10.48	1.00	9.93	2.14	0.32	0.48
222.68	419.00	300.00	46.00	25.51	2.38	2.70	2.17	0.32	0.68
194.41	427.00	350.00	53.00	29.60	2.70	21.84	2.56	0.28	0.69
213.71	477.00	410.00	58.00	32.40	2.96	35.20	2.20	0.31	0.78
199.24	517.00	460.00	61.00	34.22	3.08	61.14	2.90	0.26	0.84

PRESSURE: INJECTION PRESSURE
CUM. INJ: CUMULATIVE FLUID INJECTED
FLUID PROD.: CUMULATIVE FLUIDS PRODUCED
EFF. PROD.: BITUMEN-SOLVENT MIXTURE PRODUCED
SOL.& BIT. REC.: SOLVENT & BITUMEN RECOVERED
WOR = INSTANTENOUS WATER OIL RATIO
SOR = INSTANTENOUS SOLVENT OIL RATIO

TABLE C.15 HISTORY OF RUN 15

WEIGHT OF OIL SAND: 3800.00 g

WEIGHT % OF BITUMEN: 17.20

SLUG SIZE: 55.00 % HCPV

FLOW RATE: 300.0 ml/h

DETAILS : CONTINUOUS INJECTION OF SYNTHETIC CRUDE WAS ATTEMPTED IN THE VISUAL RECTANGULAR MODEL. THE SOLVENT INJECTION WAS POSSIBLE UNTIL THE INJECTION PRESSURE REACHED THE MAXIMUM WORKING PR

PRESSURE, kPa	CUM.INJ., CM3	FLUID PROD.	EFF. PROD.	SOL. REC., %	BIT. REC., %	WOR	SOR	BIT. CONC.	HCPV INJ.
413.64	210.00	100.00	80.00	3.07	10.92	0.00	0.15	0.87	0.33
296.44	260.00	150.00	130.00	8.24	15.96	0.00	0.57	0.64	0.41
282.65	350.00	248.00	230.00	22.56	23.83	0.00	1.00	0.50	0.55

PRESSURE : INJECTION PRESSURE
CUM. INJ.: CUMULATIVE FLUID INJECTED
FLUID PROD.: CUMULATIVE FLUIDS PRODUCED
EFF. PROD.: BITUMEN-SOLVENT MIXTURE PRODUCED
SOL.& BIT. REC.: SOLVENT & BITUMEN RECOVERED
WOR = INSTANTENOUS WATER OIL RATIO
SOR = INSTANTENOUS SOLVENT OIL RATIO

TABLE C.16 HISTORY OF RUN 16

WEIGHT OF OIL SAND: 2450.00 g

WEIGHT % OF BITUMEN: 15.80

SLUG SIZE: 216.00 % HCPV

FLOW RATE: 300.0 ml/h

PRESSURE,kPa	CUM.INJ.,CM3	FLUID PROD.	EFF. PROD.	SOL. REC.,%	BIT. REC.,%	WOR	SOR	BIT. CONC.	HCPV INJ.
178.90	138.00	0.00	0.00	0.00	0.00	0.00	0.00	0.00	0.37
151.67	210.00	100.00	60.00	18.04	5.89	1.81	1.71	0.37	0.56
124.09	240.00	150.00	110.00	31.67	9.05	0.00	3.21	0.24	0.64
110.30	280.00	200.00	160.00	41.89	11.37	0.00	4.74	0.17	0.75
68.94	380.00	300.00	260.00	52.74	15.85	0.00	4.93	0.17	1.01
62.05	480.00	400.00	360.00	59.61	19.65	0.00	6.00	0.14	1.28
68.94	570.00	500.00	460.00	65.44	23.15	0.00	6.61	0.13	1.52
55.15	670.00	600.00	560.00	69.48	25.14	0.00	12.33	0.08	1.78
55.15	770.00	700.00	660.00	72.66	26.74	0.00	15.67	0.06	2.05
55.15	860.00	800.00	760.00	76.08	28.14	0.00	18.05	0.05	2.29
48.26	960.00	900.00	860.00	77.89	29.87	0.00	14.38	0.06	2.55
48.26	1000.00	970.00	930.00	81.32	31.08	0.00	14.38	0.06	2.66

PRESSURE: INJECTION PRESSURE
CUM. INJ: CUMULATIVE FLUID INJECTED
FLUID PROD.: CUMULATIVE FLUIDS PRODUCED
EFF. PROD.: BITUMEN-SOLVENT MIXTURE PRODUCED
SOL.& BIT. REC.: SOLVENT & BITUMEN RECOVERED
WOR : INSTANTENOUS WATER OIL RATIO
SOR : INSTANTENOUS SOLVENT OIL RATIO

TABLE C.17 HISTORY OF 17

WEIGHT OF OIL SAND: 2450.00 g

WEIGHT % OF BITUMEN: 16.10

SLUG SIZE: 317.00 % HCPV

FLOW RATE: 300.0 ml/h

PRESSURE,KPa	CUM.INJ.,CM3	FLUID PROD.	EFF. PROD.	GI, CM3	GP, CM3	SOL. REC.%	BIT. REC.%	WOR	SOR	HCPV INJ.
41.364	99.00	0.00	0.00	0.00	0.00	0.00	0.00	0.00	0.00	0.26
27.58	170.00	100.00	60.00	0.00	0.00	4.17	2.46	1.67	0.16	0.44
27.58	270.00	200.00	160.00	0.00	0.00	11.68	4.75	1.00	0.09	0.71
27.58	430.00	300.00	260.00	0.00	0.00	19.45	6.25	1.00	0.06	1.12
20.68	500.00	400.00	360.00	0.00	0.00	27.17	7.88	1.00	0.06	1.31
27.58	620.00	500.00	460.00	0.00	0.00	34.85	9.64	1.00	0.07	1.62
27.58	730.00	600.00	560.00	0.00	0.00	42.76	10.69	1.00	0.04	1.91
20.68	795.00	700.00	660.00	0.00	0.00	50.69	11.67	1.00	0.04	2.08
1895.85	795.00	700.00	660.00	4300.00	0.00	50.69	11.67	100.00	0.00	2.08
1723.50	920.00	800.00	760.00	4300.00	540.00	57.63	15.77	1.00	0.16	2.40
1344.33	1020.00	900.00	860.00	4300.00	840.00	64.67	19.57	1.00	0.15	2.66
999.63	1120.00	1000.00	960.00	4300.00	1250.00	71.89	22.78	1.00	0.12	2.92
654.93	1215.00	1120.00	1080.00	4300.00	1800.00	81.03	25.13	1.00	0.08	3.17

PRESSURE: INJECTION PRESSURE
CUM. INJ: CUMULATIVE FLUID INJECTED
FLUID & EFF. PROD.: FLUID AND EFFLUENT PRODUCED
SOL.& BIT. REC.: SOLVENT & BITUMEN PRODUCED
WOR = INSTANTENOUS WATER OIL RATIO
SOR = INSTANTENOUS SOLVENT OIL RATIO
GI= CO2 INJECTED GP= CO2 PRODUCED

TABLE C.18 HISTORY OF RUN 18

WEIGHT OF OIL SAND:	2390.00 g
WEIGHT % OF BITUMEN:	15.00
SLUG SIZE:	100.00 % HCPV
FLOW RATE:	300.0 mL/h

PRESSURE,KPa	CUM.INJ.,CM3	FLUID PROD.	EFF. PROD.	GI, CM3	GP, CM3	SOL. REC.%	BIT. REC.%	WOR	BIT. CONC.	HCPV INJ.
151.67	220.00	100.00	80.00	0.00	0.00	4.68	18.31	1.25	0.80	0.63
206.82	320.00	200.00	180.00	0.00	0.00	28.47	23.25	1.00	0.17	0.92
234.40	345.00	230.00	210.00	0.00	0.00	35.61	24.73	1.00	0.17	0.99
1034.10	345.00	230.00	210.00	2560.00	0.00	35.61	24.73	---	0.00	0.99
827.28	665.00	330.00	226.00	2560.00	520.00	37.44	27.49	6.25	0.60	1.91
723.87	765.00	430.00	254.00	2560.00	800.00	40.73	32.24	3.57	0.59	2.20
620.46	865.00	530.00	268.00	2560.00	1000.00	42.38	34.62	7.14	0.59	2.49
634.25	965.00	630.00	286.00	2560.00	1200.00	44.31	37.86	5.56	0.63	2.77
289.55	1065.00	730.00	301.00	2560.00	1350.00	45.83	40.65	6.67	0.65	3.06
275.76	1305.00	980.00	333.00	2560.00	1700.00	49.04	46.63	7.81	0.65	3.75
137.88	1310.00	1048.00	353.00	2560.00	1750.00	51.04	50.38	3.40	0.65	3.76
62.05	1310.00	1082.00	357.00	2560.00	1860.00	51.43	51.14	8.50	0.66	3.76

PRESSURE: INJECTION PRESSURE
CUM. INJ: CUMULATIVE FLUID INJECTED
FLUID & EFF. PROD.: FLUID AND EFFLUENT PRODUCED
SOL.& BIT. REC.: SOLVENT & BITUMEN PRODUCED
WOR = INSTANTENOUS WATER OIL RATIO
SOR = INSTANTENOUS SOLVENT OIL RATIO
GI= CO2 INJECTED GP= CO2 PRODUCED

TABLE C.19 HISTORY OF RUN 19

WEIGHT OF OIL SAND:	2800.00 g
WEIGHT % OF BITUMEN:	15.30
SLUG SIZE:	197.00 % HCPV
FLOW RATE:	300.0 mL/h

THE RUN WAS STARTED WITH INJECTION OF SURFACTANT SOLUTION AT THE PRODUCTION WELL UNTIL THE PRESSURE WENT UP TO 1930 KPa. IT WAS LEFT UNTIL THE PRESSURE DROPPED AND THIS PROCEDURE WAS REPEATED SEVERAL TIMES AFTER WHICH 2 HCPV OF SOLVENT INJECTION WAS INJECTED. CARBONDIOXIDE STIMULATION FROM THE PRODUCING END HELPED MOBILIZE THE RESIDUAL BITUMEN WHICH WAS CHASED BY SURFACTANT SOLUTION.

PRESSURE,KPa	CUM.INJ.,CM3	FLUID PROD.	EFF. PROD.	GI, CM3	GP, CM3	SOL. REC.%	BIT. REC.%	WOR	SOR	BIT. CONC.
1930.32	83.00	28.00	0.00	0.00	0.00	0.00	0.00	100.00	0.00	0.20
1930.32	110.00	61.00	0.00	0.00	0.00	0.00	0.00	100.00	0.00	0.26
1930.32	141.00	84.00	0.00	0.00	0.00	0.00	0.00	100.00	0.00	0.34
1930.32	165.00	119.00	0.00	0.00	0.00	0.00	0.00	100.00	0.00	0.40
1930.32	200.00	140.00	0.00	0.00	0.00	0.00	0.00	100.00	0.00	0.48
1930.32	220.00	160.00	0.00	0.00	0.00	0.00	0.00	100.00	0.00	0.53
1930.32	238.00	178.00	0.00	0.00	0.00	0.00	0.00	100.00	0.00	0.57
1930.32	255.00	216.00	0.00	0.00	0.00	0.00	0.00	100.00	0.00	0.61
413.64	445.00	316.00	100.00	0.00	0.00	7.18	9.90	1.00	0.41	1.07
261.97	558.00	416.00	200.00	0.00	0.00	15.89	16.77	1.00	0.29	1.34
186.14	655.00	519.00	303.00	0.00	0.00	25.77	22.08	1.00	0.21	1.57
172.35	755.00	619.00	403.00	0.00	0.00	35.61	26.75	1.00	0.19	1.82
158.56	855.00	719.00	503.00	0.00	0.00	44.29	33.69	1.00	0.29	2.06

CONTINUED

137.88	955.00	819.00	603.00	0.00	0.00	51.20	44.11	1.00	0.43	2.30
124.09	1055.00	919.00	703.00	0.00	0.00	60.24	50.36	1.00	0.26	2.54
827.28	1055.00	919.00	703.00	0.00	0.00	60.24	50.36	100.00	0.00	2.54
482.58	1245.00	1019.00	738.00	1758.00	310.00	62.84	53.64	2.86	0.39	2.99
372.28	1375.00	1119.00	758.00	1758.00	430.00	64.41	55.35	5.00	0.36	3.31
358.49	1455.00	1219.00	772.00	1758.00	500.00	65.39	56.78	7.14	0.43	3.50

PRESSURE: INJECTION PRESSURE
CUM. INJ: CUMULATIVE FLUID INJECTED
FLUID & EFF. PROD.: FLUID AND EFFLUENT PRODUCED
SOL.& BIT. REC.: SOLVENT & BITUMEN PRODUCED
WOR = INSTANTENOUS WATER OIL RATIO
SOR = INSTANTENOUS SOLVENT OIL RATIO
GI= CO2 INJECTED GP= CO2 PRODUCED

TABLE C.20 HISTORY OF RUN 20

WEIGHT OF OIL SAND: 2750.00 g
WEIGHT % OF BITUMEN: 15.50
SLUG SIZE: 350.00 % HCPV
FLOW RATE: 300.0 ml/h

PRESSURE,kPa	CUM.INJ.,CM3	FLUID PROD.	EFF. PROD.	SOL. REC.,%	BIT. REC.,%	WOR	SOR	BIT. CONC.	HCPV INJ.
89.62	50.00	14.00	0.00	0.00	0.00	0.00	0.00	0.00	0.12
70.32	155.00	100.00	86.00	37.91	6.58	0.51	2.16	0.32	0.37
68.94	255.00	200.00	186.00	50.74	13.68	0.00	2.40	0.29	0.62
99.96	380.00	300.00	286.00	53.05	20.40	0.00	2.60	0.28	0.92
103.41	480.00	400.00	386.00	58.01	25.99	0.00	3.32	0.23	1.16
110.30	590.00	500.00	486.00	59.54	32.56	0.00	2.68	0.27	1.43
110.30	640.00	550.00	536.00	61.09	35.05	0.00	3.85	0.21	1.55
110.30	750.00	650.00	636.00	63.71	38.23	0.00	6.61	0.13	1.81
68.94	845.00	750.00	736.00	67.13	40.78	0.00	8.46	0.11	2.04
68.94	945.00	850.00	836.00	69.43	43.47	0.00	7.97	0.11	2.28
55.15	1000.00	910.00	896.00	70.96	45.05	0.00	8.21	0.11	2.42
48.26	1120.00	1010.00	996.00	71.11	48.22	0.00	6.61	0.13	2.71
55.15	1220.00	1120.00	1096.00	72.50	51.12	0.83	7.33	0.12	2.95

CONTINUED

55.15	1330.00	1230.00	1206.00	74.19	52.98	0.00	13.29	0.07	3.21
51.70	1405.00	1310.00	1286.00	75.45	54.58	0.00	11.12	0.08	3.40
48.26	1500.00	1430.00	1406.00	78.14	56.53	0.00	13.81	0.07	3.62

PRESSURE: INJECTION PRESSURE
CUM. INJ: CUMULATIVE FLUID INJECTED
FLUID PROD.: CUMULATIVE FLUIDS PRODUCED
EFF. PROD.: BITUMEN-SOLVENT MIXTURE PRODUCED
SOL.& BIT. REC.: SOLVENT & BITUMEN RECOVERED
WOR : INSTANTENOUS WATER OIL RATIO
SOR : INSTANTENOUS SOLVENT OIL RATIO

TABLE C.21 HISTORY OF RUN 21

WEIGHT OF OIL SAND: 2825.00 g
WEIGHT % OF BITUMEN: 16.50
SLUG SIZE: 331.00 % HCPV
FLOW RATE: 300.0 ml/h

PRESSURE,kPa	CUM.INJ.,CM3	FLUID PROD.	EFF. PROD.	SOL. REC.,%	BIT. REC.,%	WOR	SOR	BIT. CONC.	HCPV INJ.
978.95	290.00	100.00	100.00	22.99	7.37	0.00	2.00	0.33	0.64
330.91	385.00	200.00	200.00	34.79	14.59	0.00	2.06	0.33	0.85
220.61	495.00	300.00	300.00	43.34	18.89	0.00	4.15	0.19	1.09
213.71	600.00	405.00	405.00	50.00	23.20	0.00	4.38	0.19	1.33
193.03	695.00	505.00	505.00	55.42	26.48	0.00	5.73	0.15	1.54
137.88	810.00	610.00	610.00	59.03	29.13	0.00	7.75	0.11	1.79
137.88	915.00	715.00	715.00	62.64	31.33	0.00	9.53	0.09	2.02
137.88	1000.00	815.00	815.00	66.47	33.21	0.00	10.76	0.09	2.21
124.09	1130.00	915.00	915.00	66.36	34.98	0.00	11.50	0.08	2.50
144.77	1220.00	1015.00	1015.00	69.67	36.47	0.00	13.81	0.07	2.70
144.77	1340.00	1115.00	1115.00	70.33	38.13	0.00	12.33	0.08	2.96
151.67	1440.00	1215.00	1215.00	71.87	39.79	0.00	12.33	0.08	3.18
137.88	1500.00	1335.00	1335.00	76.40	41.77	0.00	12.33	0.08	3.31

PRESSURE: INJECTION PRESSURE
CUM. INJ: CUMULATIVE FLUID INJECTED
FLUID PROD.: CUMULATIVE FLUIDS PRODUCED
EFF. PROD.: BITUMEN-SOLVENT MIXTURE PRODUCED
SOL.& BIT. REC.: SOLVENT & BITUMEN RECOVERED
WOR : INSTANTENOUS WATER OIL RATIO
SOR : INSTANTENOUS SOLVENT OIL RATIO